Order Number 9417519

Improvement for the B-CDMA PCS links in an urban environment by using a directional antenna at the mobile terminal

Zilberfarb, Joseph, Ph.D.

City University of New York, 1994

U·M·I
300 N. Zeeb Rd.
Ann Arbor, MI 48106

IMPROVEMENT FOR THE B-CDMA PCS LINKS IN AN URBAN ENVIRONMENT BY USING A DIRECTIONAL ANTENNA AT THE MOBILE TERMINAL

by

JOSEPH ZILBERFARB

A dissertation submitted to the Graduate Faculty in Engineering in partial fulfillment of the requirements for the degree of Doctor of Philosophy, The City University of New York

1994

This manuscript has been read and accepted for the Graduate Faculty in Engineering in satisfaction of the dissertation requirement for the degree of Doctor of Philosophy.

22 December 1993
Date

Professor Donald L. Schilling
Chair of the Examining Committee

1/15/94
Date

Professor Gerard G. Lowen
Executive Officer

Professor Joseph Barba

Professor Paul Karmel

Professor Svetislav Maric

Dr. Philip Balaban

Supervisory Committee

THE CITY UNIVERSITY OF NEW YORK

ABSTRACT

Since the early days of mobile communications researchers have attempted to improve the link performance by using directional antennas. Previous research focused on the cell site antennas, for the following reasons:

1. It makes more economical sense to invest in the cell antenna that supports a multitude of users, and keep the simple low cost whip antenna at the mobile terminals.

2. The mobile user may change his relative location with respect to the cell site at any moment. Knowledge of the direction of arrival (DOA) of the signal is necessary to facilitate an effective use of a directional antenna at the mobile terminal.

3. For an efficient antenna to have a significant directivity its aperture has to be at least a half wavelength by a half wavelength. A relatively large antenna (approximately 20 cm by 20 cm) is required

for the "traditional" 800 MHz cellular band. That size is too big for a mobile or a portable terminal.

Moreover, researchers that had tried to use highly directional antennas for the mobiles, reported only a marginal improvement (or none at all). That created a myth that only an omni - directional antenna is suitable for the mobile terminals.

Increased demand for more efficient use of the spectrum, requires an innovative fresh look at this old problem. Current computing technology makes it possible to have more processing power at the mobile unit at reasonable cost and size. Allocation of higher frequencies for personal communication (1.9 Ghz) and proposals for even higher frequencies (6 Ghz, or even 60 Ghz), makes the size of an efficient directional antenna compatible with the dimensions of a mobile or even a portable terminal. Maintaining similar link budgets at higher frequencies demands the use of directional antennas at both ends of the link.

Another approach to increasing capacity is to divide the service area to smaller cells. The increased demand in urban areas has prompted proposals to build an

infrastructure of smaller cells that cover only several blocks each. Each "micro-cell" will have its own low cost low power transmitter, and its antenna will be installed on utility polls. This configuration will support communications up to approximately two hundred meter range. This microcellular (urban) environment has not been investigated until recently.

In this research I concentrated on the improvement of the B-CDMA links in urban microcellular environment, by using a directional antenna at the mobile terminal. First, I present a model that predicts the distribution of the directions of arrival of the signal in that environment. Based on that model, I show that the signals arrive from distinct directions. Thus, having an adaptive system that would direct the antenna towards that best direction will improve the received signal to noise ratio (SNR). Later, I propose a method for direction finding, and analyze how it can be applied to the cellular mobile application. Finally, I present field measurements whose results have verified the validity of the model. Field test results prove that an adaptive system can achieve the full gain advantage from a directional antenna at the mobile.

ACKNOWLEDGMENTS

First and foremost, I would like to express my appreciation to my thesis adviser, Professor Donald L. Schilling. It has been my privilege and my pleasure to study with him. Working on this research, I have benefited much from his wide knowledge, guidance and friendship.

Field tests were conducted using experimental equipment that belongs to SCS TELECOM, INC. (which later has become InterDigital Telecom, Inc.). The logistic complexity of the field tests in NY had required the active participation of my CUNY colleagues: Mr. Saeed Gassemzadeh, Mr. Maxwell Taylor, and Mr. Simon Nawrot. Without their resources and support these tests would not have been possible. Special thanks to my colleague Dr. Vinko Erceg for his valuable comments on the model, and his participation in the field tests.

I am indebted to my beloved parents, Devorah and Shalom, who have instilled in me the desire to pursue my

professional education to the fullest. This long time study would not have been possible without the love, consideration, and understanding of my dear wife Ronit and my children Liat and Orit. Their tolerance, support and encouragement has permitted me to complete this research.

Table of Contents

List of Tables

page

List of Figures

1. INTRODUCTION

The popularity of the cellular phone has created an enormous pressure on the service providers to increase the capacity of their systems. The FCC has allocated a restricted band of frequencies for the cellular application, and it is unlikely that it will always be able to add more bandwidth to satisfy the increasing demand. Developments in computing technology (palm held computers), and the wide acceptance of facsimile machines, have increased the demand for voice and data "communication on the move". People have come to expect wireless connectivity to the public telephone network (voice), or to their home and office computers (data) while they are driving their cars, or walking in the streets. This truly Personal Communication System (PCS) environment requires an increase of several orders of magnitude over the capacity of the existing system.

Several proposals for improvement are being considered by the cellular providers. They make plans to transition from the current analog (FM) modulation to a new digital modulation. Both Time Division Multiple Access (TDMA) and Code Division Multiple Access (CDMA)

offer increased capacity compared to the existing FM. However, changing the modulation scheme alone will not satisfy the demand for increased capacity, and more improvements are planed. AT&T has recently applied for an experimental license to provide cellular service in a microwave band that traditionally has been reserved for terrestrial microwave and satellite communications. The propagation characteristics at 6 GHz are inferior to UHF, and use of directional antennas at the cell site and perhaps at the mobile terminal will be required.

Another method to increase the capacity of the cellular system is to increase its frequency re-use, by designing it for operation in smaller cells (microcells). The highest demand is, of course, in the cities, that currently are served by a limited number of cells (macrocells). Currently, the base antennas are mounted on top of high buildings, that are "strategically" selected to provide a good coverage in the city. In a micro-cell system, a large area will be divided in to multitude of "microcells", each covering several blocks. There would be many base antennas, mounted on top of utility poles. The transmitter power at each site will be only a few milliwatts, but it will be enough to communicate with mobile terminals that are

only 200 m to 300 m away. This environment has not been investigated enough in the past. Recent research is focused at modeling the propagation in urban microcells environment.

In this dissertation the idea of using a directional antenna on the mobile terminal is investigated. It is shown that if the Direction Of Arrival (DOA) of the signal is known, pointing a directional antenna on the mobile terminal will improve the link. I propose a method to estimate the DOA by measuring the phase relations of the received signal in an array of several antennas. I analyze the predicted accuracy of the DOA estimate, and its time constraints. Using a multi-ray model to predict the propagation of the radio waves, I present specific recommendations for the directional antenna beam width. This result has been verified by field tests, in both Line of Sight (LOS) and out of sight streets. My conclusion that the directional antenna offers a significant improvement is contrary to common belief. Previous research and tests in urban and sub-urban environment, using narrow band modulation techniques [1-5], concluded that a directional antenna could not offer its full potential for improvement, because of the scattering and multipath effects.

The gain of an antenna is related to its physical aperture by the following formula [6]:

$$G = (4\pi Aeff)/(\lambda)^2 \qquad (1.1)$$

Where

G is the antenna gain in dBi,
Aeff is the effective aperture of the antenna, and
λ is the wavelength.

At 835 Mhz the wavelength is 36 cm, at 1900 Mhz it is 16 cm, and at 6000 Mhz it is only 5 cm. While it is difficult to implement the idea of a directional antenna (yet a compact one) at current UHF cellular frequencies, it is quite possible in higher frequencies. It is possible to imagine an array of several quarter wavelength dipoles built into the hand held terminals that operate at 6 Ghz. The 6 Ghz band is currently investigated by AT&T for future PCS applications.

The obvious advantages of the directional antenna is an increase in Signal to Noise Ratio (SNR) that is translated to higher capacity. Theoretically, the capacity of a channel is given by Shanon's theorem as:

$$C = B \log_2 (1 + S/N) \qquad (1.2)$$

Where

C is the capacity,

B is the channel bandwidth, and

S/N is the Signal to Noise (and interference) ratio.

Use of directional antennas may reduce the required radiation level towards the users' head, that has recently caused public concern over health risk due to an extensive use of cellular portable terminals. Directing the radiated power towards a specific direction will also reduce the interference level in the "unwanted" directions, which is a prime concern in a CDMA system. Following is a brief description of the

interference problem in a CDMA system, using spread spectrum modulation.

The Direct Sequence (DS) spread spectrum signal is generated by modulating the (relatively) low bit rate information with a "fast" pseudo-random sequence (PN code). This effect is called "spreading". The inverse, "de-spreading" operation, is performed at the receiver. The spreading and the de-spreading operations have no impact on the resultant thermal noise that is always present in the channel [7]. However, additional narrow band interference added by the channel (after the original signal has been spread), is attenuated by the ratio of the interference bandwidth to the PN sequence bandwidth.

That is one of the advantages of a spread spectrum modulation. Other users, each having its own unique PN code, are present at the receiver input. The receiver multiplies the input signals by a specific, desired, PN sequence. The wanted signal is de-spread, and the original information is recovered. The multiplication of the specific PN sequence with other codes produces interference called "co-channel interference". The cross-correlation properties of truly random PN

sequences is zero. Practical PN sequences are selected from a family of pseudo-random sequences that have a low cross-correlation property [7]. The designer of the link makes sure that it will maintain a certain signal to thermal noise ratio. It is unlikely that many narrow band interfaces will be present, but even if they exist, they will have virtually no impact on the spread spectrum system. It is likely that other co-users will be present. The co-channel interference generated by a multitude of co-users is a limiting factor on the capacity of a CDMA system [8].

Power control is a common technique to reduce the co-channel interference. In this technique the power levels are adjusted to prevent transmissions with excess power that has a negligible improvement on the specific link, but increases the interference into other co-users. Another technique to reduce interference is to use a Voice Activity Detector (VAD) that cuts transmit power in the silence periods during normal talk. The ratio between the "active" and the "silence" periods in a normal talk is a statistical parameter whose average is approximately thirty percent [9]. It has been shown that it offers a statistical capacity increase between two and three.

Using a directional antenna at the mobile terminal has a similar advantage. It will reduce the interference generated by a specific user into other terminals that are randomly distributed in other directions. The combination of power control, VAD, and a directional antenna is a further improvement to the link.

2. Review of Prior Work

Early research in mobile communications tried to model and characterize the unique mobile environment. Researchers tried to find ways to reduce signal fading, and to increase the average signal strength. It has been recognized that the mobile environment presents different challenges than point to point communications. In the latter there is a simple relation between the transmitted and the received power [3,6,7]:

$$Pr = Pt + Gt + Gr - L \qquad (2.1)$$

where

- Pr is the received power at the mobile terminal [dBm],
- Pt is the transmitted power level [dBm],
- Gt is the transmitter antenna gain (in the direction of the receiver) [dBi],
- Gr is the receiver gain (in the direction of the transmitter) [dBi], and
- L is the propagation loss between the transmitter and the receiver [dB].

In an ideal "free space" environment the "free space loss" (in dB) is [3]:

$$L = 20 \text{ Log } (4\pi d/\lambda) \qquad (2.2)$$

where

- d is the separation between the receiver and the transmitter and the receiver, and
- λ is the wavelength (both expressed in same units).

As the distance between the transmitter and the receiver increases, the received signal power decreases. The received power is inversely proportional to that distance squared. The attenuation is 20 dB per decade (in a logarithmic scale).

Propagation over smooth conducting plane earth has been investigated by Norton [11], and by Bullington [12]. Assuming a perfectly conducting flat earth, and a large separation between the transmitter and the receiver (compared to the difference in the height of the antennas), it can be shown that [3,4,9,11,12,17]:

$$L = 20 \text{ Log } (d^2 / Hb\ Hm) \qquad (2.3)$$

where

Hb is the height of the base antenna, and

Hm is the height of the mobile antenna.

Under these conditions the attenuation is at a rate of 40 dB per decade. To predict precisely the propagation loss in another environment, other models were investigated by Bullington. To apply those techniques one must know the details of the topographic environment in the vicinity of the two antennas, and the exact topographic cross section of the path.

In point to point communications it may be possible to predict the propagation loss based on those techniques. In mobile applications it becomes much more difficult. The topographic data is generally not available in details for the base site, and it is meaningless for a mobile terminal whose environment changes on the move. Studies and field tests (for example [13]) have shown that the attenuation is a function of the "type" of the propagation environment (e.g. urban, sub-urban, open

area, etc..). The attenuation is always greater than 20 dB per decade, and its slope is sharper than 40 dB per decade for practical measurements in cities. Actual measurements show attenuation in the range of 50 dB in some cities or even 60 dB per decade in NYC. In a large city there are more reflections, not only the reflection from an ideal flat earth, but also reflections from buildings and other objects. Those reflected waves cause more attenuation. Hence, the attenuation rate in cities is larger than the 40 dB per decade predicted by the two ray model. It becomes more difficult to build a deterministic model to predict the attenuation in a city, yet the simplified models help establishing a lower bound on the attenuation rate.

Instead of predicting the propagation in deterministic terms, a statistical approach has been suggested by many. Hata [15], in a classical paper, suggests an empirical formula that is based on measurements in the 100 - 1500 Mhz range, distances of 1 -20 km, a base station antenna height of 30 - 200 m, and a mobile antenna height of 1 - 10 m.

Much attention has been paid to all the parameters that appear to impact the received power level. Among them the base antenna height, and the mobile antenna height. Again, an empirical data, and the Hata's model on which it is based, show that the effect of the base station antenna height is 6 dB per octave (as predicted by the flat earth model) for distances up to 10 km. Changing the mobile antenna height from 1.5 m to 3.0 m, Okumura observed a height-gain advantage of 3 dB. At higher frequencies, and in a medium city he observed a steep height-gain dependence. It is not surprizing that there seems to be better agreement between the theoretical model and the base antenna height dependence, than the dependence of the signal strength on the mobile antenna height. The base site is generally on top of a high building, where the mobile antenna is in the street in a strong and changing multi-path environment.

Use of directional antennas for both the base site and the mobile terminals has been investigated at the early stages of mobile communications research. The base site antenna is supposed to serve users that could be at

any random azimuth direction. Therefore, it is desirable to have an omni-directional azimuth pattern for the base antenna [4]. Directivity in the elevation pattern would be beneficial, as long as the antenna covers well the elevation angles from which the mobile terminals are communicating. Reference [3] records the results of an un - published research of Bell Laboratories with a directional dish as the base site antenna. The measured free space beam width was 1.2 degrees, and the average of the measured beam width (using a stationary mobile terminal) was 2.6 degrees. The median was 1.7 degrees, meaning that for half of the measurements the effective gain was only 3.6 dB lower than the free space value.

Generally, omni-directional antennas are used in the cell site. The antenna is shared by the cell site transmit and receive equipment. When traffic demands, "sector" antennas are used. Each "sector" antenna has its own set of transmit and receive resources. For economical reasons, each antenna usually cover either a 120 degrees sector (in azimuth), or a 60 degrees sector [4].

Using a directional antenna at the mobile terminal could further improve both the forward and the reverse links. Indeed, researchers have tried to explore that possibility since the early days of mobile communications research. In a set of experiments done by Bell Laboratories in 1966 (the pre-cellular era), a directional antenna at the mobile terminal was tried at 836 Mhz [1,2]. Lee used several directional antennas, and compared their received signal strength to that received by an omni-directional antenna in the same locations [1]. The reference 'omni' antenna was a whip antenna. The same element in front of a large (one wavelength by six) reflector constituted the directional antenna. Arrays of two, four, and eight elements (with same reflector) were also measured. The peak signal strength of the eight elements array was the same as that for the four elements array. The difference between the two elements array to the four elements was only 2.0 dB. The same difference of peak signal strength was observed comparing the single element (with the reflector) to the two elements array (with the reflector). Only the difference between the reference omni-directional antenna (whip without a reflector) and the directional single element in front of the reflector

was 3.0 dB. Similar comparison of average signal strength, showed only 2.2 dB of increase when the reflector was added in front of the omni-directional antenna. The theoretical (and free space measured) difference is 3 dB. There was no significant difference of the average signal strength received by the two, four, and the eight element arrays. The obvious conclusion was that there is only a marginal advantage to using a directional antenna at the mobile terminal. Using a highly directive antenna (eight elements as compared to four elements) did not produce any advantage that would have been realized under free space conditions.

Both Lee [1] and Stidham [2] concluded that there is only a limited potential of improvement by the (horizontal) directional mobile antenna. Also, both observed a reduction in the fading rate using a directional antenna. Those findings were attributed to the fact that the signal was received from directions that were almost uniformly distributed in the horizontal plane. Lee and Brandt [15] checked the actual gain of a mobile terminal with a directional antenna that was omni-directional in the horizontal plane, but had a

narrow beam width in the elevation plane. The free space difference in gain between the high (elevation) gain antenna and the whip antenna was 4.0 dB. Measurements taken in LOS conditions showed almost 4.0 dB advantage for the directional antenna. However, the average difference for measurements taken in locations that were out LOS conditions was only 2.3 dB.

Independent tests and measurements [5] confirmed that high gain antennas have significantly less effective gain when used at the mobile terminal. Davidson and Turney [5] have found a 2.0 dB advantage for a directional antenna that had 3.0 dB higher gain (measured at free space), and only 2.2 dB gain difference for a higher gain antenna (whose free space gain advantage would be 5.0 dB). All antennas were omni-directional in azimuth, the gain difference was achieved by different elevation patterns. All those measurements (that were done with narrow band systems) discouraged the use of directional antennas at the mobile. Reference [4] goes as far as stating that "an omni-directional antenna must be used" (-at the mobile terminal).

It has been generally accepted that the received

signal is a sum of a local mean (that 'slowly' changes in reference to location) and a 'fast' changing component due to multi-path
(for example [1, 4, 8]). The multi-path components arrive with random phase (uniformly distributed) and their relative amplitudes have Gaussian distribution. Having many components justify the normal distribution, at least in the limit. Field tests of narrow band systems in a macro-cellular environment agree with those models. Recently, several propagation models for the micro-cellular environment were proposed. In reference [16] a LOS model based on six rays is proposed. In reference [17] a multi-ray model is proposed for both LOS and out of LOS conditions. The models try to estimate the average levels of the received power at the mobile end, but there was no attempt to analyze individual rays.

3. CONTRIBUTION

In this research I present a model that concentrates on the distribution of individual rays in a "regular" urban micro-cellular environment. I show that the waves arrive at the mobile terminal from distinct directions. Most of the times the energy is carried by a "dominant" ray at any given location. The direction from which that "dominant" ray arrives varies as the mobile terminal changes its location. I propose a method for DOA estimation. The results of the DOA algorithm are the (maximum likelihood) estimator of the DOA and a quality criterion. The quality criterion can be used to characterize the multi-path environment. A high quality means that we can assume (with a high level of confidence) that the signal arrives from a distinct direction. In that case it would be advantageous to use a directional antenna, and point it towards the estimated DOA. When the DOA estimate is "poor" it is due to strong multi-path, in which case the best strategy is to use an omni-directional antenna.

The idea is to look at the mobile antenna as a

"spatial filter". The proposed strategy is to estimate the DOA and the characterize the environment. Based on that estimate the best antenna will be used. The antenna is the "matched spatial filter". The proposed system cannot be worse than an omni-directional antenna, currently used for the mobile terminal.

This adaptive strategy is new. The suggestion to use a directional antenna on the mobile terminal is contrary to the common belief, that was based on earlier research of narrow band systems in a cellular environment. The simulation and the field test results suggest that using this adaptive strategy, one could get the full potential for improvement using a directional antenna at the mobile PCS terminal in a micro-cellular urban environment.

4. SIMULATION OF THE PROPAGATION IN URBAN ENVIRONMENT

4.1 Basic Propagation Model

The propagation characteristics in "regular" urban environment are determined by the fact that rays are reflected from the road surface, and bounce off the walls of the buildings on both sides of the road. The basic two ray model ("Propagation over Flat Earth " [3,4,6 16,17]) is described in figure 1. The details are repeated here for completeness. The free space field intensity for the direct ray is given by:

$$E_0 = k/d_1 \qquad (4.1)$$

The field intensity of the ground reflected ray is given by:

$$E_r = R(\phi)\ k/(d_2+d_3)e^{j\Delta} \qquad (4.2)$$

where

$R(\phi)$ is the reflection coefficient,

ϕ is the angle between the ground and the reflected ray, and

$\triangle$ is the phase difference between the two rays.

The phase difference can be approximated by the following expression:

$$\triangle = 4\, h_b h_m / \lambda d \qquad (4.3),$$

if $d > 5\, h_b h_m$ [3].

For vertical polarization the reflection coefficient is:

$$R(\phi) = \frac{e_o \sin\phi - \sqrt{e_o - \cos^2\phi}}{e_o \sin\phi + \sqrt{e_o - \cos^2\phi}} \qquad (4.4.1),$$

$$e_0 = e - j60\sigma\lambda \qquad (4.4.2).$$

The dielectric constant e is typically 15 for the

road surface, and σ is the conductivity of the ground (expressed in mhos per meter). We have used $\sigma = 7$ as per reference [17].

The 40 dB per decade dependance is a special case when we assume that the reflection coefficient is -1.0, and that the distance d is much greater than the difference between the mobile and the base antenna heights .

4.2 Multi - Ray Model

In an urban environment the streets usually maintain regular geometry (figure 2). The received signal comprises of the direct ray (and its correspondent ground reflected ray), and a multitude of rays that bounce off the walls of the buildings on both sides of the street. The amplitude of those rays depends on their incident angle (in reference to the side -wall) and the distance they traveled from the source. The reflection coefficient may be close to 1.0, but is always smaller than 1.0. Thus, the "higher order" bounces will be further attenuated, because of many more reflections,

and because of the extra distance those rays travel to the receiver. The presence of these extra rays creates the "fading" observed in field measurements. To develop the model, it was assumed that the reflected rays are dominant over the diffracted rays. That is certainly the case in the main street when LOS conditions prevail, and also true for the first 300 m after turning into the side street. It would be logical to expect that most of the energy is carried by several dominant rays.

Figure 3 describes the streets geometry, and identifys the geometrical parameters that are used to develop the model. Once the mobile turn into the "side street", a sharp drop in signal level has been observed [17,18]. The reflection coefficient in the side street depends on the incident angle in the side street. The power of each individual ray obeys the "free space" square law attenuation:

$$P_r = P_t \, (\lambda/4\pi)^2 \, R^2 / D^2 \qquad (4.5) \quad ,$$

and

$$R = R^n(\gamma) \, R^m(\delta) \qquad (4.6) \quad ,$$

where:

γ is the incidence angle in the main street (LOS),

δ is the incidence angle in the side street,

n is the number of reflections in the main street,

m is the number of reflections in the side street,

D is the path length,

P_t is the transmitted power, and

P_r is the received power.

The total power received by the mobile (with an omni-directional antenna) is:

$$P_r=\sum_{i=1}^{n}(\lambda/4\pi)^2(R_i/D_i)^2P_t+\sum_{i=1}^{n}\sum_{j=1}^{n}(\lambda/4\pi)^2(R_iR_j/D_iD_j)^2\cos(\Delta_i-\Delta_j)P_t, \quad (4.7)$$

where:

n is the number of rays reaching the mobile, and

$(\Delta_i-\Delta_j)$ is the phase difference between ray i and ay j.

For simplicity, only rays that pass through point A in

figure 4 are summed. There are number of rays that could pass through to the side street (see figure 5), therefore we multiply that ray by a density function [17]:

$$\alpha_i = \frac{\alpha_{2i} - \alpha_{1i}}{\pi} \qquad (4.8) \quad .$$

Figure 6 shows the relative power versus distance as measured in Manhattan [17], the data agrees with the model. Similar results were reported in [11].

The first expression in (4.7) represents the average value of the power in the side street. Each component of the 'sum' expression represents a ray that propagates into the side street.

The second expression is the "fading" component that is typical of a multipath environment. This model explains why less fading is observed when the mobile uses a directional antenna [1,2,5,16]. If its beam width is narrower than the spatial spread of the various rays,

fewer rays will produce the "fading". This is true for both macro-cellular and micro-cellular environment.

However, the gain advantage that we can expect depends on the rays spatial distribution, the directional antenna beamwidth, and the direction towards which it is pointing. If the directional antenna will block several rays (that may carry a significant fraction of the total energy) the total signal power may be inferior to using an omnidirectional antenna. That happens when the signal arrives from a specific direction while the directional antenna points to another direction. Lee [4,9] has shown that for a uniform distribution of the directions of the rays there is no theoretical advantage to a directional antenna. The problem of the distribution of the directions from which the rays arrive has not been investigated before. This problem will be discussed in the next section.

4.3 Distribution of DOA for Multi-Ray

Based on the same assumptions discussed earlier a

model describing individual rays was developed. Figure 7 is based on the theoretical model. It shows the variation of power associated with each ray as a function of its distance from the transmitter. In this simulation d1 = 300 m (the transmitter is located 300 m from the corner of the side street), the same conditions as Figure 6. Figure 6 shows the average power measured in a field trial in Manhattan [17]. Comparing figures 6 and 7 it seems that most of the energy is carried by few rays, and some times most of it may be carried by a single ray. Figure 8 is a similar presentation, but d1 is shorter (50 m). It illustrates better that in any given location in the main street the "direct" ray is significant, but as you turn into the side street, that ray attenuates sharply. For most of the locations shown in the side street there is a dominant ray.

In the main street it is logical to expect that the signal would come from the direction of the transmitter for the following reasoning:

The "direct" ray is always present, and for short distances it is the dominant ray (see figure 7 and 8). Only at larger distances the relative power of the other rays becomes significant.

Our model assumes perfect symmetry, thus, pairs of rays arrive from both sides of the 'main' street. Those rays travel the same distance, and have bounced the same number of "bounces". As a result they have equal amplitude, and same phase. Under those conditions, the vectorial sum of each pair is an equivalent signal that comes from the transmitter. The interference of those rays with the direct rays (and with themselves) will produce changes in amplitude. However, in an ideal street (infinite reflecting walls from both sides of the street), the DOA in the main street should remain the same.

The distribution of the DOAs for the multi rays in the side street is not symmetrical, even with an ideal model. Computer simulation were run to produce typical distributions of relative power and directions for various configurations. Figures 9.1 through 9.4 show the DOA and relative power distribution for the individual rays in the side street, when the transmitter is at a fixed distance of 50 m (d1 = 50 m) from the corner. The set of figures 10.1 through 10.10 shows the distribution for d1 = 100 m.

5. Direction Of Arrival (DOA) Estimate

This chapter starts with an introduction to the basic concepts of the interferometer that can be used to estimate the DOA. I will explain the relation between the accuracy of the DOA estimate, and the measurement time constraints. I will show that this technique may be used for a cellular application.

5.1 Basic Interferometer

A basic phase interferometer is diagramed in figure 11a, and 11b. The simplest implementation (11a) consists of a linear array of two antennas, a dual channel receiver, a phase detector, and a processor. If a signal arrives from the boresight, it will reach both antennas at the same exact time. Signals arriving from other directions will arrive at each antenna at different times. Figure 12 shows the phase relation between the angle of arrival, the antennas separation, and the frequency. From the geometry:

$$\phi_1 = k \sin(\alpha) \qquad (5.1.1)$$

$$k = 2\pi d/\lambda \qquad (5.1.2)$$

where:

ϕ_1 is the phase difference between the signal arriving at antenna # 1 and the signal at antenna # 2,

α is the angle of arrival,

d is the separation of the antennas (also called "base-line"), and

λ is the wavelength.

The processor translates the phase information into a DOA estimate by computing the inverse sine function (see 5.1.1). The baseline has to be shorter than half a wavelength, for an un - ambiguous estimate. In practice the baseline is kept bellow 0.3 - 0.4 wavelength, to provide additional noise margin. The accuracy of that

estimate can be computed by differentiating (5.1.1) with respect to ϕ_1. For a given phase measurement error (σ_{ϕ_1}), the larger the baseline the better accuracy of the DOA estimate is achieved. The accuracy is also a function of the DOA itself. Best accuracy is for signals arriving from the boresight, as indicated by:

$$\sigma_\alpha = \sigma\phi_1/k \cos(\alpha) \qquad (5.1.3)$$

where

σ_α is the estimated DOA error, and
σ_{ϕ_1} is the phase measurement error.

The sensitivity of the DOA estimate to measurement phase error is proportional to $1/\cos(\alpha)$. Clearly, for signals arriving 90 degrees from the boresight, there are singular points . In many practical tracking applications the general direction is usually known, and the interferometer is used to provide just the "final" tracking correction. For those applications the array can be pointed towards that general direction, and a single baseline interferometer will work fine. If there is no prior knowledge of the general direction from

which the signal may arrive, those singular points present a problem. A better arrangement is to have another orthogonal baseline, and measure the phase relations between the second pair as well. A switching mechanism allows measurement of either pair of antennas using only one set of a two channel receiver. The phase relations for the second pair is:

$$\phi_2 = k \cos(\alpha) \qquad (5.1.4).$$

The processor estimates the DOA by computing:

$$\hat{\alpha} = tg^{-1}(\phi_1 / \phi_2) \qquad (5.1.5).$$

5.2 DOA Accuracy

Using a DOA estimator as a mean to point the (mobile) directional antenna towards the best receiving direction does not require a highly accurate system. However, one may want the DOA estimation error to be smaller than the directional antenna beam - width. Following is a discussion of the interferometer accuracy.

The DOA accuracy is a function of the phase

measurement errors σ_{ϕ_1}, and σ_{ϕ_2}. The exact dependence is found by differentiating (5.1.5) with respect to ϕ_1, and ϕ_2. Assuming that the phase errors in each measurement are independent Gaussian random processes, with zero mean and same variance - σ_ϕ, the DOA error is given by:

$$\sigma_\alpha = \sigma_\phi / k \qquad (5.1.6) \ .$$

The sensitivity of the dual (orthogonal) baseline interferometer to phase errors is not dependent on the exact DOA. No prior knowledge about the DOA is required to properly estimate the DOA. Once an estimated DOA is computed, one can compute the phase errors by substituting $\hat{\alpha}$ instead of α in (5.1.10, and in (5.1.4). Now we have:

$$\Delta\phi_1 = \phi_1 - k \sin(\hat{\alpha}) \qquad (5.1.7),$$

$$\Delta\phi_2 = \phi_2 - k \cos(\hat{\alpha}) \qquad (5.1.8),$$

and

$$\Delta\phi = \sqrt{\Delta\phi_1^2 + \Delta\phi_2^2} \qquad (5.1.9).$$

The calculated phase error ($\Delta\phi$) can serve as a

quality criterion. For an ideal system (no noise, interference, or any other measurement error) the estimated DOA will be exactly the same as the actual DOA, and the quality criterion ($\Delta\phi$) will be zero. In practice the DOA estimate will be close to the actual DOA, but the "quality criterion" will not be zero. Intuitively, we expect it to be larger, as system errors are large. In the next paragraph several causes of errors are discussed. It is important to remember that the DOA estimate will be inaccurate, and the quality criterion will be greater than zero, whenever phase errors are present, regardless of their cause.

5.3 Quality Criterion

In the previous paragraph, I introduced the concept of a "quality criterion" whose value will be large whenever phase errors are associated with the DOA estimate. Practical systems are subject to several sources of measurement errors, for example: difference phase response of antenna elements, slight differences in cables' lengths, final resolution of the phase

processor, etc. It is possible to measure all the fixed errors, and to store them in the memory. Only the measurement errors resulting from sources external to the system can not be calibrated. The prime contributors to the (un - controlled) phase errors are:

a. Thermal Noise
b. Co - Channel Interference
c. Multi - Path.

First I will derive the relation between the thermal phase error to the SNR. For generality of the discussion I will use the Cramer Rau bound [19,20] given by:

$$\mathrm{Var}\,(\hat{\theta}) \;>\; 1/\,E\{\,[\,\partial \ln P\,(\phi/\theta)/\,\partial\theta\,]^2\,\} \qquad (5.3.1)$$

where:

$\hat{\theta}$ is the (un-biased) estimator of θ from measurements of ϕ .

The probability of measuring the phase angle ϕ given an actual phase θ , has been investigated by Rice [21], and has been repeated in many references, for example [20]. Rice has shown that for a noisy channel the

conditional probability density function is:

(5.3.2)

$$P_{(\phi/\theta)} = e^{-\rho}/2\pi + 1/2\frac{\sqrt{\rho}}{\sqrt{\pi}}\cos(\theta-\phi)\exp[-\rho\sin(\theta-\phi)]^2\{1+\mathrm{erf}[\sqrt{\rho}\cos(\theta-\phi)]\}$$

where:

ρ is the SNR (not in dB!), and

$$\mathrm{erf}(x) = 2/\sqrt{\pi}\int_0^x e^{-t^2}\,dt \quad .$$

For a high SNR the following approximations will simplify that expression:

a. $e^{-\rho} = 0$

b. $\sin(\theta-\phi) = (\theta-\phi)$

c. $\cos(\theta-\phi) = 1.0$

d. $\mathrm{erf}(\sqrt{\rho}) = 1.0$

$$P_{(\phi/\theta)} = \sqrt{\frac{\rho}{\pi}}\, e^{-\frac{(\theta-\phi)^2}{1/\rho}} \qquad (5.3.3)\,.$$

The conditional probability density function $P_{(\phi/\theta)}$ is the normal density function. The average of ϕ is

zero, and its variance is $1/\mathcal{S}$. For a high SNR:

$$\ln P(\phi/\theta) = K - [1/(1/\mathcal{S})](\theta - \phi)^{-2}$$

$$\frac{\partial^2 \ln P(\phi/\theta)}{\partial^2 \theta^2} = -2\mathcal{S} \qquad (5.3.4).$$

Substituting (5.3.4) in (5.3.2),

$$\mathrm{Var}(\phi) = 1/2\mathcal{S} \qquad (5.3.5).$$

So far we have found the relation between the variance of the phase estimate and the SNR of the single noisy channel. In our case the two channels are noisy. Assuming that there is a similar SNR in each antenna, and that the noise is uncorrelated, the variance of the phase measurement between two noisy channels is given by:

$$\mathrm{var}(\phi) = 1/\mathcal{S} \quad \text{(radians)} \quad , \text{ or}$$

$$\sigma_\phi = 1/\mathcal{S} \qquad (5.3.6).$$

Figure 13 illustrates the inaccuracy of the DOA

estimate as a function of SNR for a single phase measurement in each baseline. The graph is plotted for an interferometer whose baseline is half a wavelength long.

Other sources of (un - calibrated) phase errors will increase the phase measurement variance, and as a result also the DOA error (as per 5.1.6). It is important to note that a CDMA system is less sensitive to narrow band interference. Its impact will be reduced by the "processing gain". After de-spreading, the narrow band interferer will slightly increase the thermal noise level. Also, the effect of other CDMA co-users will be an increase of the noise level after de-spreading, that is where the phase estimate will be done. However, the multipath will always be present in CDMA PCS signal in urban environment. Reflections that will arrive with time separation greater than one chip rate will be de-spread, like other co-users that have a different PN code. The net effect of such reflections will be an additional increase of the effective noise level. That is a typical case for a B-CDMA system. However, multi-path that arrives within a shorter time difference will not be resolved, and has the potential of further

degrading the DOA estimate.

Ideally, one would like to have a "sophisticated rays separator" that can resolve the received signal into individual rays and can find for each ray its relative amplitude, time (or phase) relation, and its DOA. Having such knowledge one may be able to built a "sophisticated rake receiver" that picks each ray with its best directional antenna, compensates for its time (or phase) delay, and combines all rays coherently.

For simplicity, I assume that the DOA estimator will "duel" only on the dominant ray that carries most of the total energy, and will estimate the best direction of that ray. For that system we need to estimate the DOA accuracy due to thermal noise and other sources of errors.

Thermal noise is always present, and calculation of its effect will provide the lower bound of the DOA accuracy. To estimate the effect of the thermal noise and the other sources of interference, one has to calculate the effective S/(N+I), and substitute that value in (5.3.6). Since all the noise and interference sources are un-correlated to each other, the effective

N+I variance will be the sum of the individual variance contributions of each N or I source:

$$\sigma^2_{N+I} = \sum_{n=1,2..} (\sigma^2_n) \qquad (5.3.7) .$$

In a strong multi-path environment, the interference from the multi-path will cause a substantial increase in the N+I level. That increase will degrade the DOA estimate, but at the same time will cause the "quality criterion" to be higher as well. That high value of the "quality criterion" will be an indication for the adaptive system that it operates in a strong "multi-path" environment, in which there is no preference to either direction. In other words, there is no single ray that arrives from a distinct direction, carrying with it most of the total energy. Since we have stated earlier that we seek to optimize the behavior of a "simple" system (one that can estimate the DOA only for single ray), then the best strategy will be to use an omni - directional antenna. The omni-directional antenna serves as the optimum (or matched) "spatial filter" for those conditions.

5.4 Timing Constraints

Equation (5.3.5) gives the relation between the DOA error to the SNR. Figure 13 is a graphical presentation of that relation for a specific half a wavelength baseline, assuming a single phase measurement for each baseline. Current analog FM systems operate at a minimum SNR of 18 dB, that corresponds to less than 5 degrees of DOA error. New digital system are designed to operate at lower SNR. Minimum Eb/No requirement for a BPSK signal (with coding rate of 2.0) is 7.5 dB. That translates to SNR of 8.0 dB (assuming a digital carrier that occupies the whole BW). For an 8.0 dB SNR, the DOA error may be as high as 20 degrees, due to thermal noise alone. As stated earlier, the degradation of the DOA accuracy due to thermal noise is only a lower bound. Other imperfections may further degrade the DOA estimate by a factor of two or more. That may be considered a bit too high even for a simple system that has only four directional antennas (each covering a 90 degrees sector).

A common technique for improving the DOA accuracy is by averaging consecutive phase measurements for each baseline. It is well known that averaging a set of n

independent measurement will reduce the variance of the mean by a factor of - $\sqrt{n}$. For the measurements to be un -correlated, one has to take samples that are least one over the signal bandwidth apart. The trade off is between accuracy and time. There is no need to reduce the variance due to thermal noise too much, because (5.3.7) shows that other system errors will become dominant. Since the purpose of the DOA estimate is to provide only a 'coarse' direction, it seems that a good design will try to reduce the thermal noise contribution to a fifth of the directional antenna beam width. Typical numbers are 10 to 15 degrees of DOA error. Using the example above it implies that averaging four consecutive phase measurements will ensure DOA error that is less than 10 degrees.

The total time required to complete a DOA measurement is:

$$T_{total} = N_b N_n (1/f_s) \qquad (5.4.1)$$

where:

N_b is the number of baselines,

N_n is the number of samples for each baseline, and

f_s is the symbol rate.

For the digital example above let us assume a symbol rate of 10 kbps, and four phase samples for each of the two base-lines. Total time required for DOA estimate is 0.8 milli-seconds. A car traveling at 30 km per hour will travel a distance of only 1.4 cm during that time. That distance is less than a tenth of a wavelength at the 1.9 Ghz PCS band. At 850 Mhz that car would not travel even 1/20 wavelength. It seems that timing will not limit the validity of the DOA approach for pedestrians, or even for a moving car in urban areas.

6. FIELD TESTS

6.1 Measurement Set Up

Two sets of measurements were performed. The first set of field tests was done at Flushing, Queens. The second set of tests took place in Port Washington, Long Island (LI). The measurement set up, and the test methodology was similar for all tests. The differences in the set up used in the different locations will be explained as appropriate. The measurement set up consisted of a Direct Sequence (DS) spread spectrum transmitter and a separate mobile receiver (figure 14a for Queens, and 14b for LI). The transmitter maximum power was 37 dBm. In Queens I used a vertical monopol with a circular ground plan as the transmit antenna. It was mounted on top of a 6 m mast. the antenna has an omni-directional pattern in azimuth, its gain is 0.0 dBi (zero elevation -looking at the horizon). In the second location I used a directional antenna (in azimuth) whose gain is approximately 9.0 dBi. It transmits to a wide sector of 180 degrees.

The receiving equipment and the computer were installed in a van. The receive antenna was mounted on top of the roof of the van. Two types of receive

antennas were used: an omni-directional antenna (similar to the transmit antenna used in Queens), and an 8.0 dBi log-periodic antenna. The latter has a beam width of 90 degrees (in azimuth).

For the first field trial, I used a receiver that measured the signal strength before de-spreading. The receiver consisted of a log amplifier, whose output was buffered, and an analog to digital (A/D) converter. A photo-interrupter wheel triggered the sampling. Data was captured every centimeter, and stored in the computer for future analysis. the test set up is depicted in figure 14a.

In the second field trial the receiver measured the signal strength after de - spreading. The computer triggered the A/D that sampled 15,000 data points within 10 seconds. We drove the van at a constant speed of 10 miles per hour (mph).

6.2 Measurement Procedure

The methodology used for the tests was the same in all the field trials. In each location we first took a set of data with the omni antenna being the receive

antenna. That set of data served as a reference. The next step was a repetition of the measurements but with the directional antenna connected to the receiver. Consecutive runs were made with the directional antenna, where all conditions were same except for the antenna pointing to different direction in each run. The direction of the antenna (relative to the vehicle) was changed in 45 degrees increments. We recorded the direction of the antenna for each run. For reference, 0 degrees was marked when the antenna pointed towards the back of the vehicle.

In the first field trial, measurement were taken in Flushing, NY. The transmitter was stationary at the corner of 34th street and 90th street. We drove the van in the main street, and then turned into a side street. One set of measurement was taken in 34th street and 91st street, in the other set we drove in 34th street into 92nd street. Streets layout is a grid, typical of urban environment. The buildings were three stories high (92 street), six stories high (91st street), or a mix of four to six stories height (34th street). Figure 15 shows typical buildings in those streets.

Measurements were taken during the day, with normal traffic conditions. We drove the van at average

speed of 15 -20 mph. To check repeatability, we repeated several measurements with same conditions, but traffic conditions and the exact path on the same road varied.

The second field trial took place in Port Washington, LI. The transmitter was stationary at 107 New Haven Avenue. we drove the van in five different locations. One location was on New Haven avenue (- the 'main street' in the terminology used in this work). The other locations were on side streets that branch off the 'main' street. The Port Washington locations represent a sub-urban environment. The streets are perpendicular, but the houses are spaced more gracefully. The environment is not homogeneous: some houses are smaller, others are two or even three stories high. Several houses have a brick front, while others are constructed of wood only and have a vinyl siding. There were differences from street to street (see figures 15g - 15l). All measurements were taken during the day, under normal (but very light) traffic conditions. The measurements were taken while driving the van at a nearly constant speed of 10 mph.

6.3 Measurement Results

The measurement results are presented as sets of graphical data. The first set is the data from 91nd street. It contain runs with the omni antenna, and eight additional runs with the directional antenna, rotated 45 degrees for consecutive runs. All the results are presented graphically in figures 16a through 16h. Likewise, the second set is similar measurements for 92st street, presented in figures 18a through 18k. During the field test one file was inadvertently purged (-270 degrees). In each street we repeated at least one run with the directional antenna, and several runs with the omni. All the repeatability measurements are presented as the third set of data, figures 17a through 17d. For example: a run marked 405 degrees is a second run for the directional antenna pointing at (405 -360) = 45 degrees.

The results of the second field trial are presented in a similar way. The data from the first location (Cypres St.) is presented in the set of figures 19a through 19i. The data from the second location

(Birchwwod St.) is presented in the set of figures marked 20a etc. Those streets are 'side streets', where data that was taken in the 'main street' (New Haven Ave.), is presented as figures marked 21a and up. the last set represents LOS conditions.

7. Analysis of the Field Test Results

7.1 Gain Improvement for the Directional Antenna

I compared the difference between the relative power of each of the directional antennas (at a given location) to the power received with the omni antenna (at the same location). That difference vector is called - the "differential gain". I computed the average and the mean value for (the differential gain in) each direction. The results from 91st street are shown in Table 7.1:

Direction	Average (dB)	Median(dB)
0	5.5	5.0
45	4.5	4.0
90	-1.0	0.0
135	-5.7	-5.0
180	-6.8	-6.0
225	-5.5	-5.0
270	-0.8	0.0
315	4.0	4.0
BEST	7.3	7.0

Table 7.1: Differential Gain Advantage (Omni -Direct.)
91 St.

The last row (named BEST) represents the gain of an adaptive system that would have used the same directional antenna, pointing to the "best" direction at each location. This concept is explained in details in the next paragraph.

In this dissertation I prove that the directions

from which the signal arrives are not distributed uniformly across all possible directions in the urban micro -cellular environment. As a first step I built a simulator to predict the DOA for the signal in a 'regular' urban environment. The simulation results suggest that at each location there is a 'dominant' ray that arrives from a specific direction. That ray is called 'dominant' since it carries most of the total energy. Only in the side street there are isolated points at which two rays have similar power level. As you walk further away from those transitional regions, one of those rays becomes dominant (see figures 7 and 8).

Analyzing the field test data, we observe that if the differential gain for all directions was similar, it would have implied that the signals were coming from all possible directions. On the other hand, if we are able to demonstrate a clear advantage to a specific direction (at least for significant sections of the travel path), it proves that the signals indeed come from a distinct direction. As you walk in the side street, you may find out a change of that direction. However, there is a significant impact of pointing the directional antenna either to the "best" or to another less favorable

direction. The results of the field test agree with the predictions of the simulation.

Since the DOA changes as the receiver moves from one location to another, we can not select any fixed direction that will always remain superior to the others. In fact, the simulation proved the need to have an adaptive system that can estimate the direction in real time. I did not have such a system in the field, but sorting the computer files off-line, I created a new file that has the "strongest" received power from all the eight directions that were recorded in each location. By this technique, I created an adaptive "artificial antenna" that would have always looked at the "best" direction. Comparing the "best" antenna to the omni, gives the potential gain improvement for an adaptive system that uses the same directional antenna under those conditions. That data is presented in the raw marked "best" in table 7.1.

Review of the table 7.1 data indicates that there is a potential for gain improvement higher than the 2.0 or 3.0 dB that were reported in [1,2,4,] for earlier measurements (done using narrow band signals). It seems

that the measured gain improvement is significantly higher, but trying to estimate it requires similar analysis of the data from 92nd street, and review of the results of the second field trial. Table 7.2 presents the data from 92nd street:

Direction	Average (dB)	Median(dB)
0	5.7	5.0
45	3.8	3.5
90	-0.5	0.0
135	-2.7	-3.0
180	-3.6	-4.0
225	-2.2	-2.8
270	1.3	1.0
315	4.8	4.0
BEST	6.6	6.2

Table 7.2: Differential Gain Advantage (Omni -Direct.)
92 St.

The data from the second set of measurement is similar to the first set. It shows a significant improvement, but the differential gain is about 0.7 dB

lower. To verify that the data is stable I repeated the analysis for the first set, but changed the reference file to another data that was taken with the omni antenna, on the same path at a different run. The results changed by 0.1 dB only. For example the differential gain for the "best" antenna in table 7.1 changed from 7.3 dB to 7.2 dB.

Before presenting the data from the second field trial, there is another observation to be made from the previously described field data. By creating the artificial adaptive best antenna, we have created a selection vector. That vector tells us which antenna (or which direction) has been selected in each location. Presentation of that vector as a histogram gives an important insight to the data. Again, if the signals were arriving from all possible directions, one would expect to see equal distribution of the selections among all possible selections. Obviously, that is not the case which proves to verify the validity of our model.

Figure 22a presents the 'selection histogram' for 91st street. It seems to indicate that at least in the main street, the signal arrives from the "obvious" direction of the transmitter. Note that 160 times out of 281 samples the best direction was the '0' degrees

direction. The '0' corresponds to the antenna looking at the back of the vehicle, driving a way from the transmitter into the side-street. Note, that the (measured) distance to the corner is approximately 150 meter. The simulator predicts that immediately after turning to the side street, the distribution of the "DOA"s is still in the general direction of the corner. Only as you step further into the side street, the directions begin to present the reflections from the side walls.

Once you are in the side street, the selected (- the best) direction is no longer the '0'. Indeed, it is divided (almost symmetrically) between the 45, and 315 degrees. The best direction in the side street is that which "picks -up" the rays bouncing off the walls. Note that in our model the DOAs are distributed mostly between +/-90 degrees (left or right walls). The directional antenna beam width is almost 90 degrees. It makes sense that the best direction is that which picks the ray bounced from one side of the street, and combines it with other rays coming from the same walls, or closer to the '0' degrees. That is why the +/- 45 degrees was selected so many times. Indeed the number of times that either +45 or - 45 degrees were selected is

approximately 120, exactly the travel length in the side street.

The '0' degrees is not selected in the side street, because, our 90 degrees beam width directional antenna would pick up the reflections from the two walls. Since the reflections from opposing walls are out of phase, they will cancel each other! This set of measurements was taken with a simple receiver that did not have a de-spread circuitry. In reality, the building surfaces are not an ideal reflector, so we did not observe a "true" zero power for the antenna pointing at '0', but that direction is not the "best" in the side street.

The results from the second field trial are summarized in table 7.3. Measurements were taken in five locations. Locations # 1 and # 3 represent data taken in the side streets. Location # 5 is the 'main street, where LOS conditions exist. Locations # 2 and # 4 are in McKean street that is parallel to the 'main street'. That location was up a small hill, that shadowed the transmitter. Locations # 2 and # 4 represent a typical sub - urban environment in which the propagation mechanism is governed by reflections from various scattered objects, as opposed to the 'regular' city structure of the other locations.

Location	Mean (dB)	Median (dB)
1	7.7	7.0
2	3.6	4.5
3	7.5	6.5
4	3.7	4.0
5	5.4	5.0

Table 7.3: Differential Gain for Port Washington data

The results agree with the first set of data. It seems that the potential for gain improvement with an adaptive directional antenna is between 6.5 dB to 7.0 dB for a highly directional antenna that has an 8 dB gain advantage in free space conditions.

7.2 Repeatability of the Results

As explained earlier I repeated several measurements, to verify the repeatability of the data. The four plots in figures 17a through 17d are two pairs of data that was taken in the first trial at different times, with different traffic conditions. The data looks almost identical. To quantify the repeatability, I repeated the "differential" gain analysis and found that it change the results by a fraction of a dB. The data from the second field trial was not as stable. Several factors contributed to that. Firstly, the data was taken in reference to time, which required driving at constant speed. Variations of the speed affected the stability of the data. Also, the de - spread circuitry was locked on a specific ray, but when signal reception was poor (and that happened when the directional antenna was pointing towards the wrong direction), it lost lock. That produced deep fades is some data files.

An obvious observation is that the data from the LOS street (Location # 5) does not have as deep a fade as the side streets data. Note that in that location the best direction was '180', since the van was driving

towards the transmitter. The fade depth for that direction is smaller than the fade of other directions, and that of the omni antenna. Previous researches have observed that directional antenna helps reducing the fades (for example [3, 4, 9, 16]).

8. CONCLUSIONS

A multi - ray model was developed to predict the relative strength and DOA of the rays propagating in a 'regular' urban environment. Field measurements have verified the validity of the model. There is a clear advantage to using a directional antenna at the mobile terminal for a B - CDMA spread spectrum signal at 1.9 Ghz. To be able to realize the full advantage of the directional antenna , one must estimate the DOA. field data proves an improvement of 6.5 to 7.0 dB for an 8.0 dBi directional antenna as compared to a 0.0 dBi omnidirectional antenna. That is contrary to previously reported results (that were based on measurements of narrow band signals in a macro -cellular environment). The directional antenna helps in reducing the fade depth and duration, when it is pointing to the right direction.

The ray distribution model can be used as a design tool to optimize PCS parameters. In a typical urban environment it predicts a time delay spread that can be as low as 50 nano-seconds. For that environment a B-CDMA system may offer an advantage, being able to resolve short delay spreads.

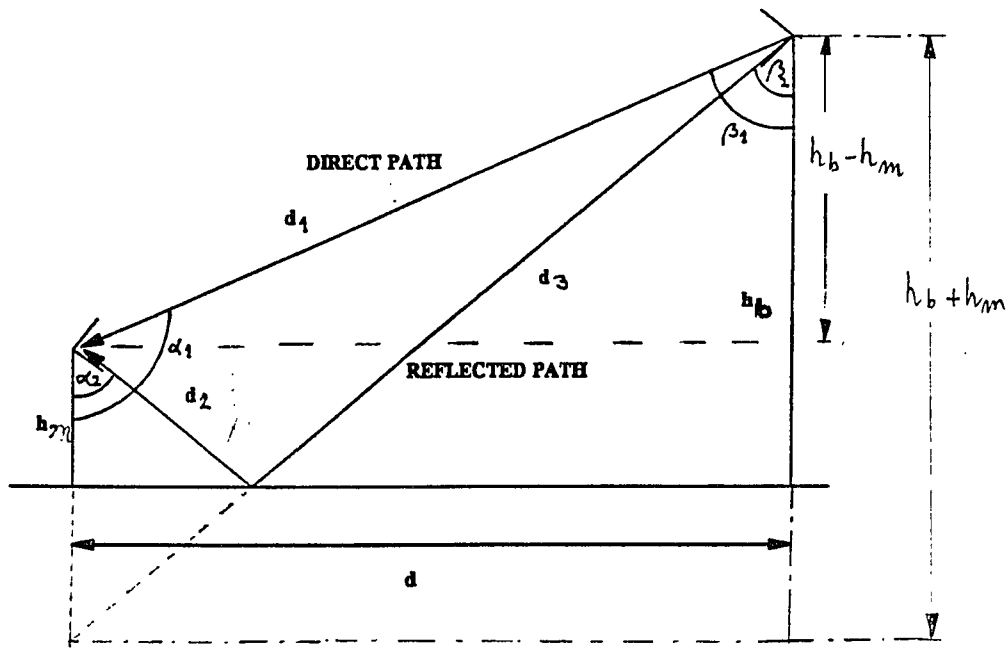

Figure 1 Two-ray propagation

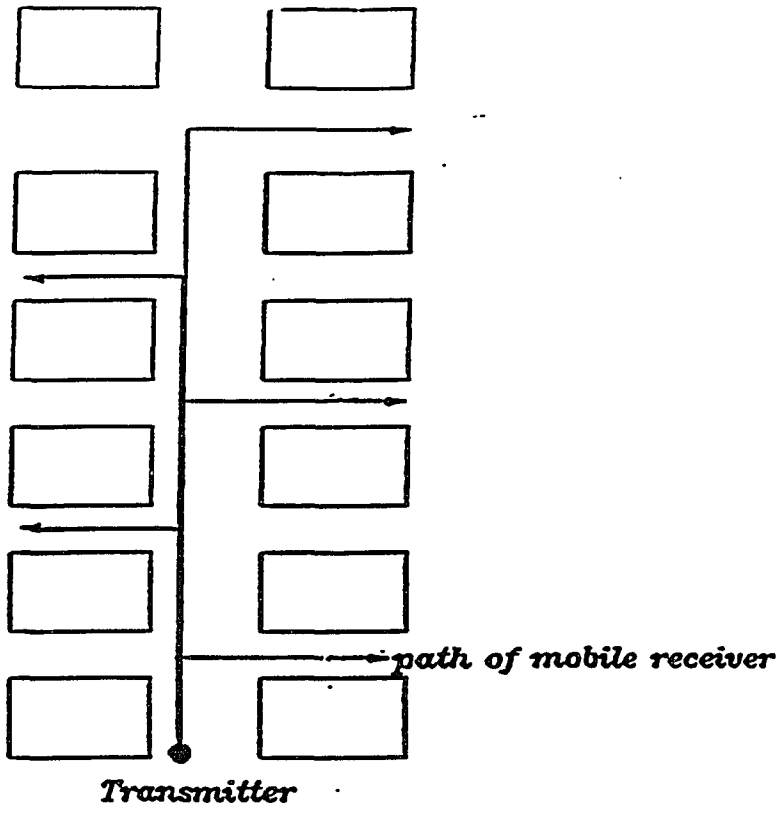

Figure 2 Out-of-sight propagation

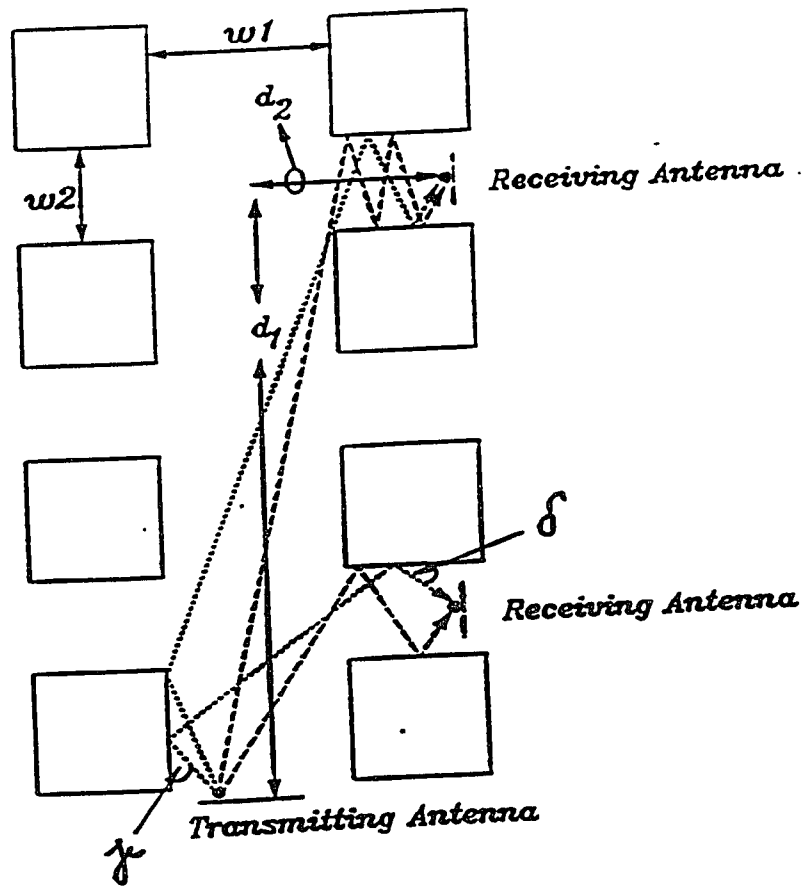

Figure 3 Rays entering out-of-sights streets

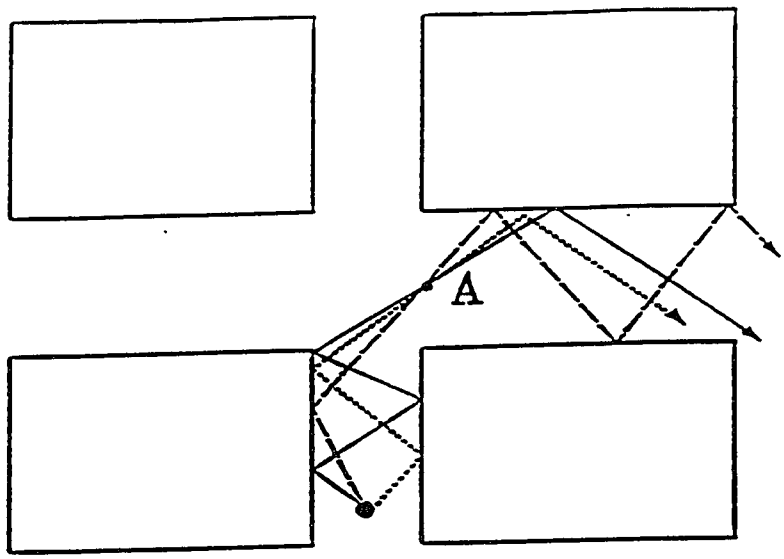

Figure 4 Only the rays passing through Point A are summed

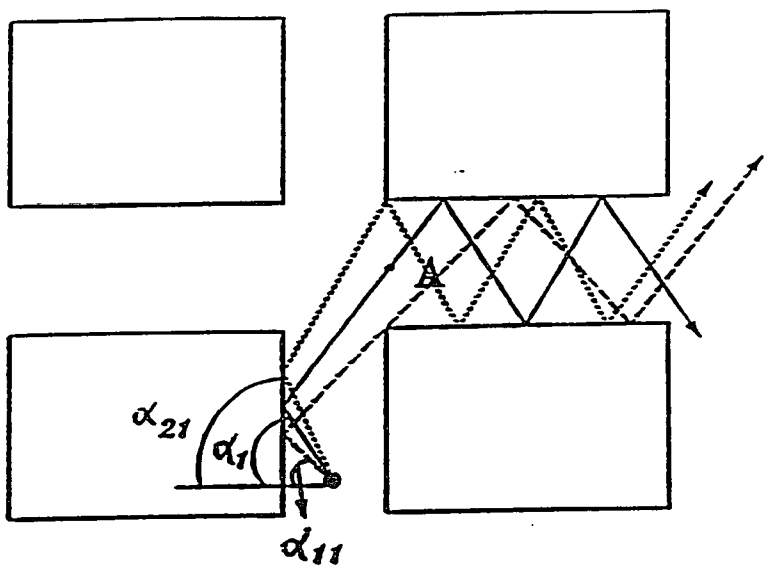

Figure 5 Rays with the minimum angle α_{11} and the maximum angle α_{21} of rays which leave the transmitter and which enter the out-of-sight street

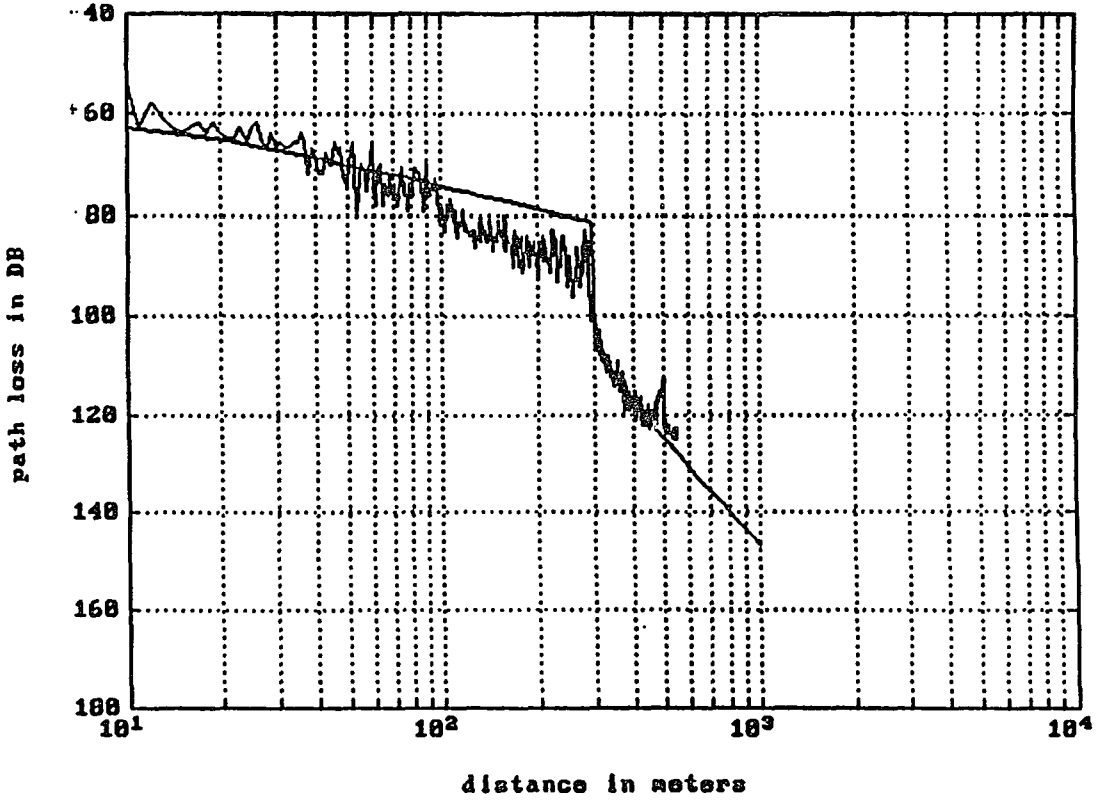

Figure 6 Manhattan, out-of-sight propagation (d_1 =290m, h_b = 6.6m)

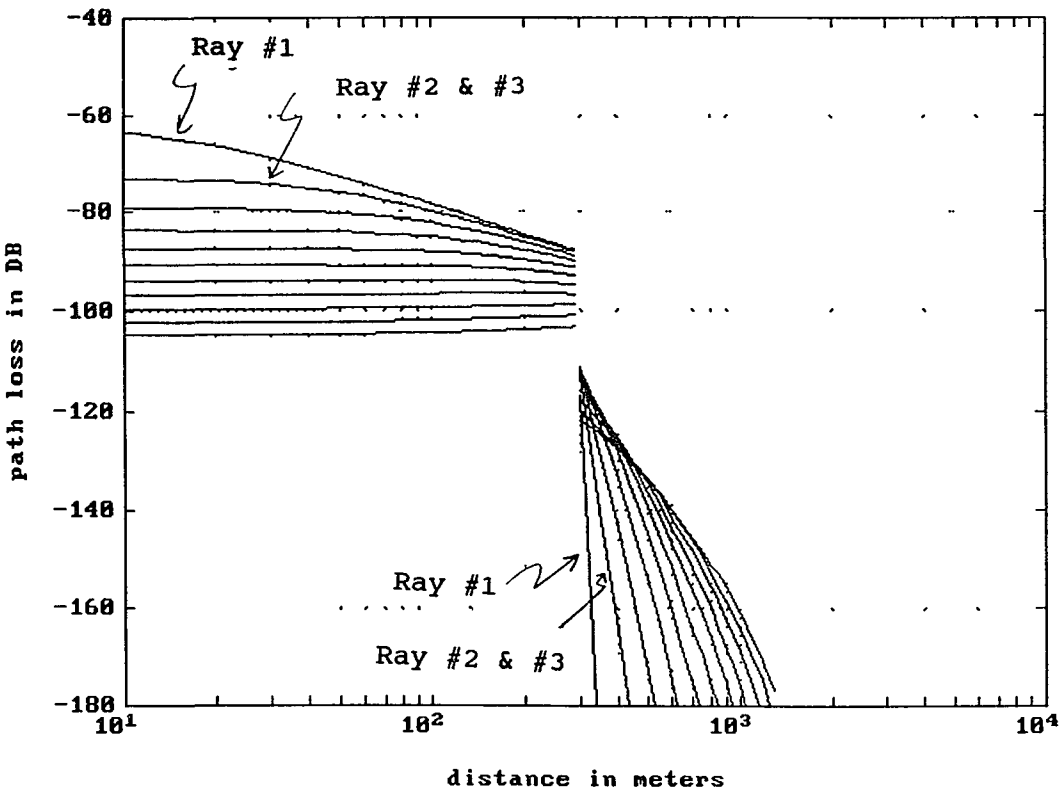

Figure 7 Theoretical Multi - Ray Model

$d_1 = 300$

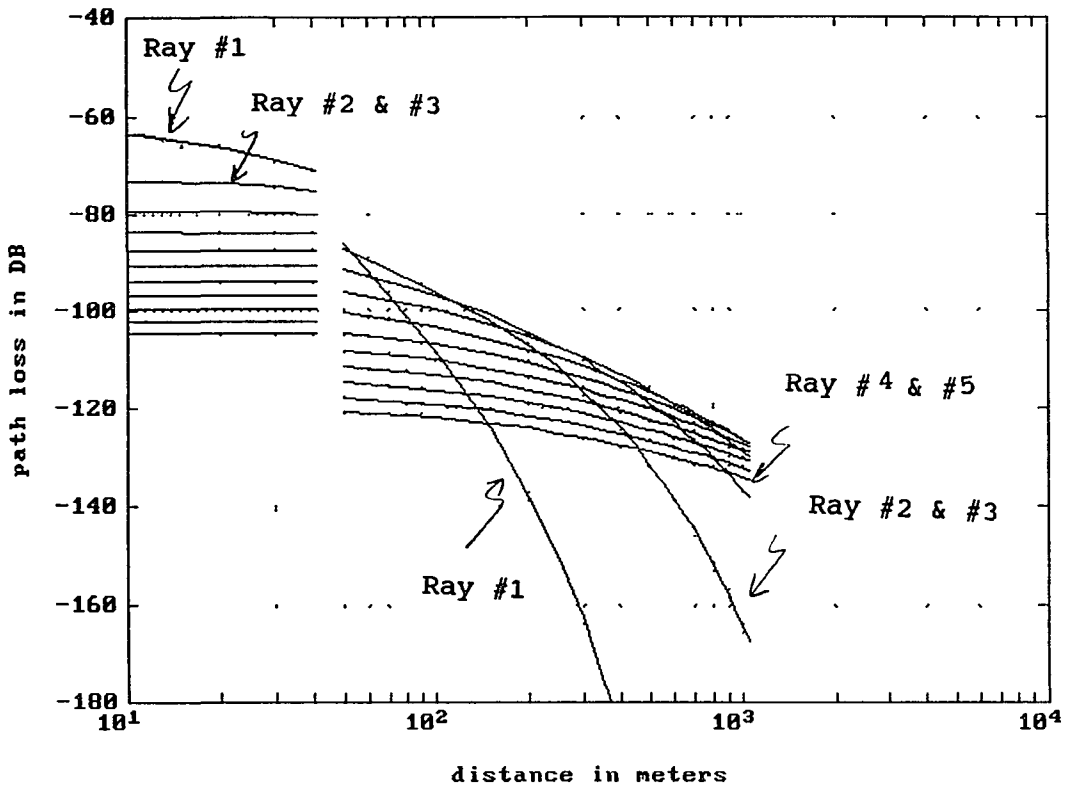

Figure 8 Theoretical Multi - Ray Model

$d_1 = 50$

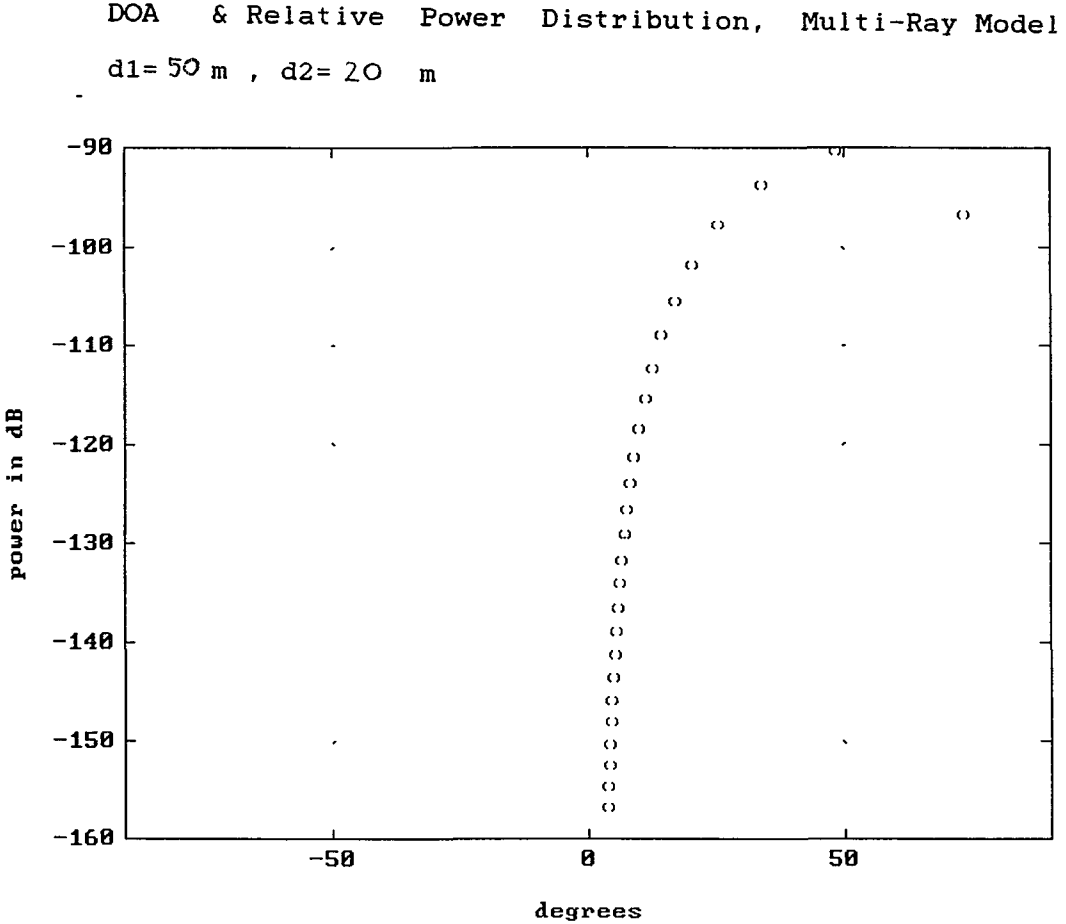
DOA & Relative Power Distribution, Multi-Ray Model
d1= 50 m , d2= 20 m
-90
-100
-110
-120
-130
-140
-150
-160
power in dB
-50
0
50
degrees

Figure 9.1

DOA & Relative Power Distribution, Multi-Ray Model

d1= 50 m , d2= 50 m

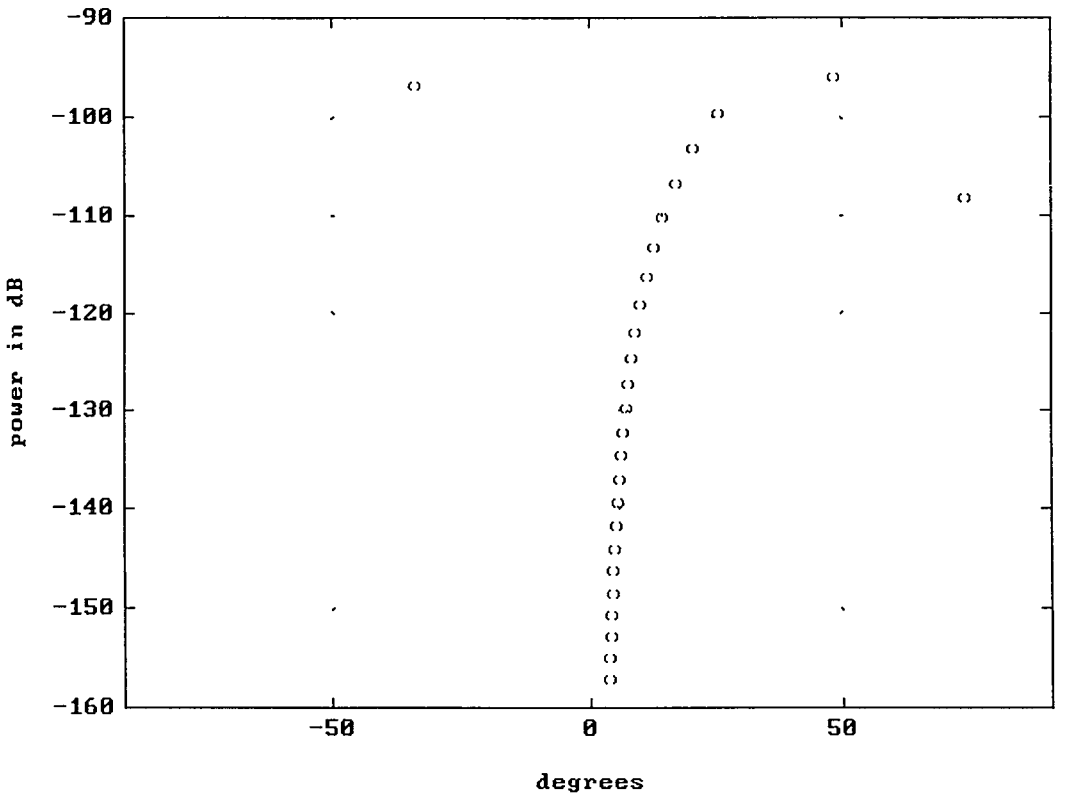

Figure 9.2

DOA & Relative Power Distribution, Multi-Ray Model

d1= 50 m , d2= 100 m

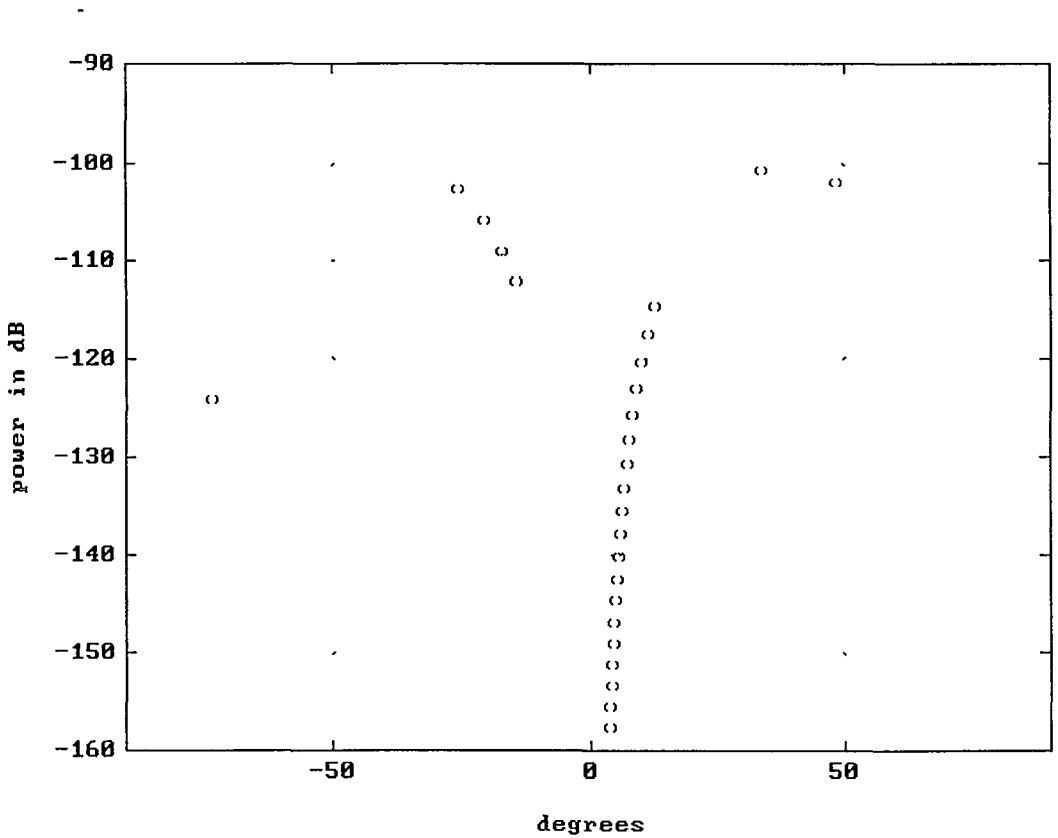

Figure 9.3

DOA & Relative Power Distribution, Multi-Ray Model

d1=50 m , d2=200 m

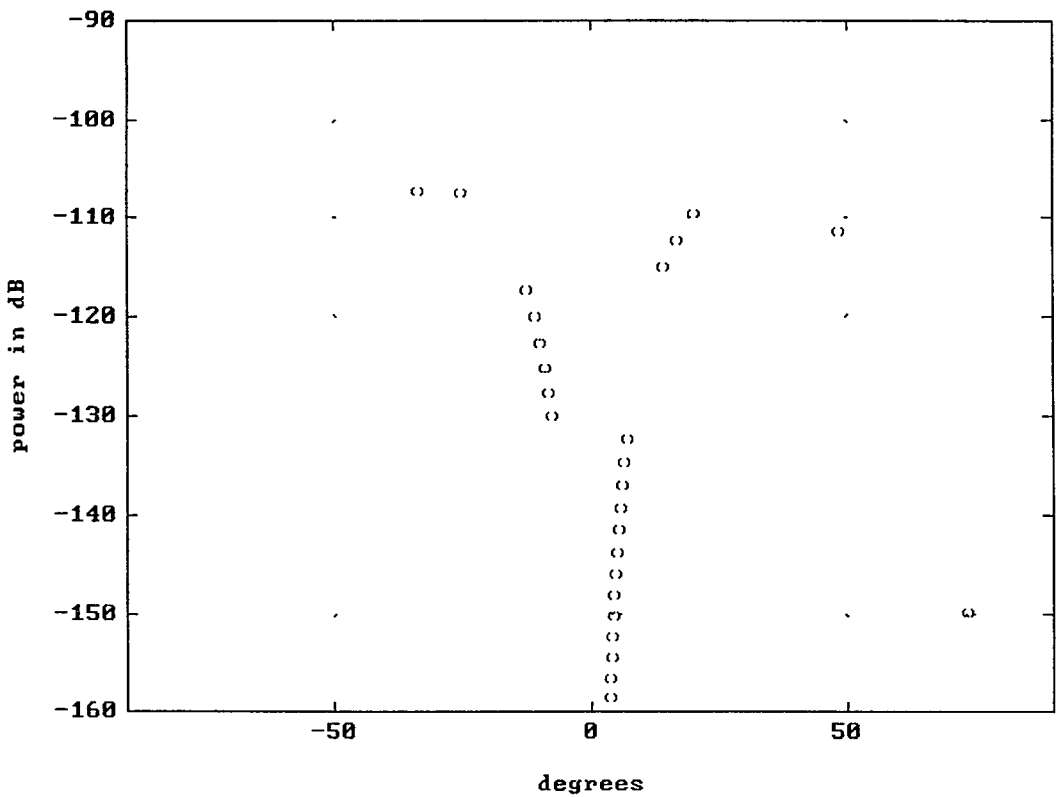

Figure 9.4

DOA & Relative Power Distribution, Multi-Ray Model

d1=100m , d2= 20 m

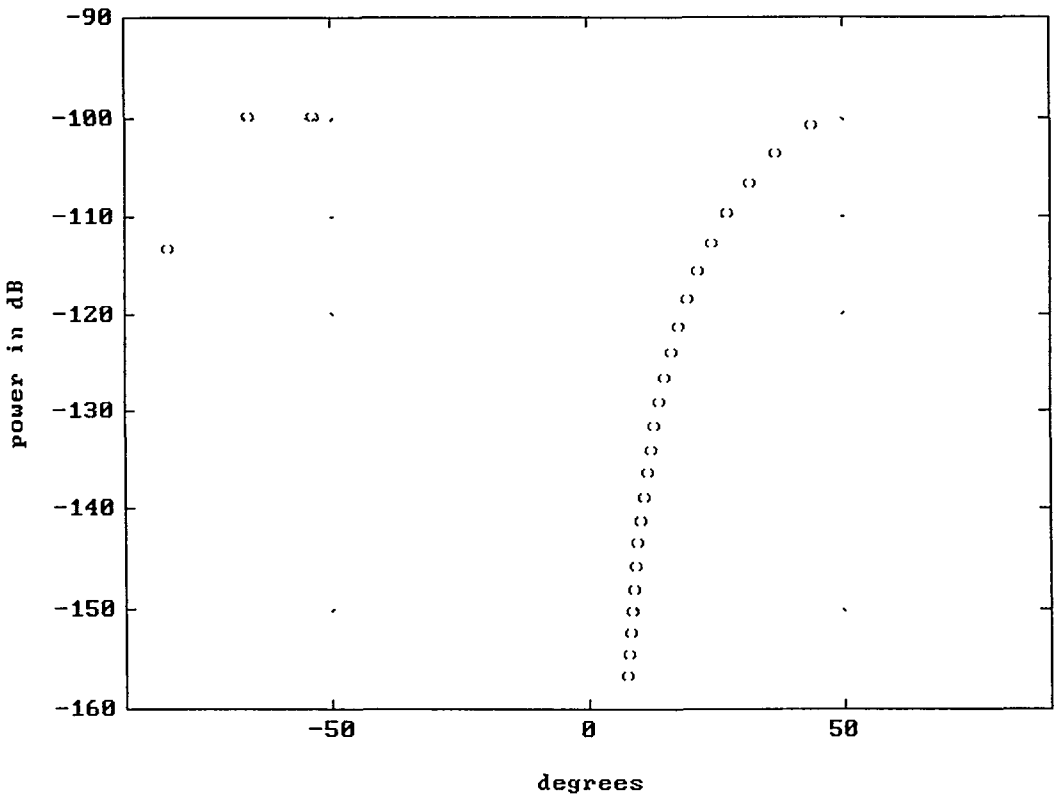

Figure 10.1

DOA & Relative Power Distribution, Multi-Ray Model

d1=100m , d2= 33 m

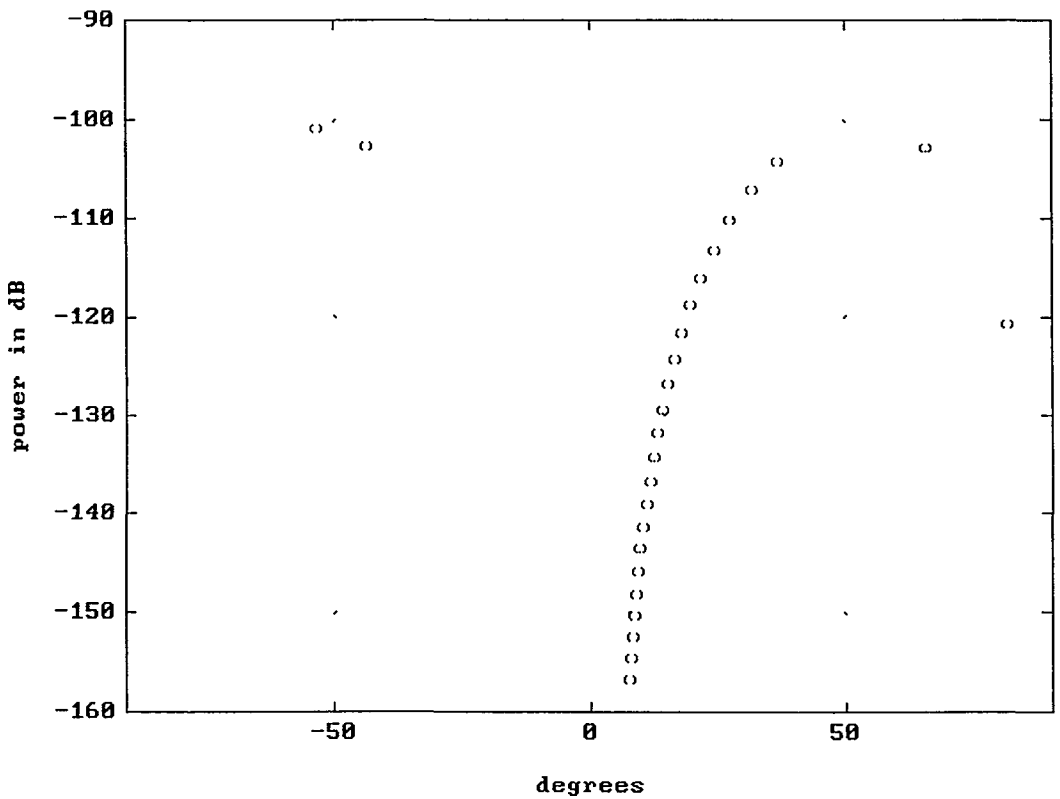

Figure 10.2

DOA & Relative Power Distribution, Multi-Ray Model

d1=100m , d2= 50 m

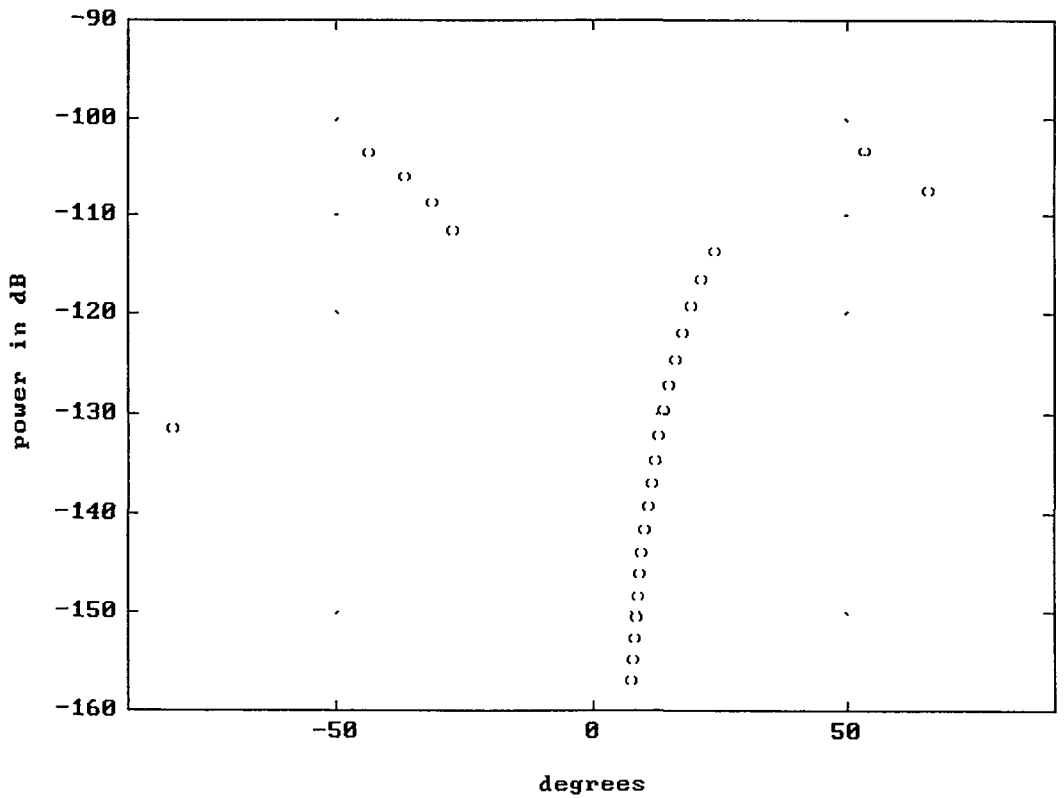

Figure 10.3

DOA & Relative Power Distribution, Multi-Ray Model

d1=100m , d2= 75 m

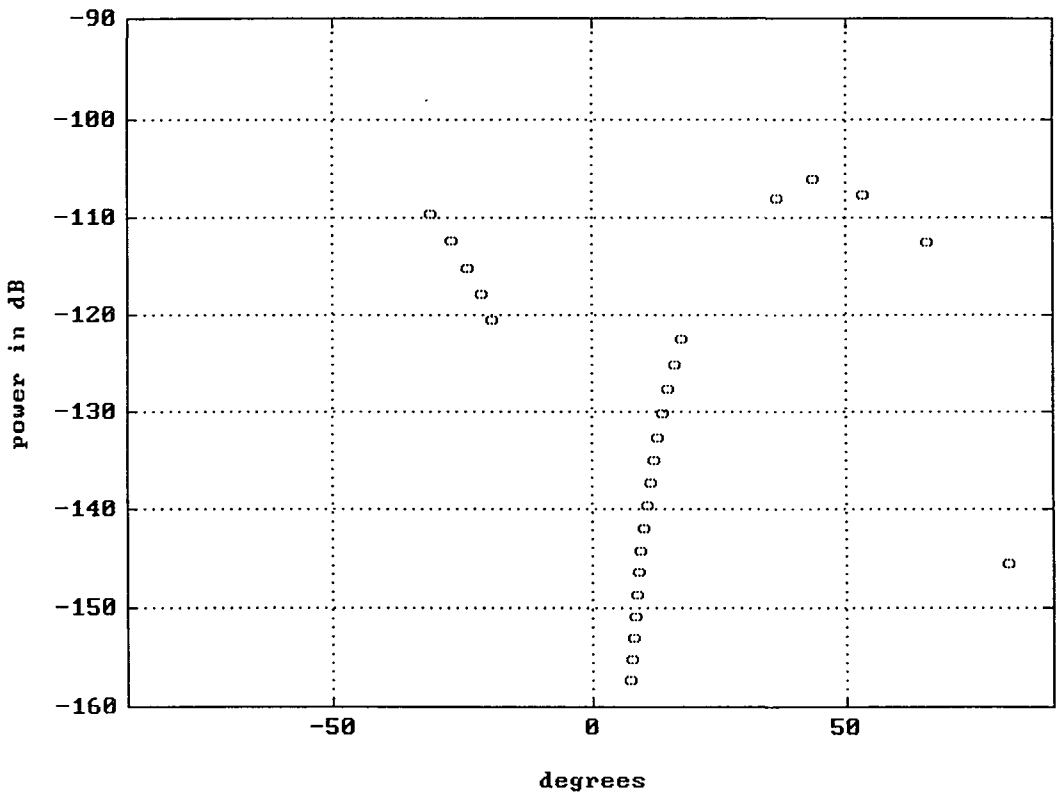

Figure 10.4

DOA & Relative Power Distribution, Multi-Ray Model

d1=100 m , d2= 100 m

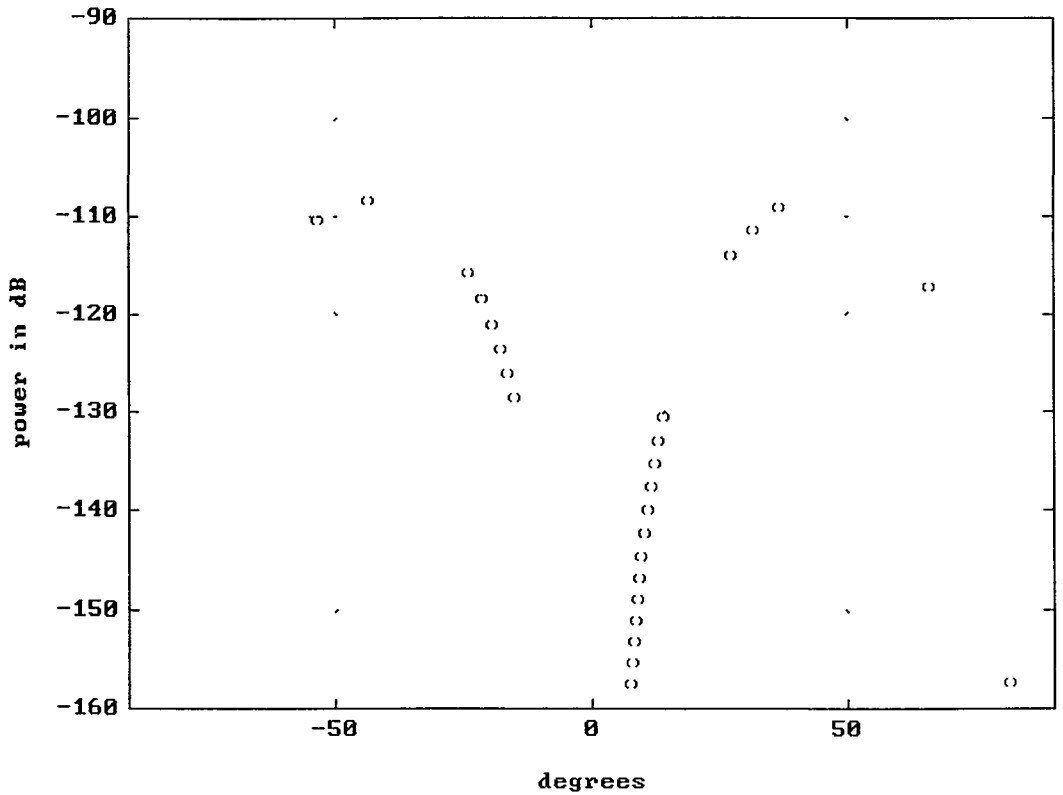

Figure 10.5

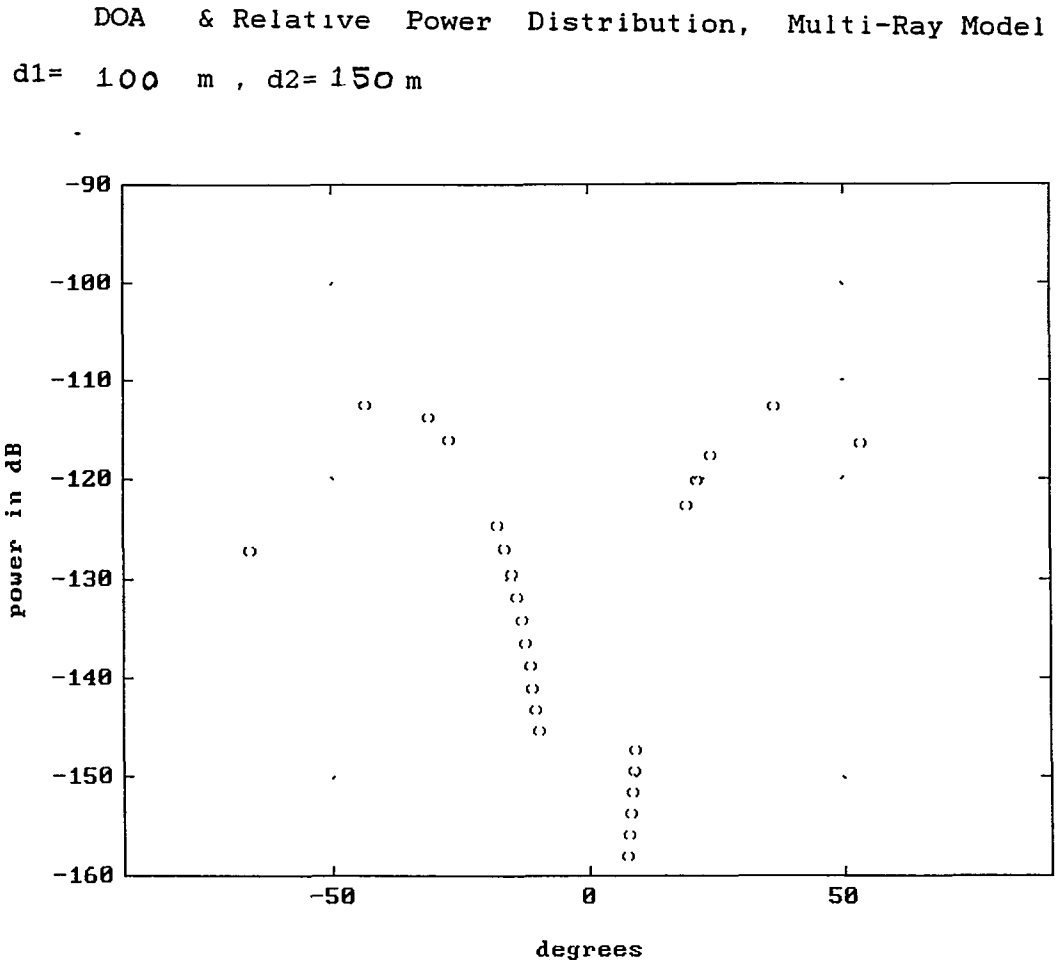
DOA & Relative Power Distribution, Multi-Ray Model
d1= 100 m , d2= 150 m
power in dB
-90
-100
-110
-120
-130
-140
-150
-160
-50
0
50
degrees

Figure 10.6

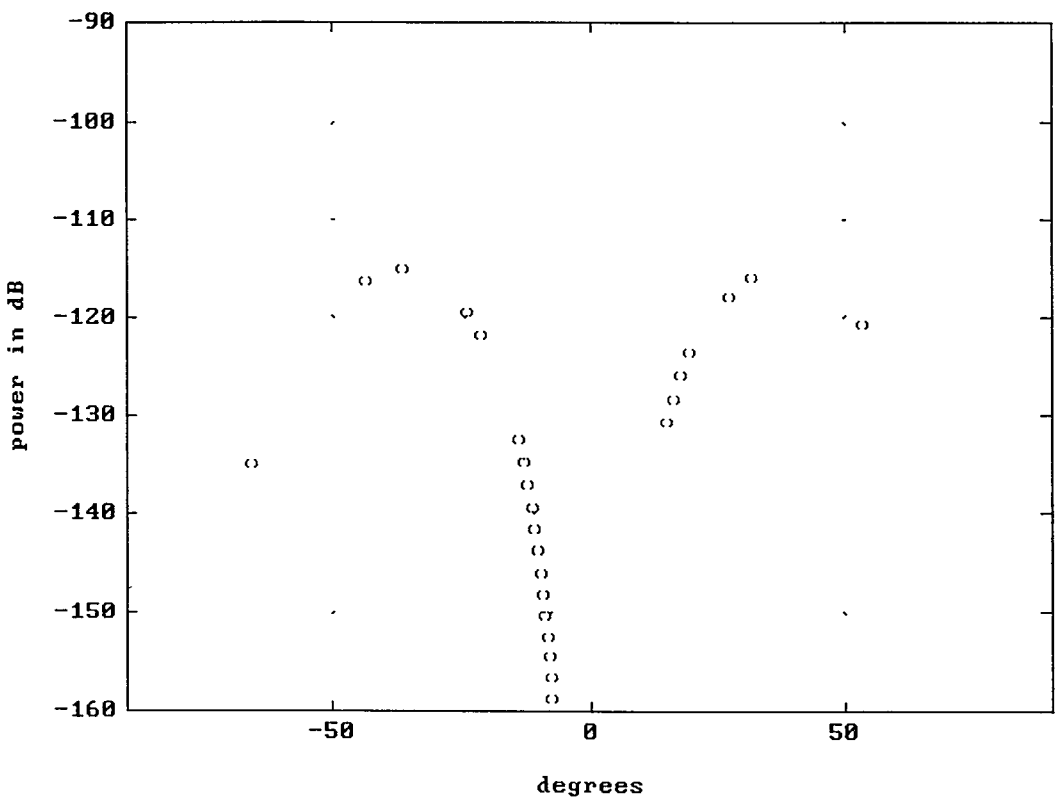
DOA & Relative Power Distribution, Multi-Ray Model
d1= 100 m , d2= 200 m
power in dB
-90
-100
-110
-120
-130
-140
-150
-160
-50
0
50
degrees

Figure 10.7

DOA & Relative Power Distribution, Multi-Ray Model

d1= 100 m , d2= 250 m

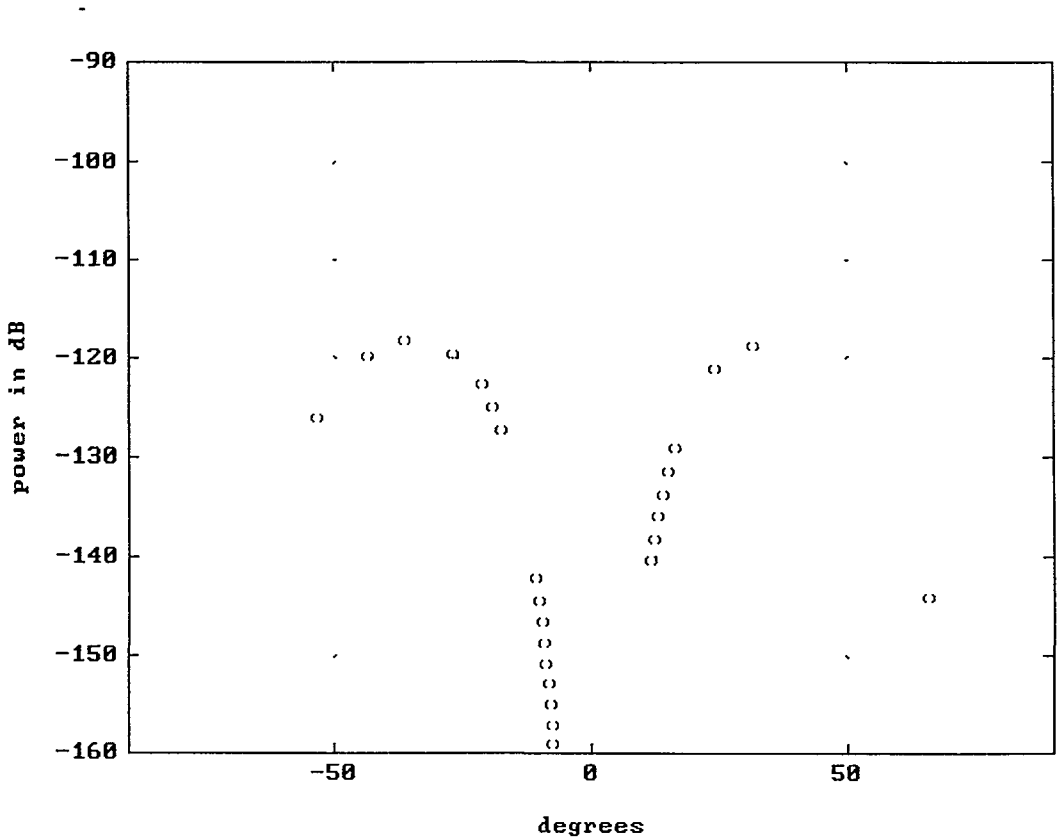

Figure 10.8

DOA & Relative Power Distribution, Multi-Ray Model

d1= 100 m , d2= 300 m

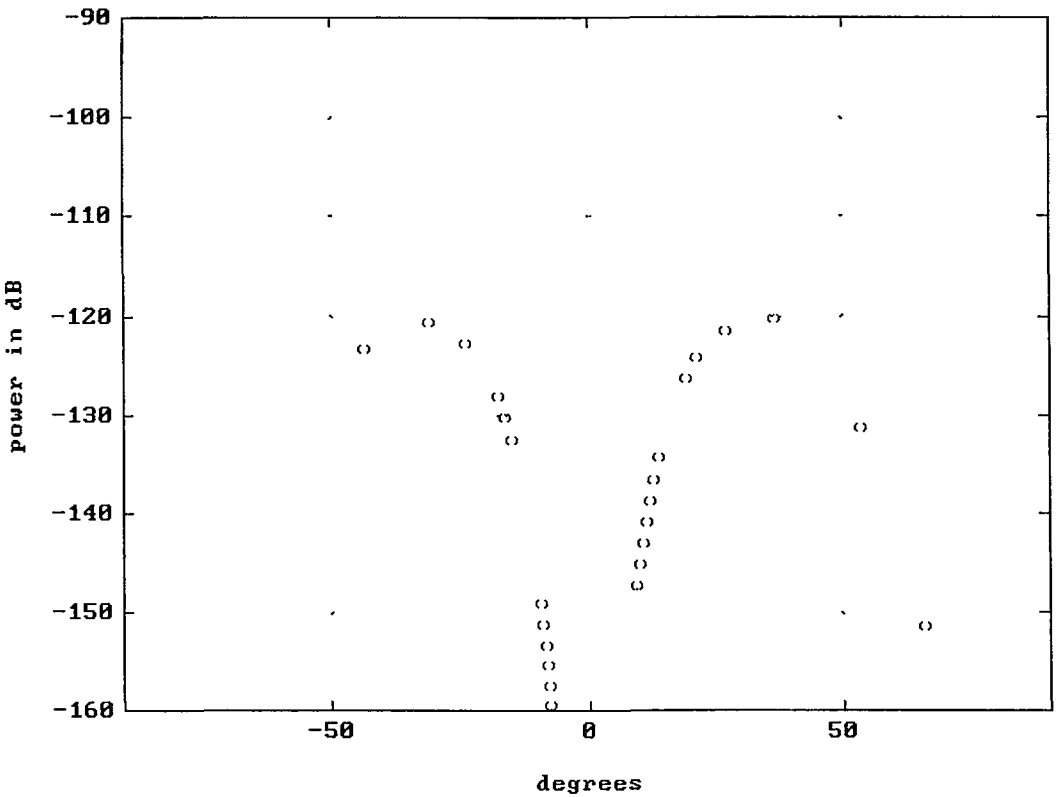

Figure 10.9

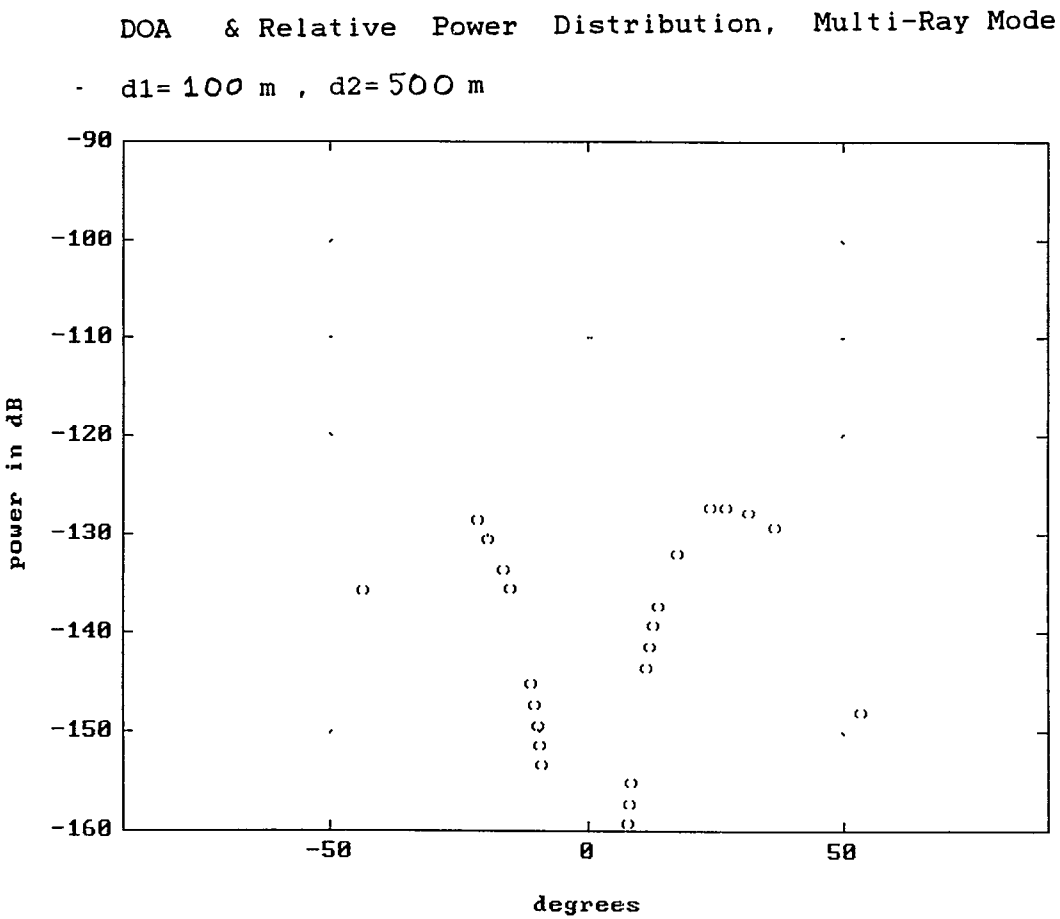
DOA & Relative Power Distribution, Multi-Ray Model
d1= 100 m , d2= 500 m
-90
-100
-110
-120
-130
-140
-150
-160
power in dB
-50
0
50
degrees

Figure 10.10

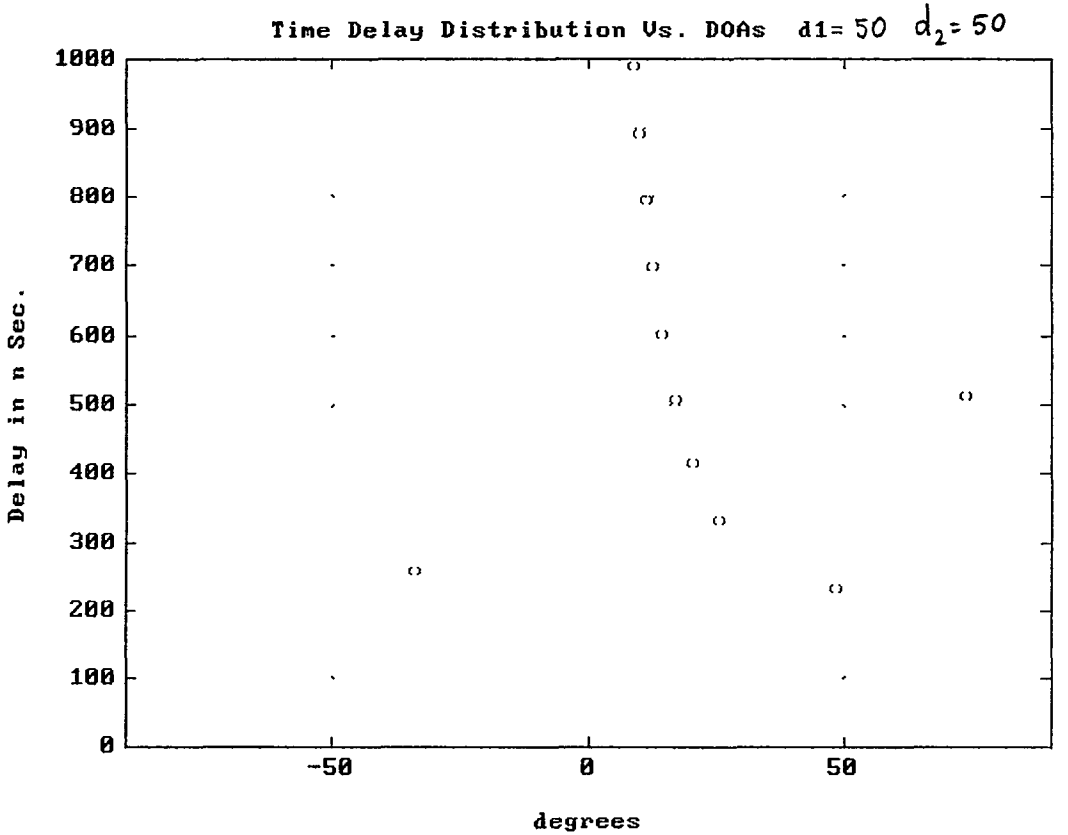
Time Delay Distribution Vs. DOAs d1= 50 d2= 50
1000
900
800
700
600
500
400
300
200
100
0
Delay in n Sec.
-50
0
50
degrees

Figure 10.11

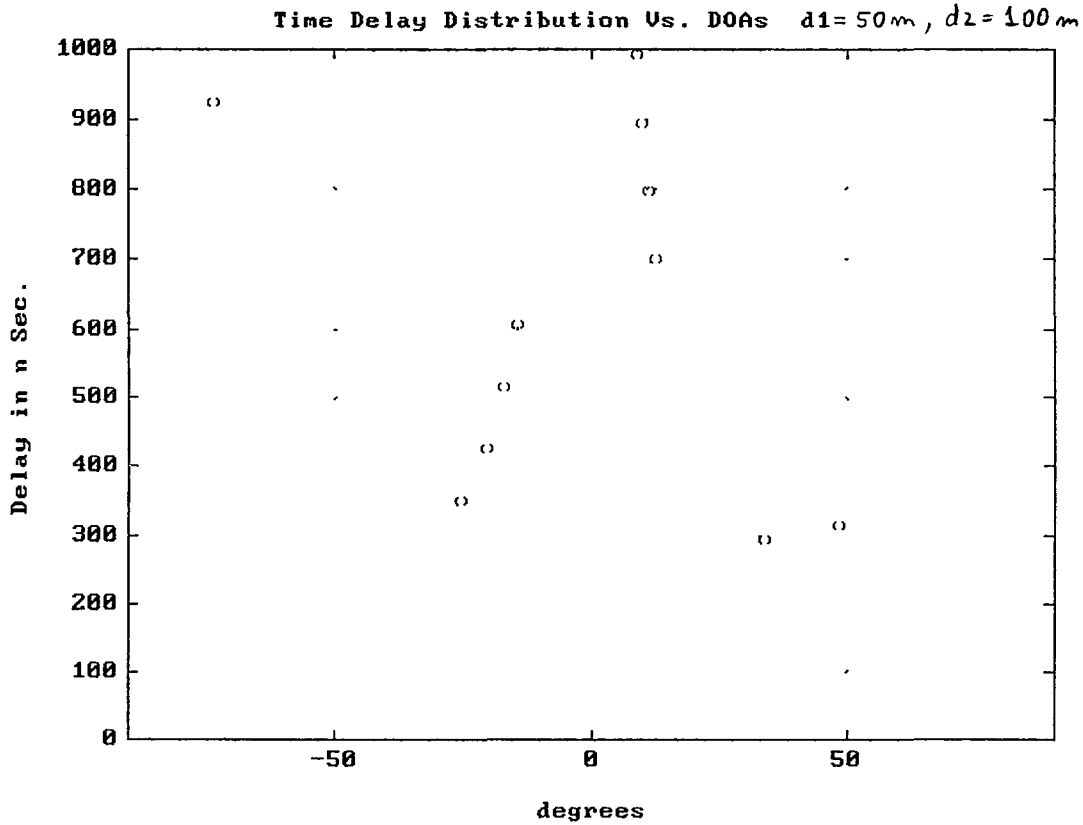
Time Delay Distribution Vs. DOAs d1= 50 m, d2= 100 m
Delay in n Sec.
1000
900
800
700
600
500
400
300
200
100
0
-50
0
50
degrees

Figure 10.12

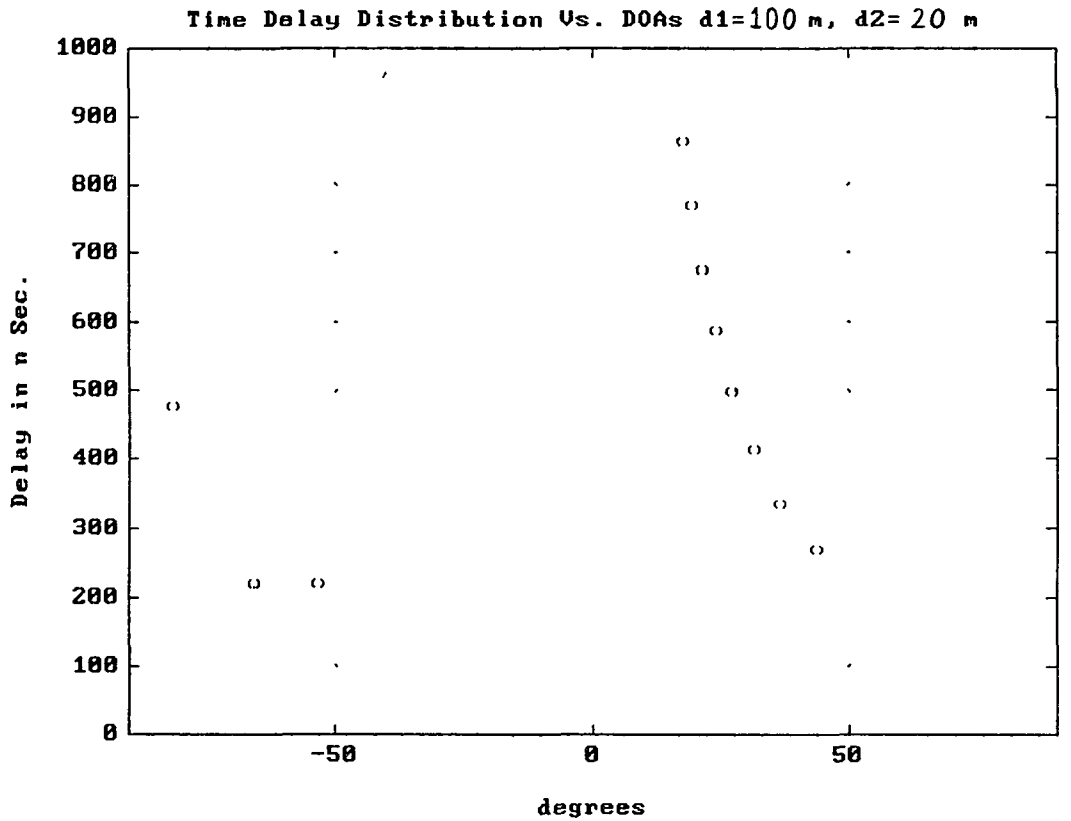
Time Delay Distribution Vs. DOAs d1=100 m, d2= 20 m
1000
900
800
700
600
500
400
300
200
100
0
Delay in n Sec.
-50
0
50
degrees

Figure 10.13

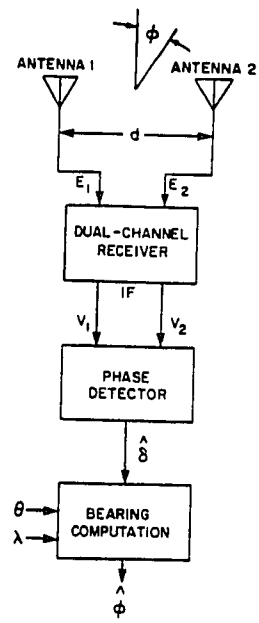

Phase comparison using a single-baseline antenna and a dual-channel receiver.

Figure 11a

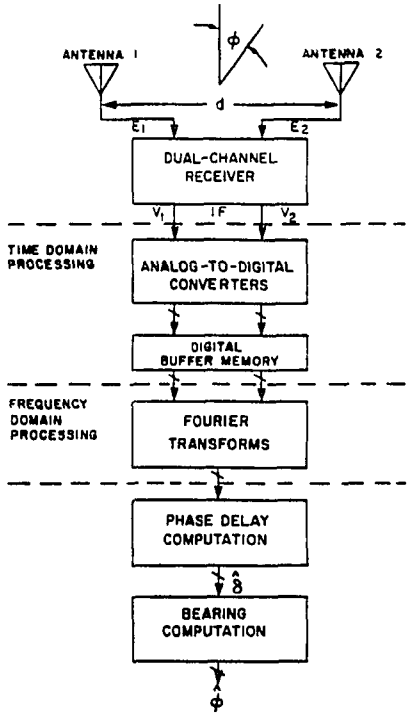

Fourier transform phase comparison DF technique.

Figure 11b

PHASE DIFFERENCE RECEPTION BY TWO ANTENNAS

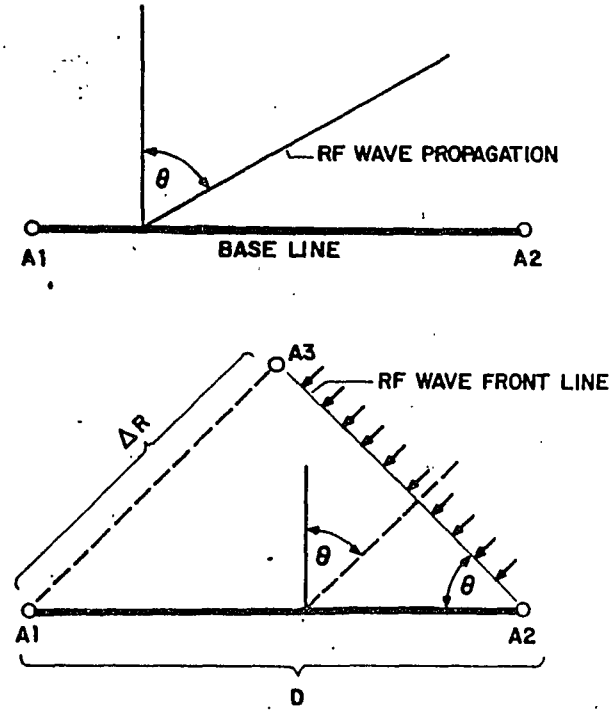

$$\Delta R = D \sin\theta$$

$$\Delta\phi = \frac{2\pi D}{\lambda} \sin\theta$$

$$\therefore \theta = \sin^{-1}\left[\frac{\Delta\phi \cdot \lambda}{2\pi D}\right]$$

Figure 12

plot of estimated azimuth angle of arrival error *versus* SNR for a d/λ value of 0.5

$$\hat{\phi}_\epsilon = \frac{1}{(\pi d/\lambda)\sqrt{\text{SNR}}}$$

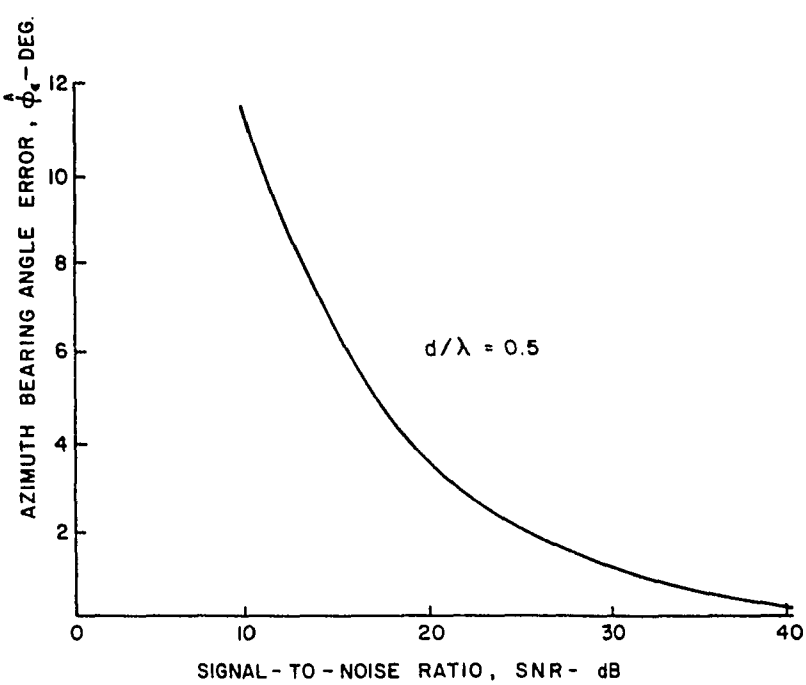

Figure 13 Phase comparison bearing error *versus* SNR.

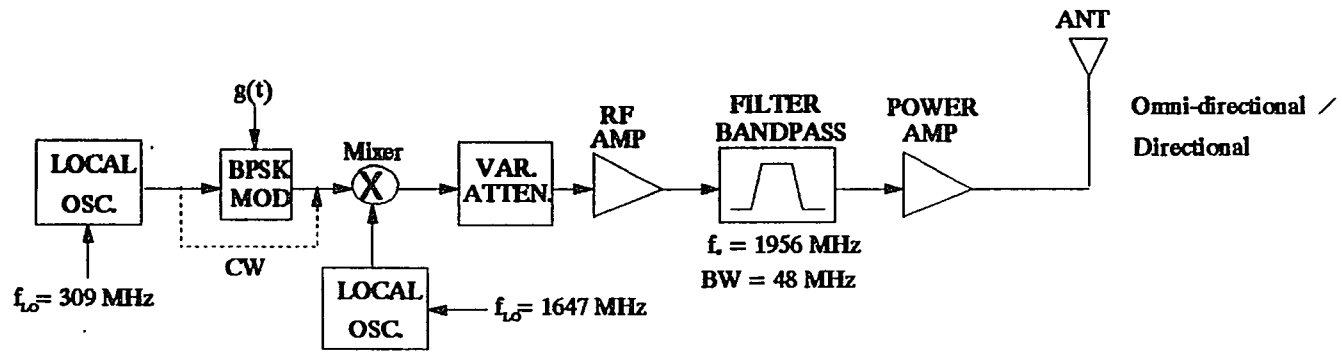

Figure 14.a DS-BPSK SPREAD SPECTRUM TRANSMITER

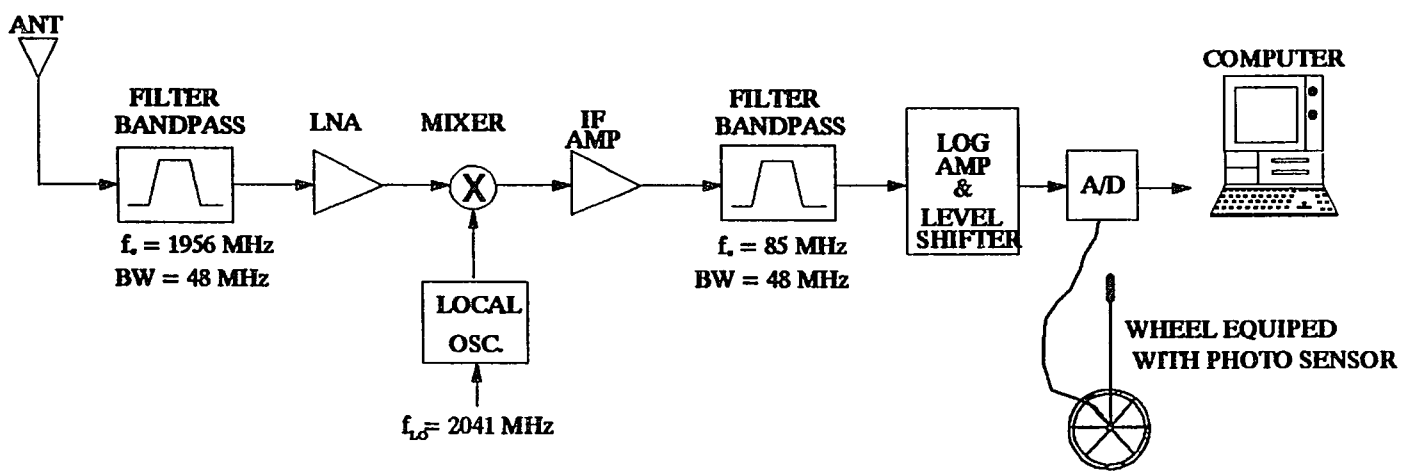

Figure 14.b SPREAD SPECTRUM RECEIVER

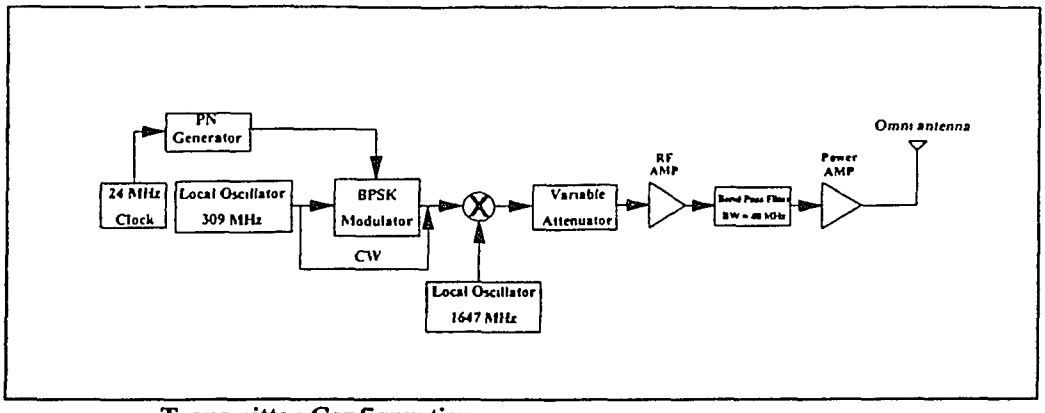

Transmitter Configuration

Figure 14.c

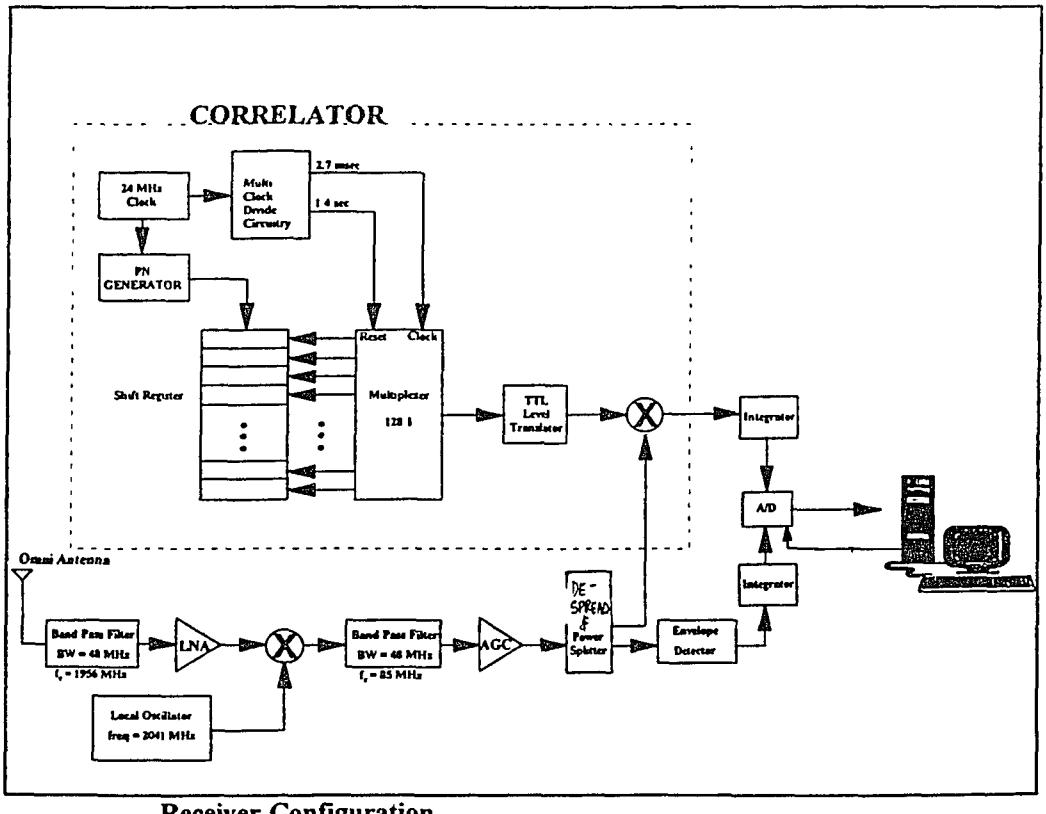

Receiver Configuration

Figure 14.d

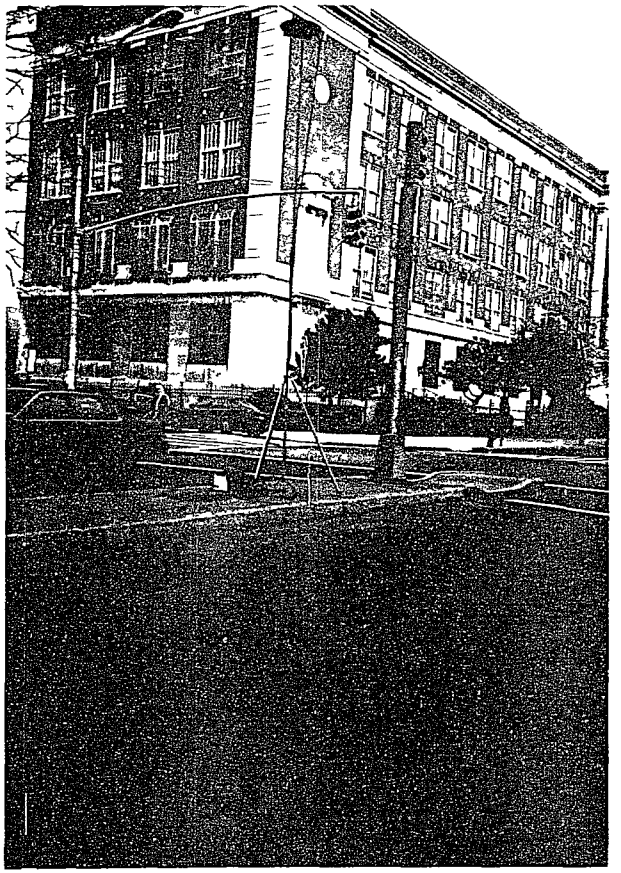

Figure 15.a Tx Antenna

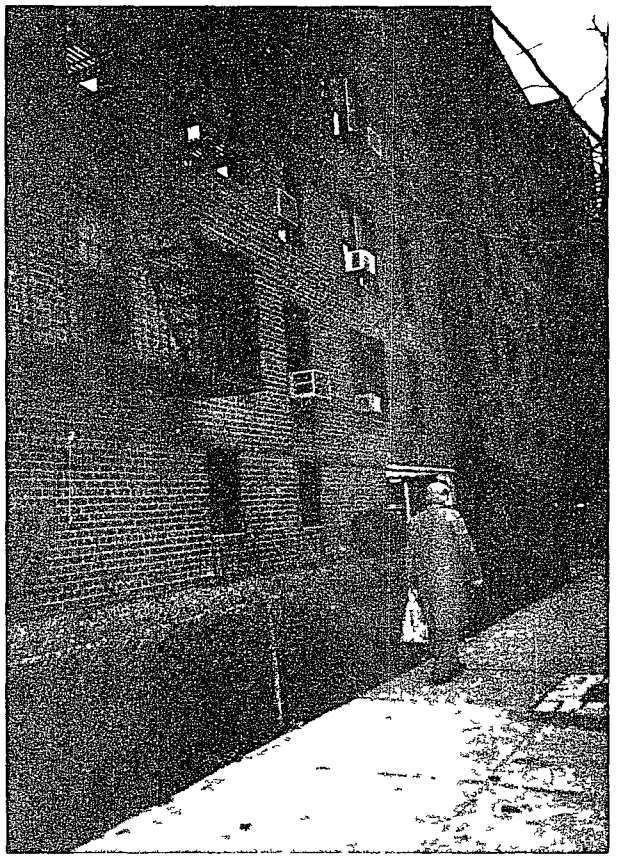

Figure 15.b 91st Street

Figure 15.c 91 St. Second View

Figure 15.d 34 Street

Figure 15.e 92nd Street

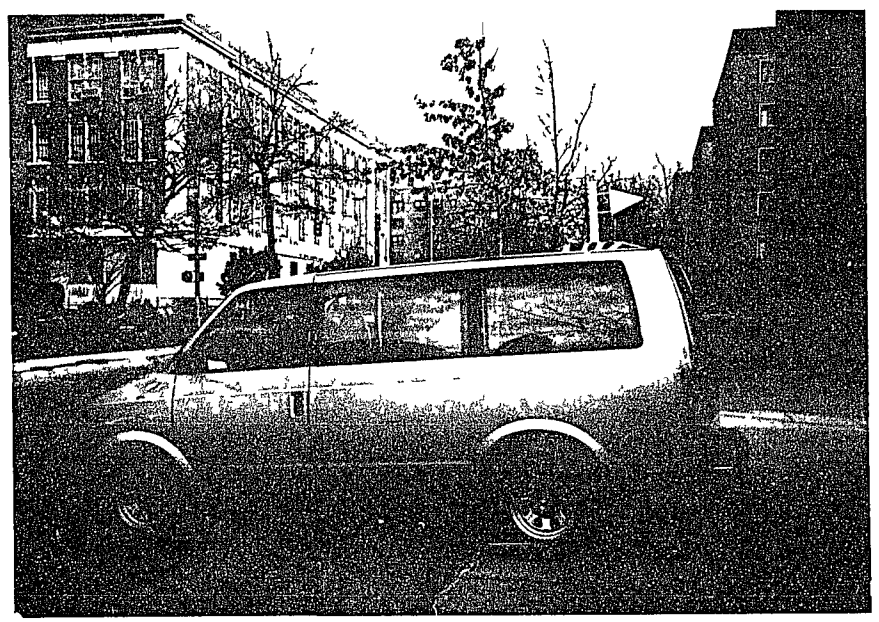

Figure 15.f Rx Antenna Pointing at 0 degrees.

Figure 15.g Port Washington Directioal Antenna Pointing at 0 degrees.

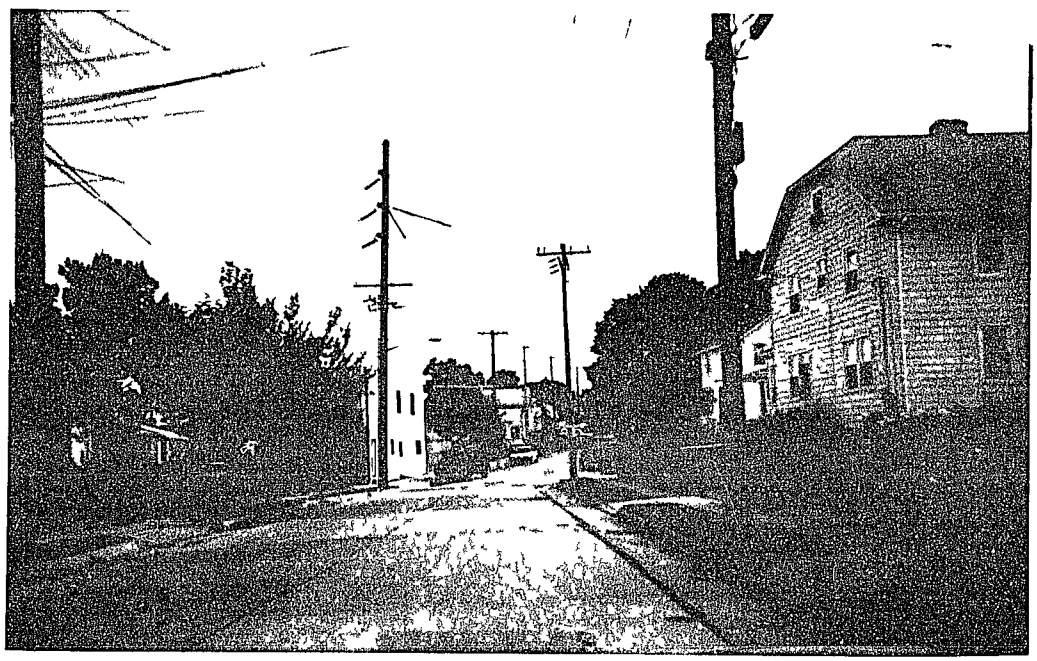

Figure 15.h New Haven St., Port Washington -LOS Conditions

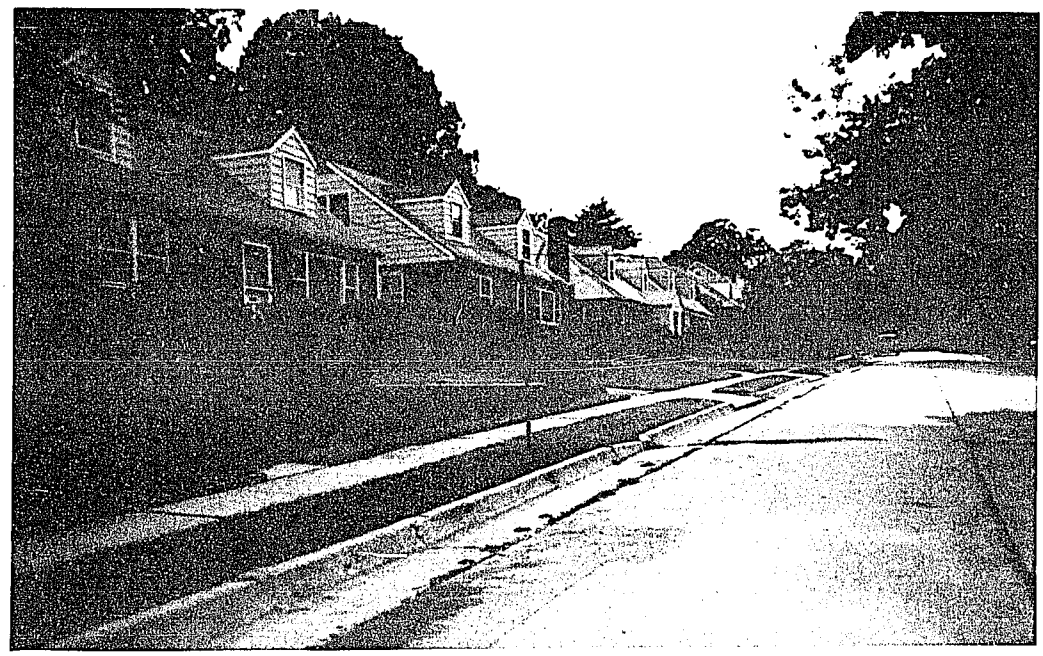

Figure 15.i Location # 2, Port Washington - 'Regular' Street.

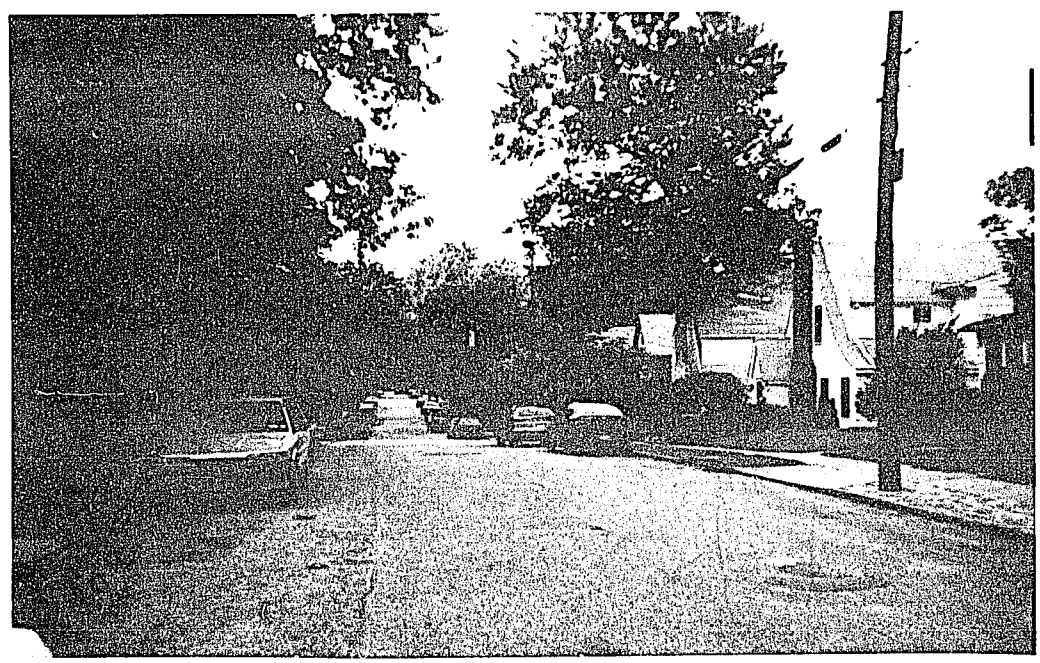

Figure 15.j Port Washington - Typical sub urban environment

Figure 15.k Location # 4, Port washington - Typical sub urban environment

Figure 15.l McKeay Ave.

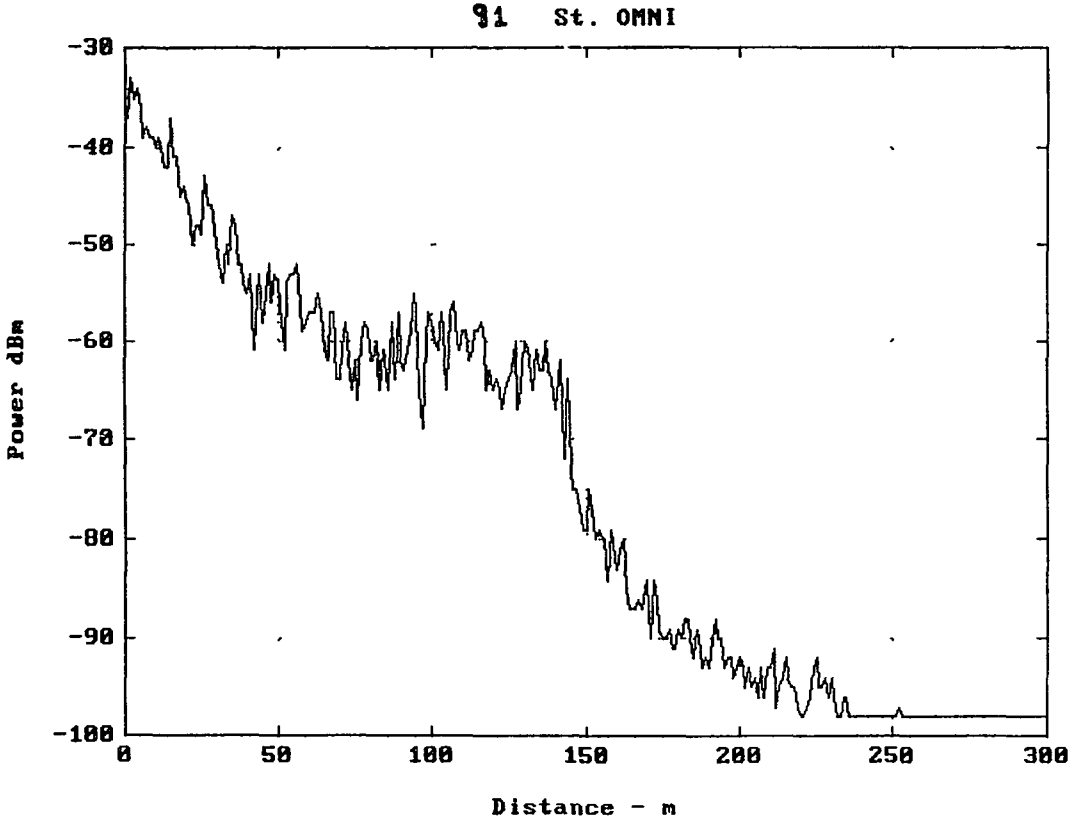
91 St. OMNI
-30
-40
-50
-60
-70
-80
-90
-100
Power dBm
0
50
100
150
200
250
300
Distance - m

Figure 16.1

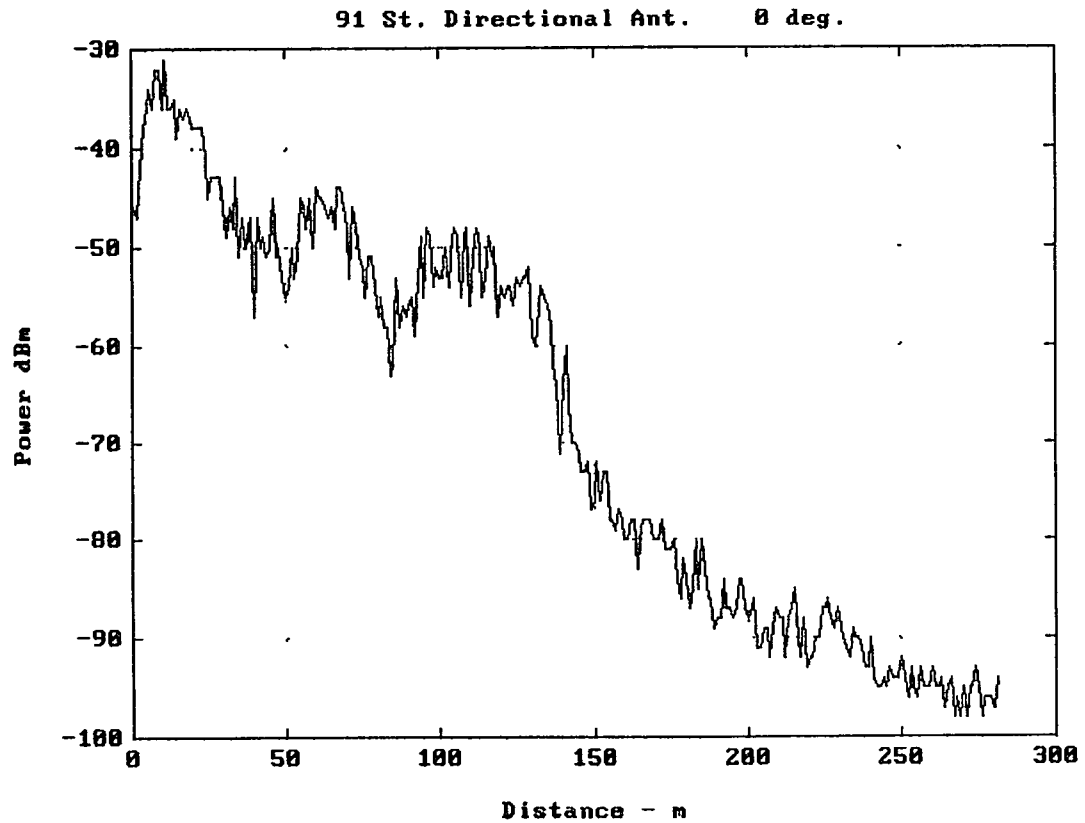
91 St. Directional Ant. 0 deg.
Power dBm
-30
-40
-50
-60
-70
-80
-90
-100
0
50
100
150
200
250
300
Distance - m

Figure 16.2

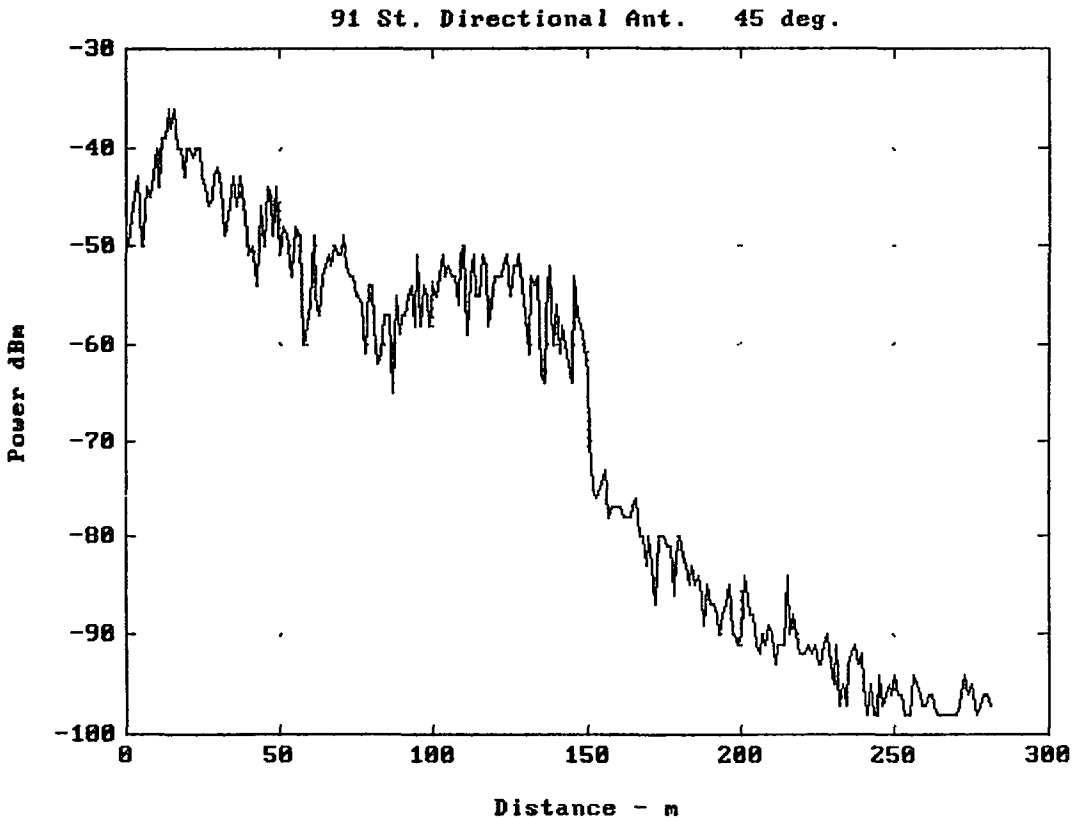
91 St. Directional Ant. 45 deg.
-30
-40
-50
-60
-70
-80
-90
-100
Power dBm
0
50
100
150
200
250
300
Distance - m

Figure 16.3

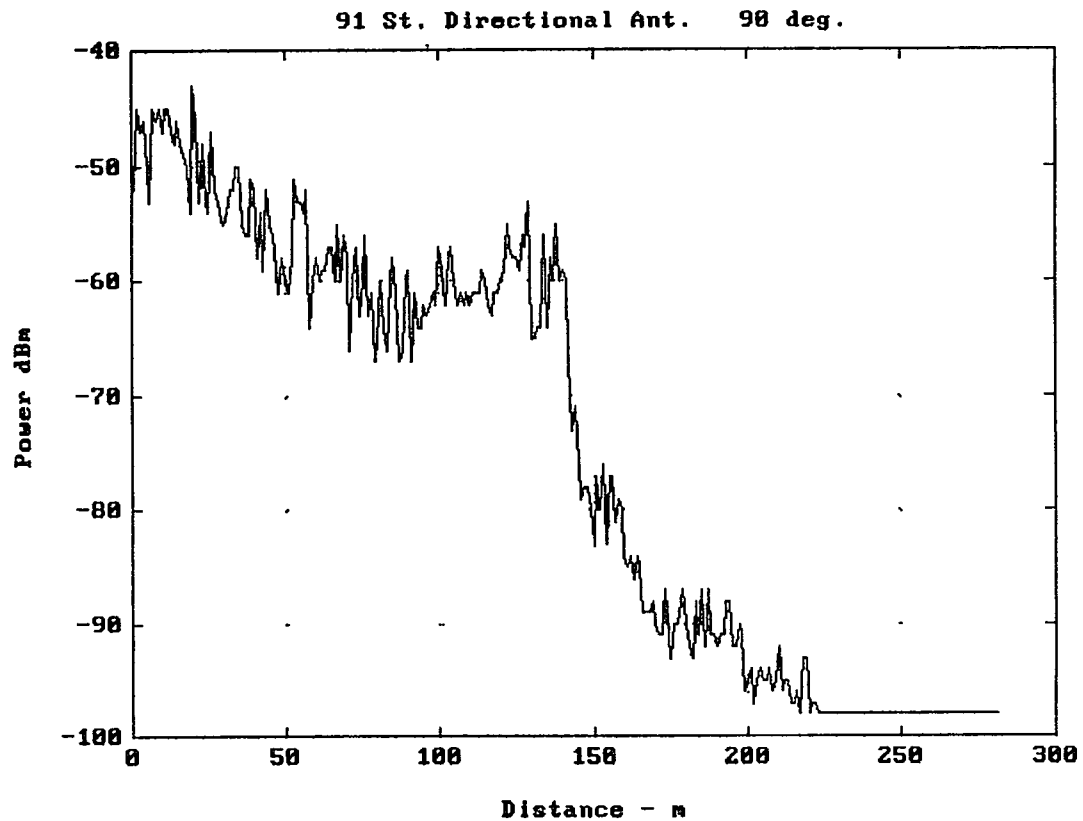
91 St. Directional Ant. 90 deg.
Power dBm
-40
-50
-60
-70
-80
-90
-100
0
50
100
150
200
250
300
Distance - m

Figure 16.4

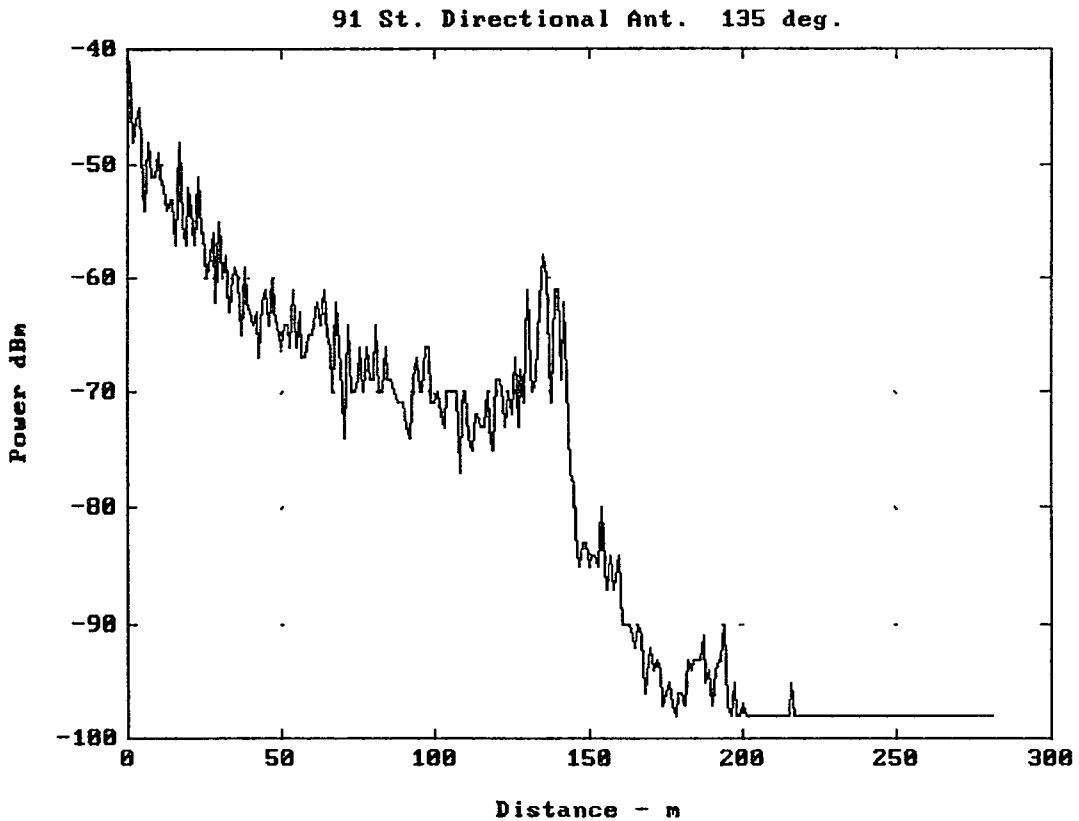
91 St. Directional Ant. 135 deg.
-40
-50
-60
-70
-80
-90
-100
Power dBm
0
50
100
150
200
250
300
Distance - m

Figure 16.5

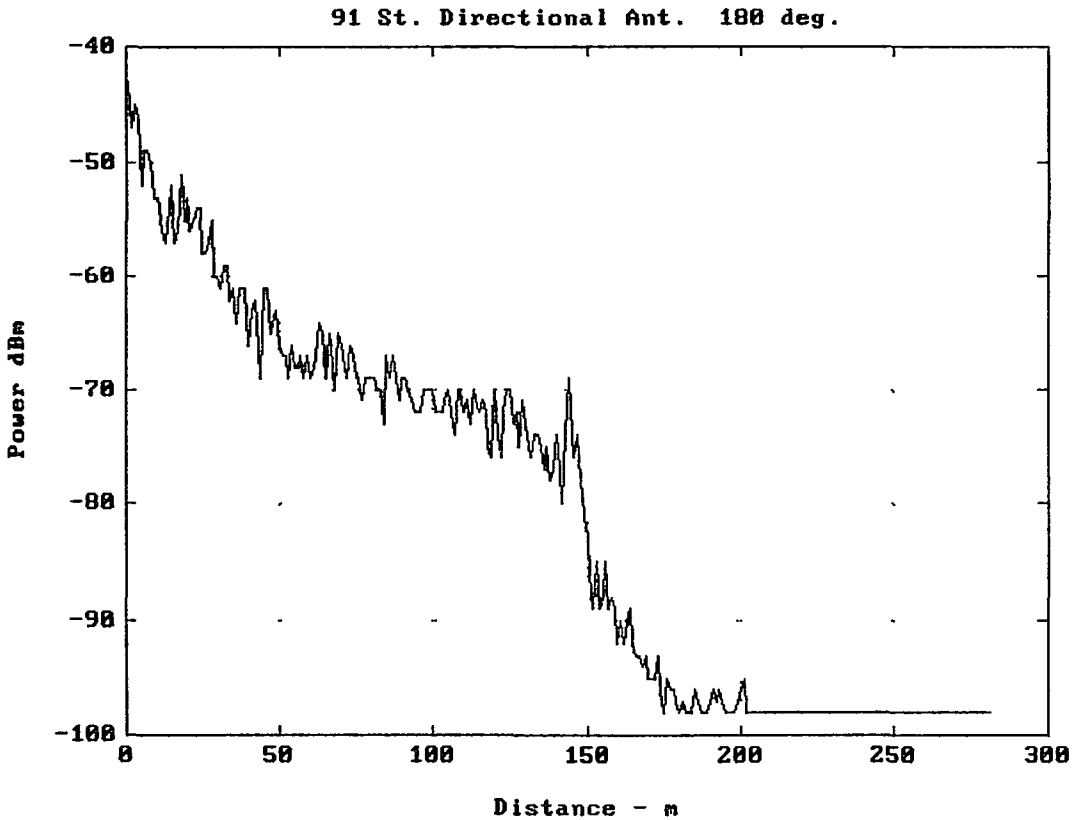
91 St. Directional Ant. 180 deg.
-40
-50
-60
-70
-80
-90
-100
Power dBm
0
50
100
150
200
250
300
Distance - m

Figure 16.6

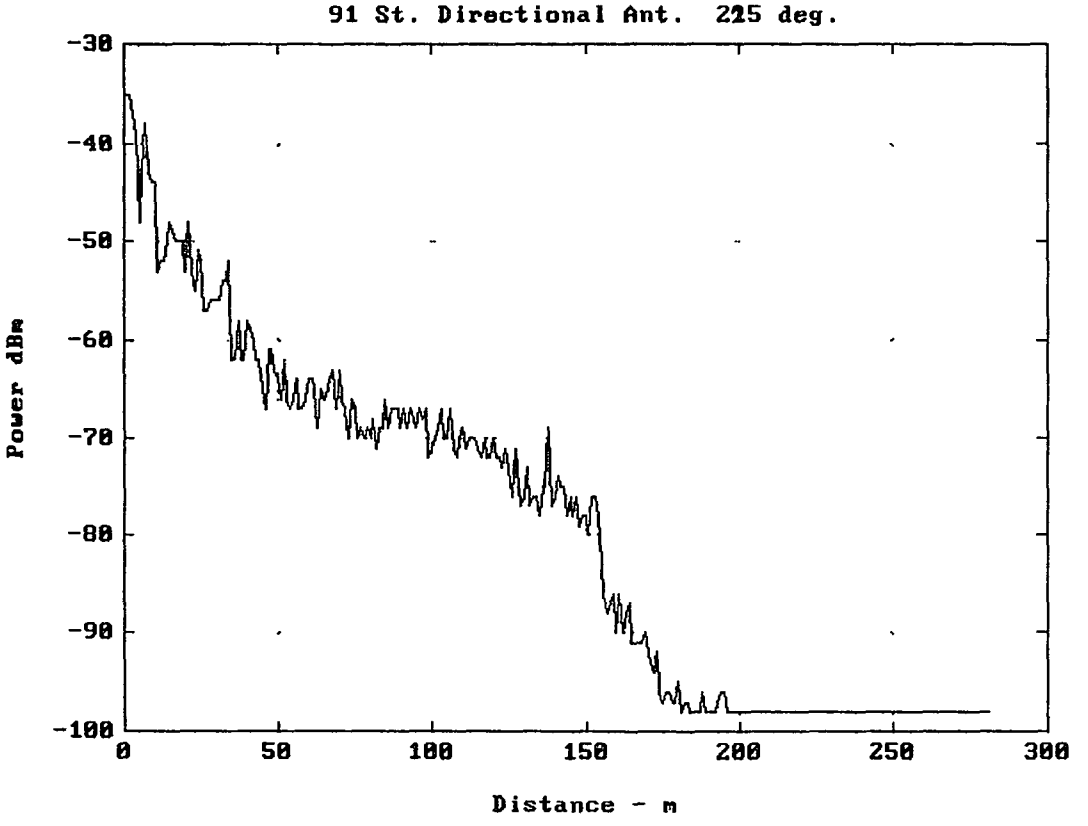
91 St. Directional Ant. 225 deg.
Power dBm
-30
-40
-50
-60
-70
-80
-90
-100
0
50
100
150
200
250
300
Distance - m

Figure 16.7

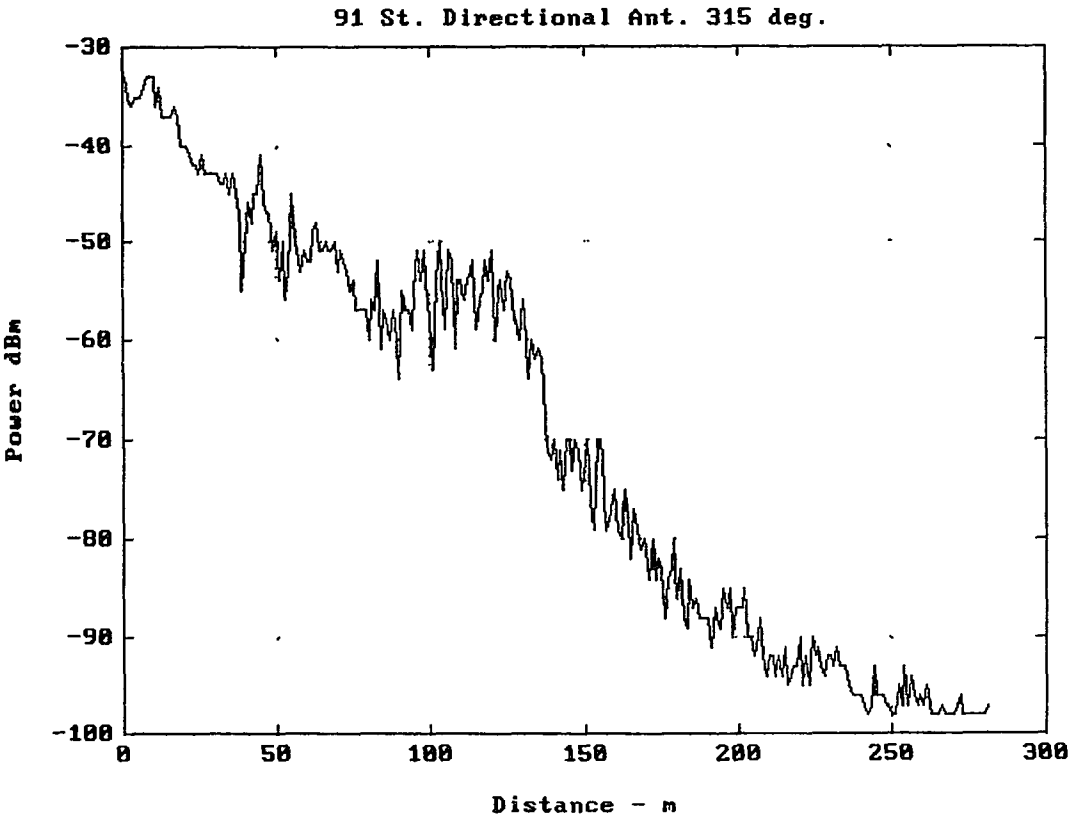
91 St. Directional Ant. 315 deg.
Power dBm
-30
-40
-50
-60
-70
-80
-90
-100
0
50
100
150
200
250
300
Distance - m

Figure 16.8

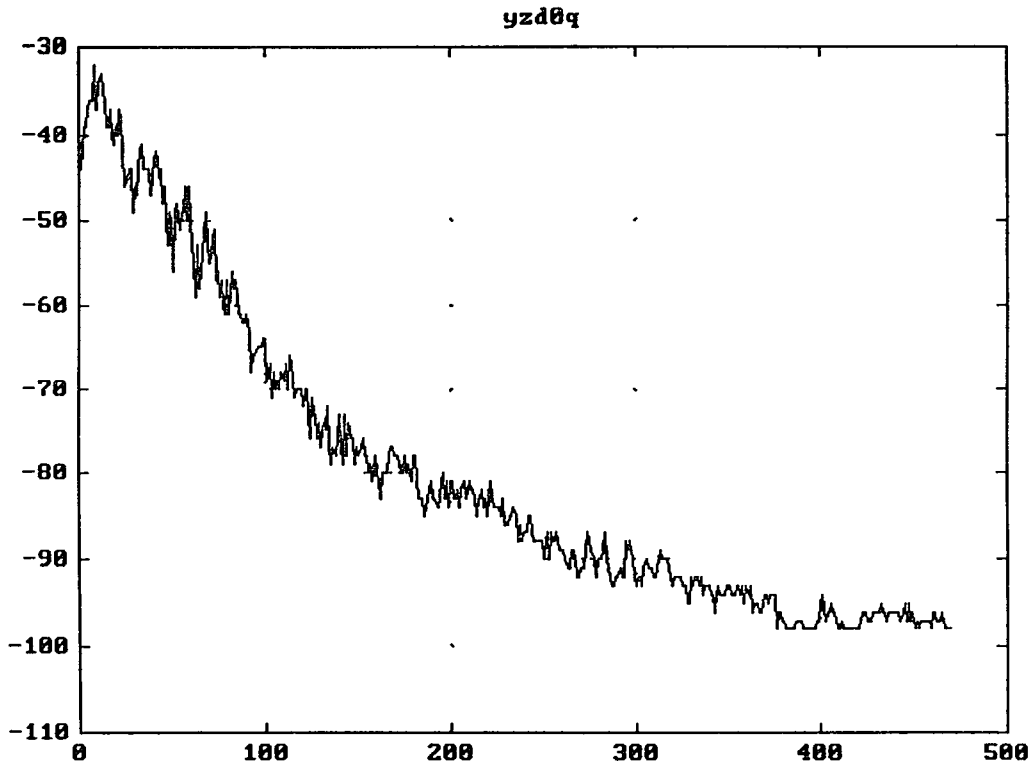

Figure 17.a Directional Ant. pointing at o degrees

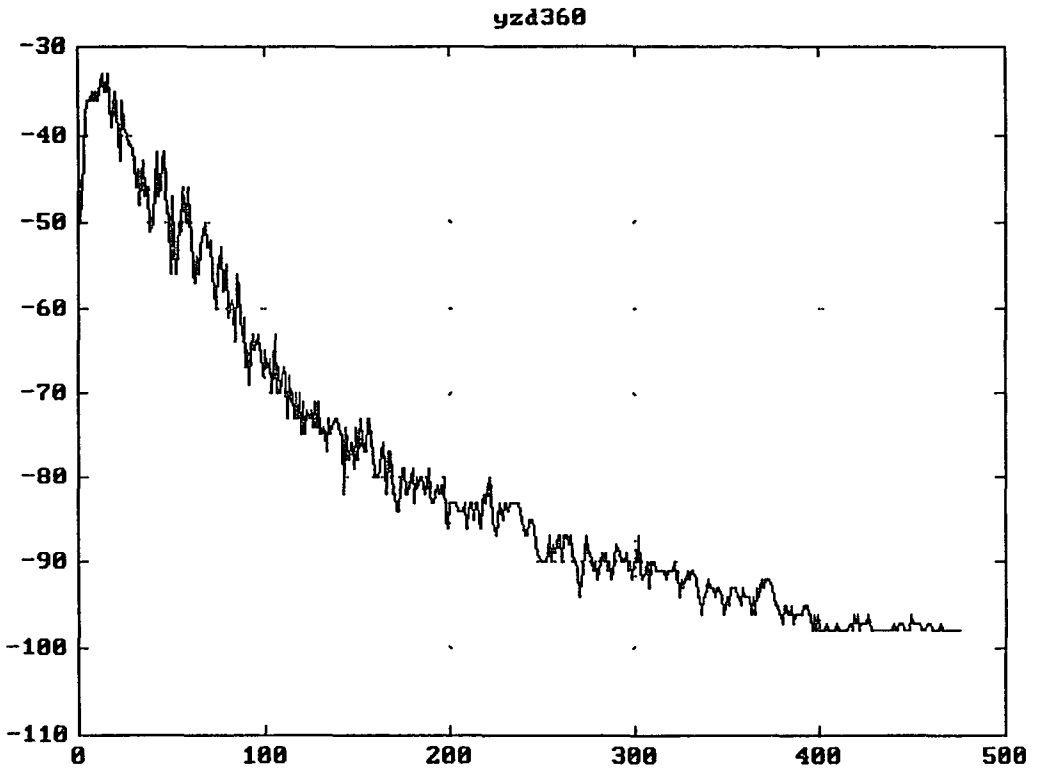

Figure 17.b Directional Ant. pointing at o degrees - second run

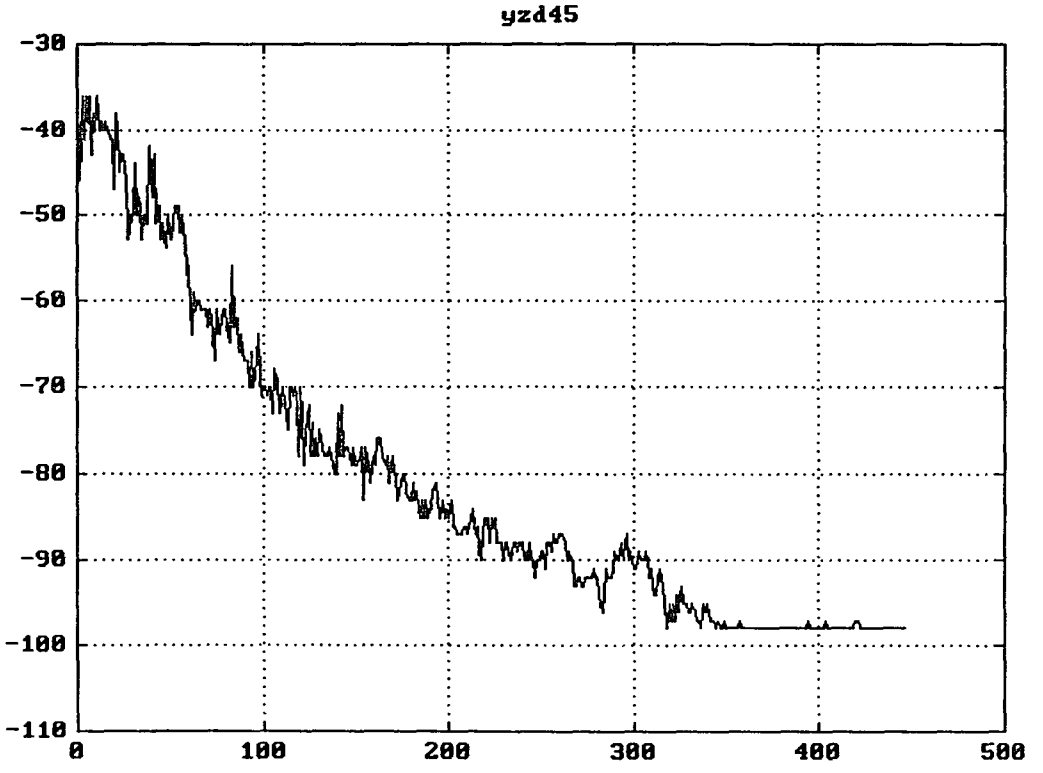

Figure 17.c Directional Ant. pointing at 45 degrees

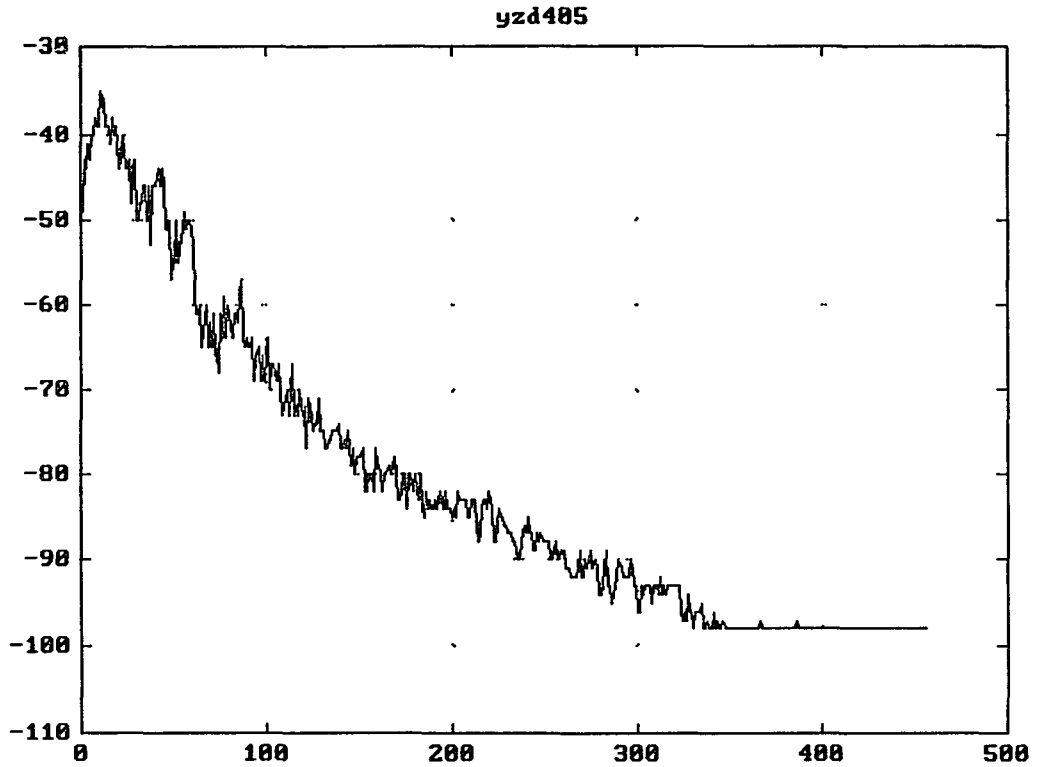

Figure 17.d Directional Ant. pointing at 45 degrees - second run

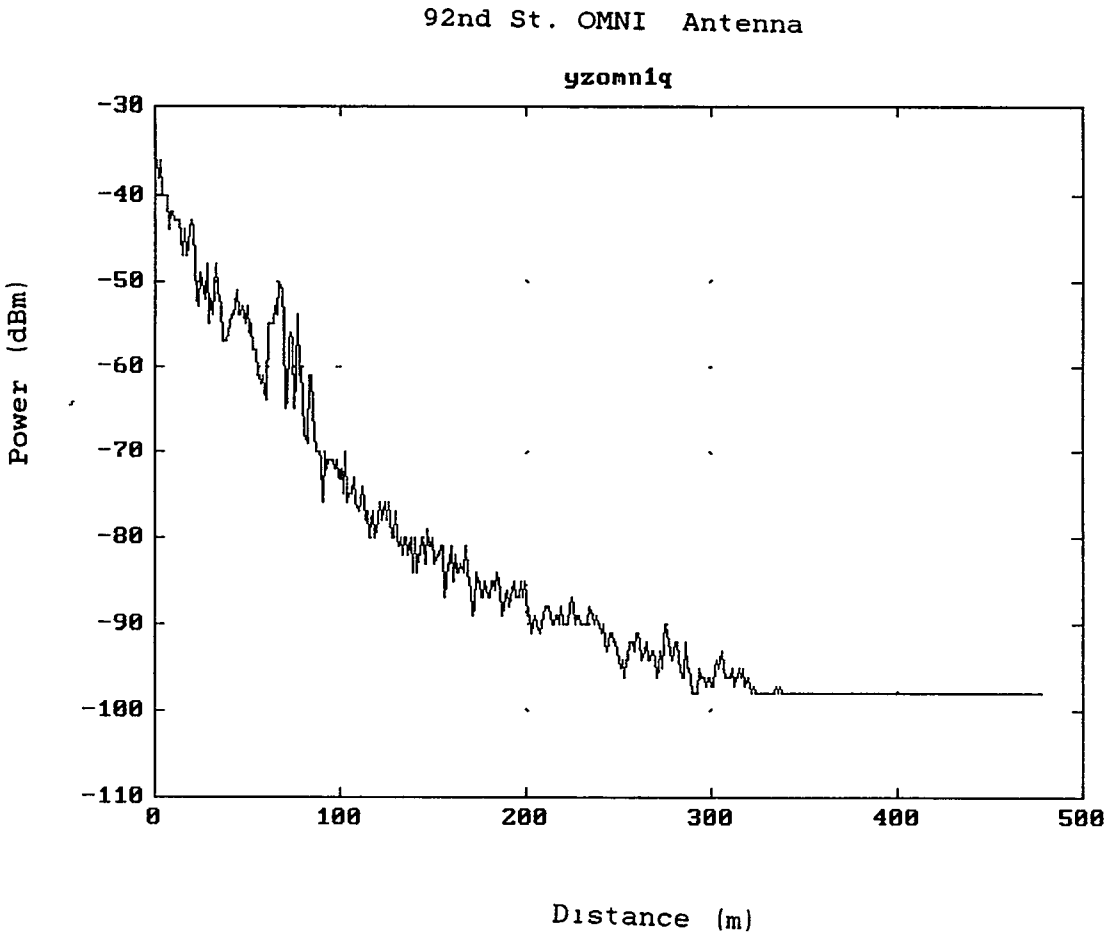
92nd St. OMNI Antenna
yzomn1q
Power (dBm)
-30
-40
-50
-60
-70
-80
-90
-100
-110
0
100
200
300
400
500
Distance (m)

Figure 18.a

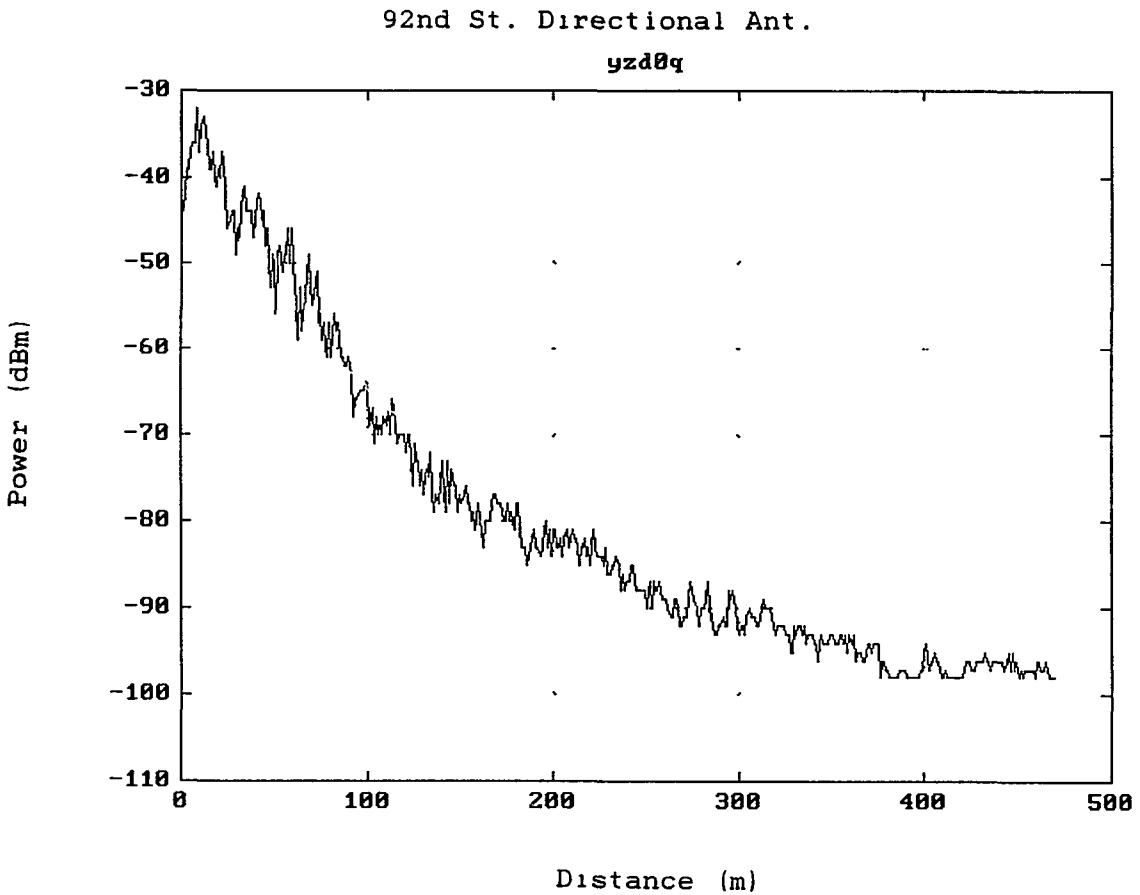
92nd St. Directional Ant.
yzd0q
Power (dBm)
-30
-40
-50
-60
-70
-80
-90
-100
-110
0
100
200
300
400
500
Distance (m)

Figure 18.b

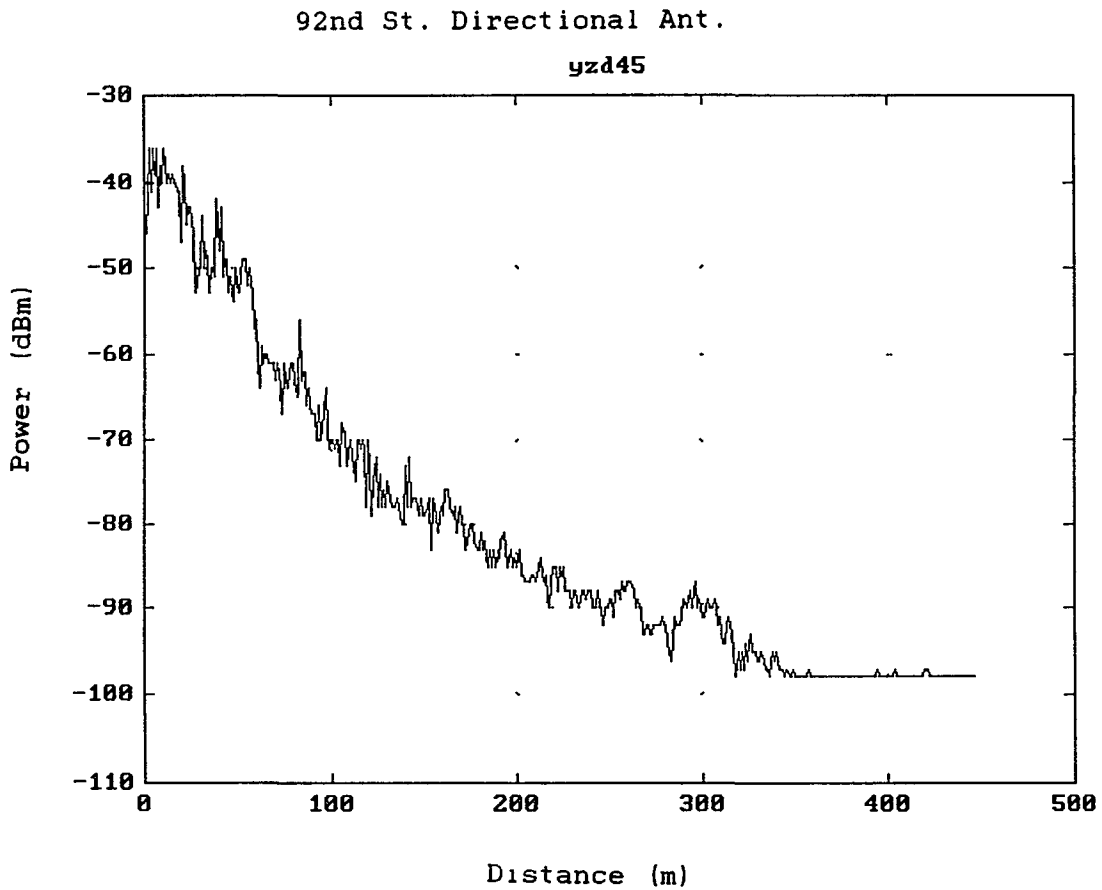
92nd St. Directional Ant.
yzd45
-30
-40
-50
-60
-70
-80
-90
-100
-110
Power (dBm)
0
100
200
300
400
500
Distance (m)

Figure 18.c

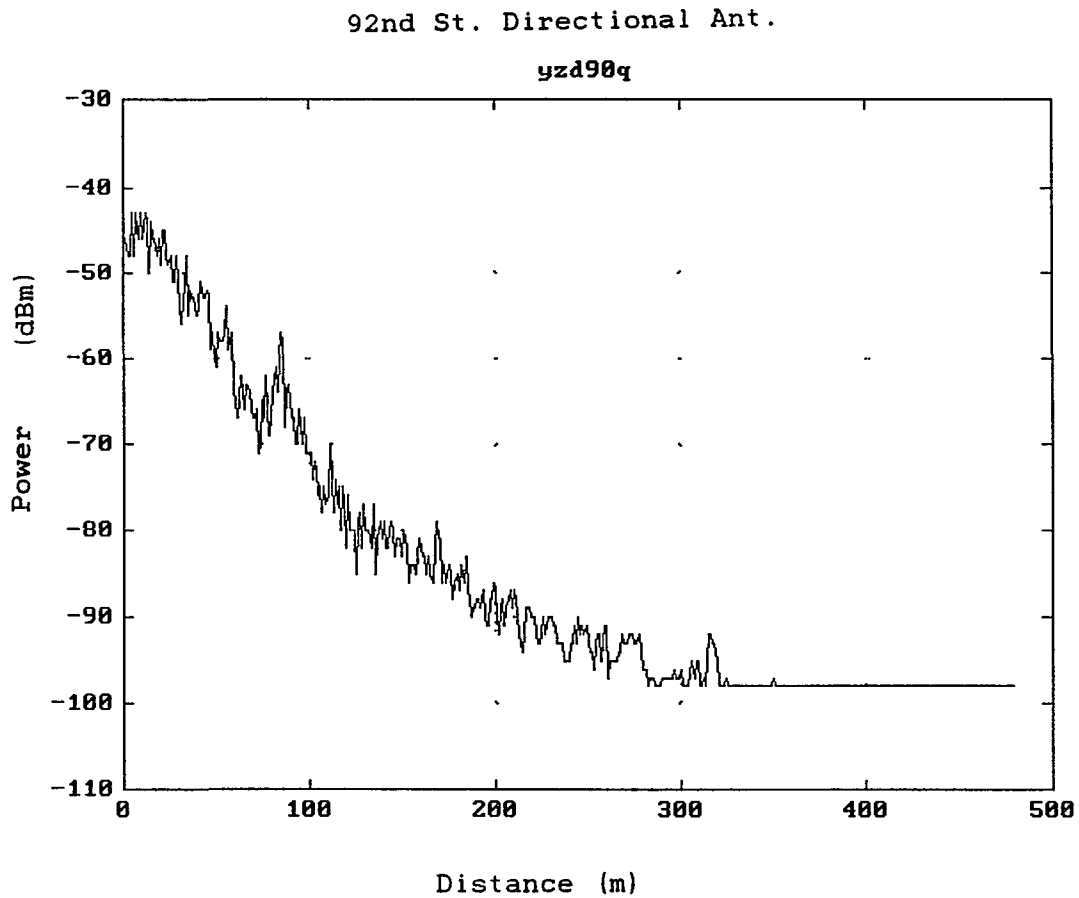
92nd St. Directional Ant.
yzd90q
Power (dBm)
-30
-40
-50
-60
-70
-80
-90
-100
-110
0
100
200
300
400
500
Distance (m)

Figure 18.d

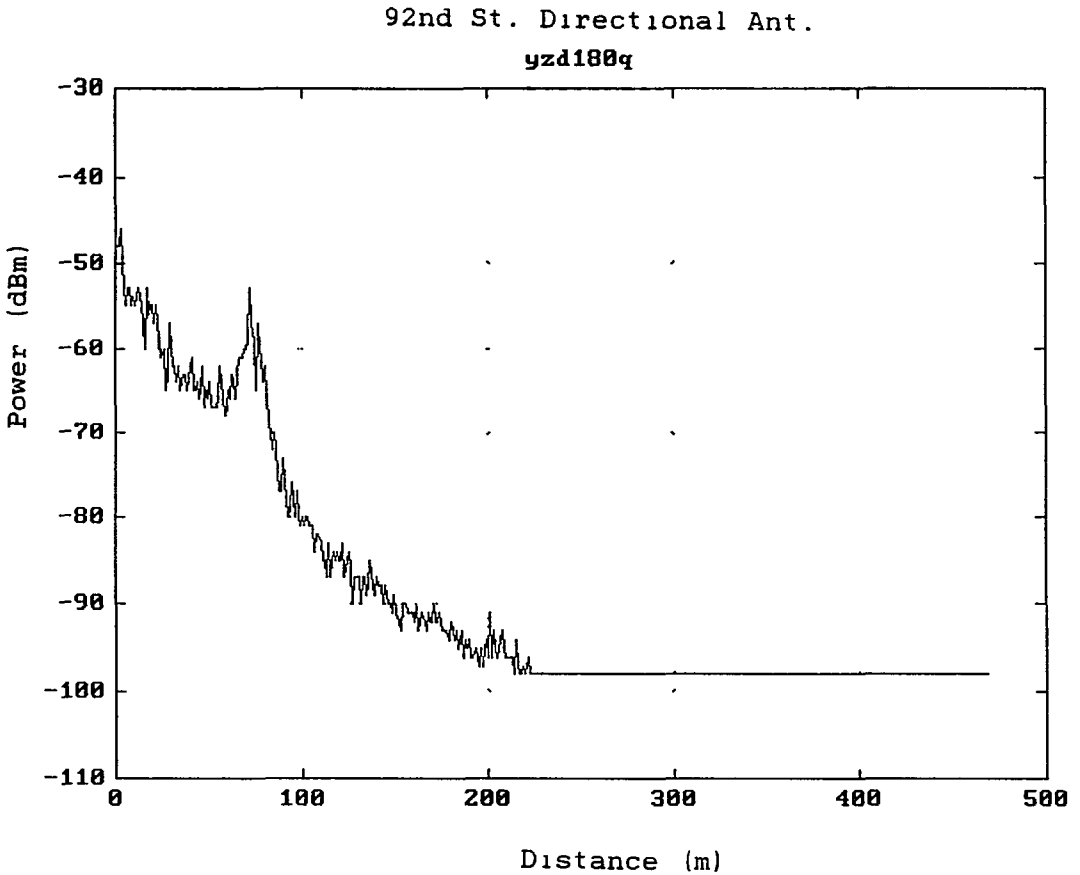
92nd St. Directional Ant.
yzd180q
-30
-40
-50
-60
-70
-80
-90
-100
-110
Power (dBm)
0
100
200
300
400
500
Distance (m)

Figure 18.e

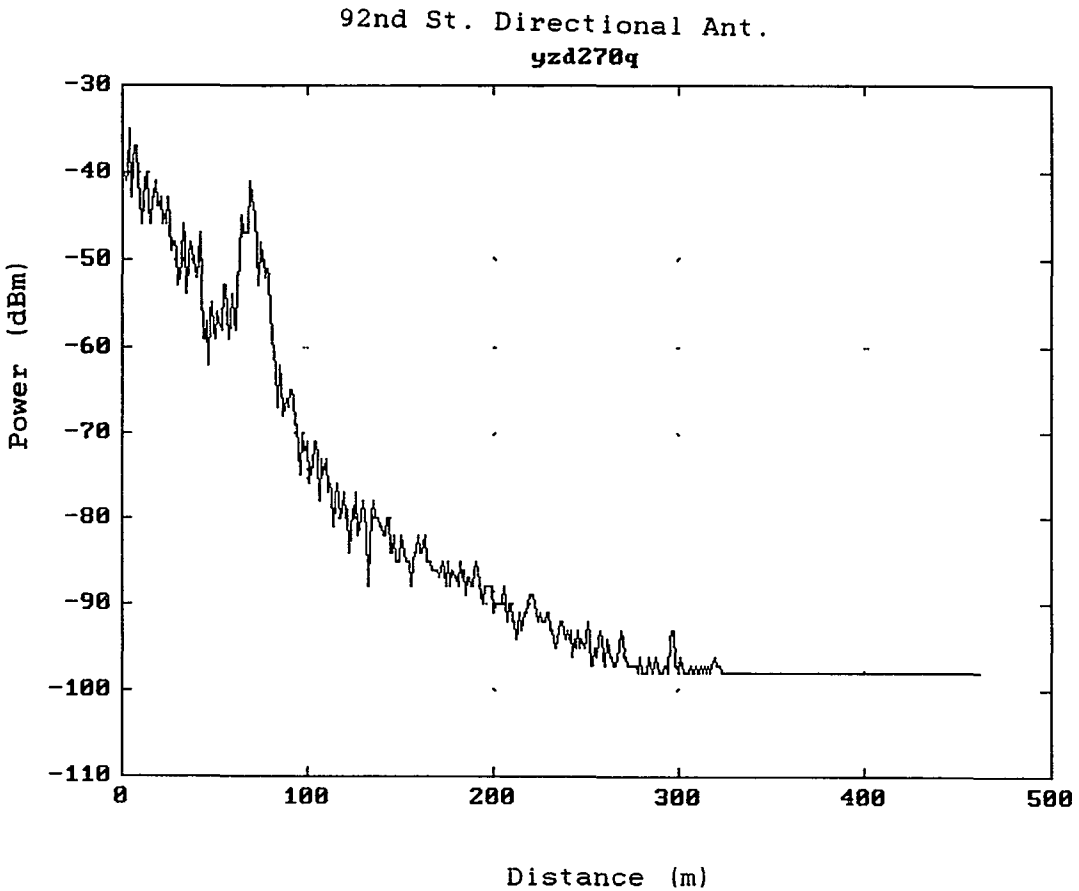
92nd St. Directional Ant.
yzd270q
Power (dBm)
-30
-40
-50
-60
-70
-80
-90
-100
-110
0
100
200
300
400
500
Distance (m)

Figure 18.f

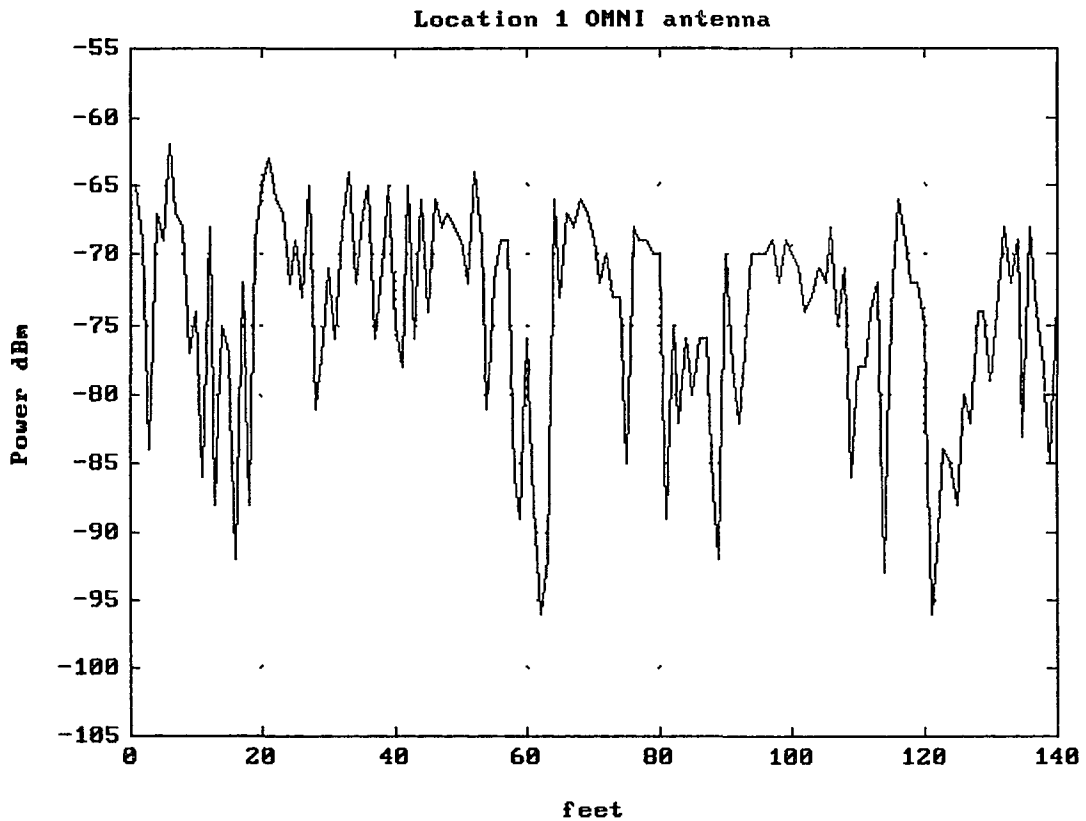
Location 1 OMNI antenna
Power dBm
-55
-60
-65
-70
-75
-80
-85
-90
-95
-100
-105
0
20
40
60
80
100
120
140
feet

Figure 19.a

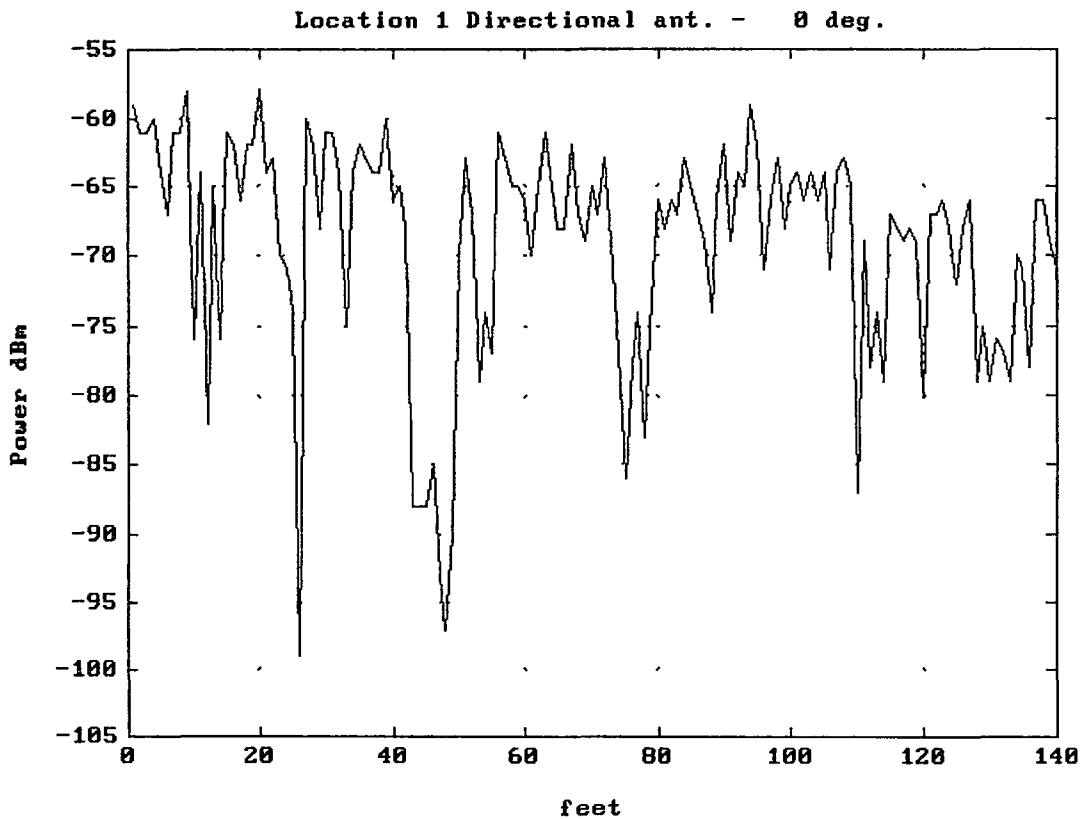
Location 1 Directional ant. - 0 deg.
Power dBm
-55
-60
-65
-70
-75
-80
-85
-90
-95
-100
-105
0
20
40
60
80
100
120
140
feet

Figure 19.b

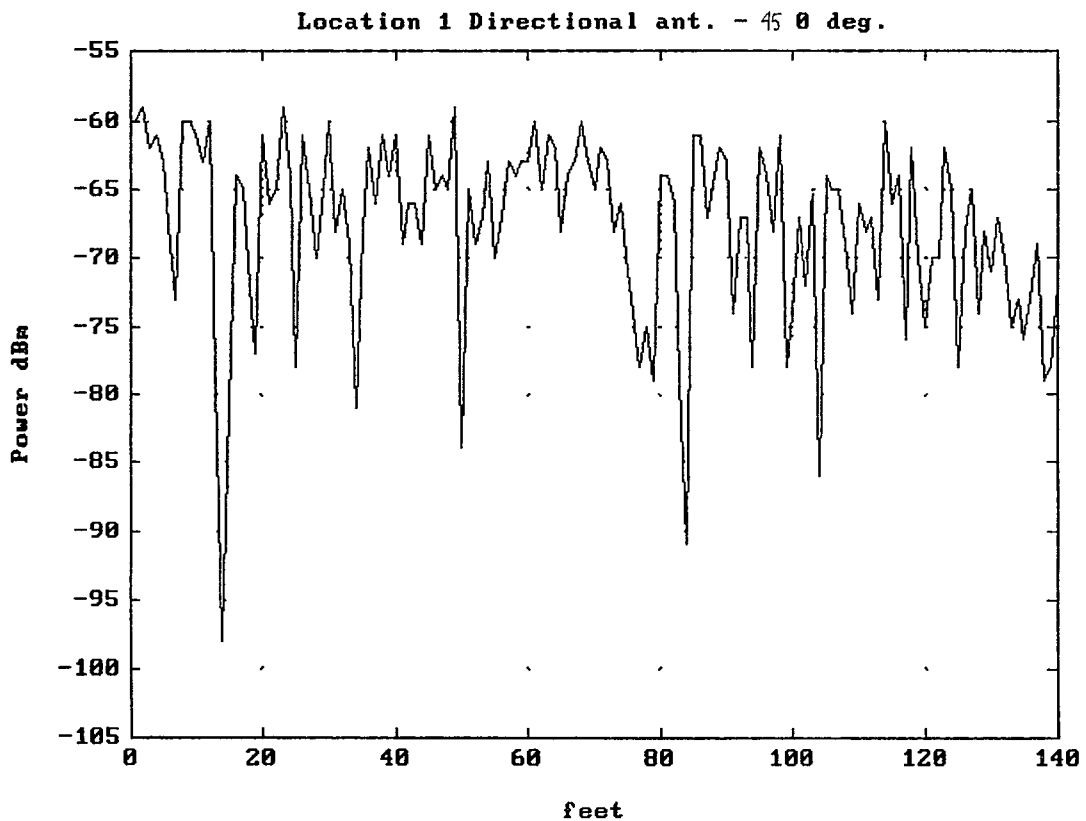
Location 1 Directional ant. - 45 0 deg.
Power dBm
-55
-60
-65
-70
-75
-80
-85
-90
-95
-100
-105
0
20
40
60
80
100
120
140
feet

Figure 19.c

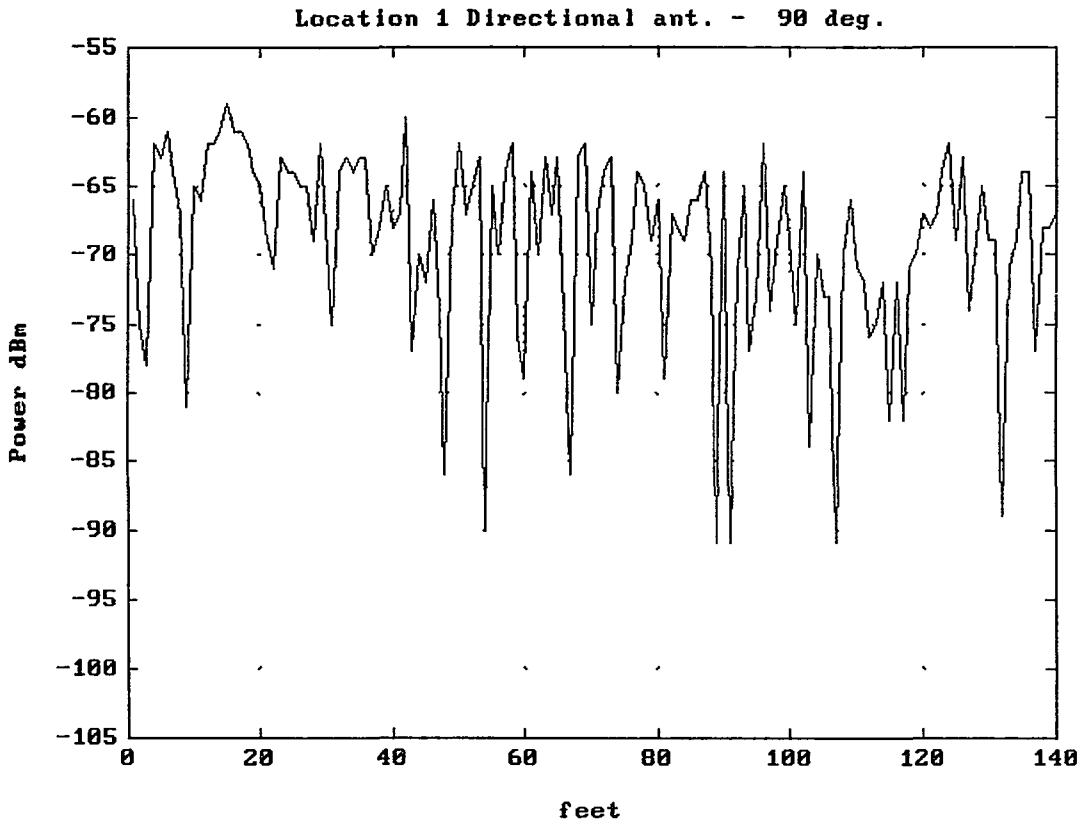
Location 1 Directional ant. - 90 deg.
Power dBm
-55
-60
-65
-70
-75
-80
-85
-90
-95
-100
-105
0
20
40
60
80
100
120
140
feet

Figure 19.d

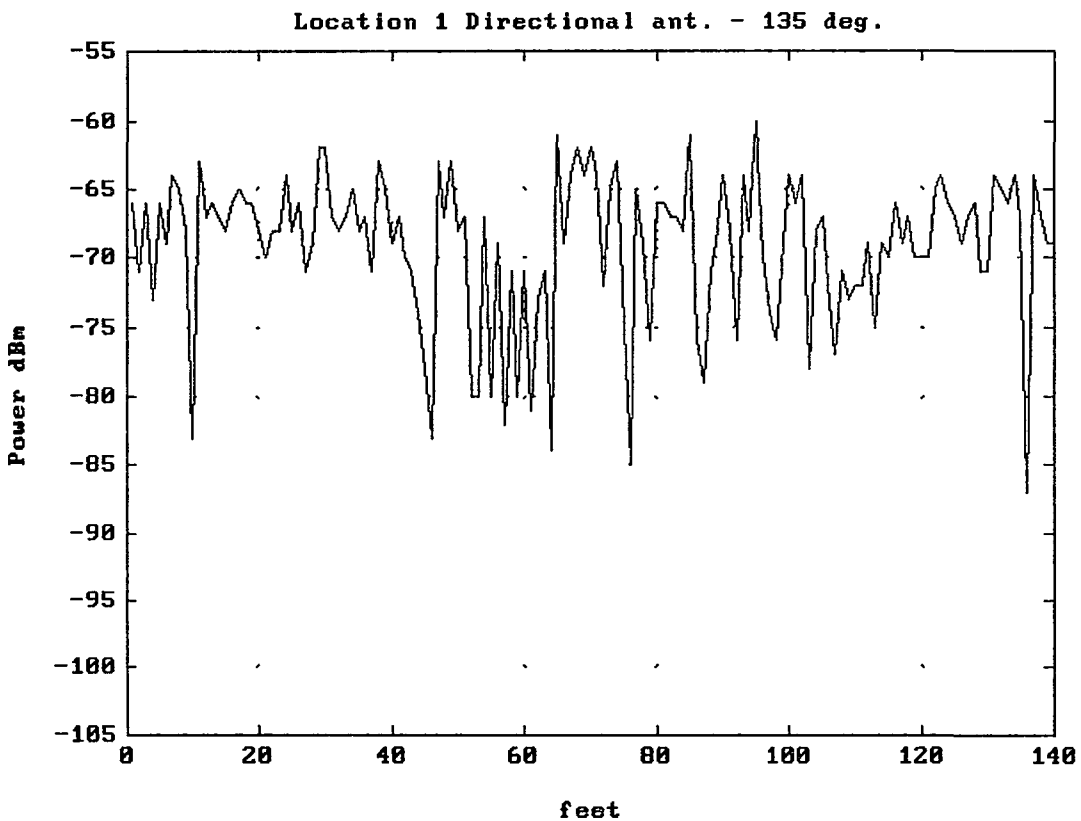
Location 1 Directional ant. - 135 deg.
Power dBm
-55
-60
-65
-70
-75
-80
-85
-90
-95
-100
-105
0
20
40
60
80
100
120
140
feet

Figure 19.e

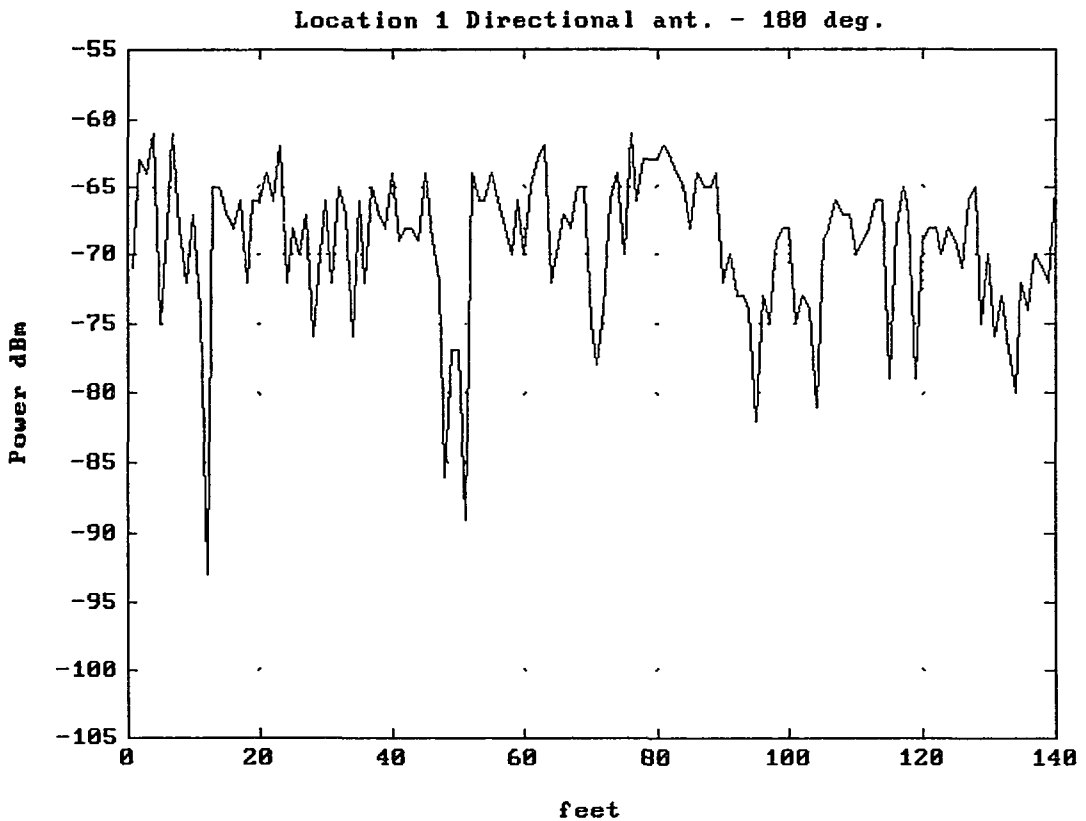
Location 1 Directional ant. - 180 deg.
Power dBm
-55
-60
-65
-70
-75
-80
-85
-90
-95
-100
-105
0
20
40
60
80
100
120
140
feet

Figure 19.f

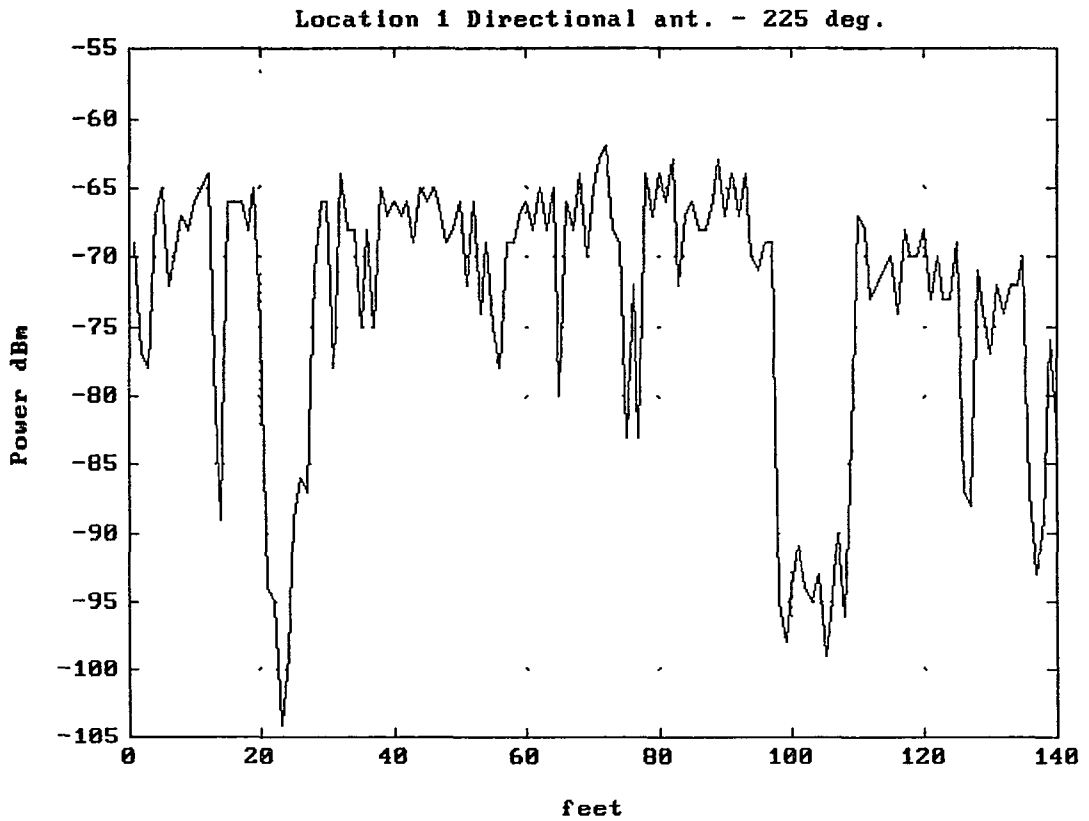
Location 1 Directional ant. - 225 deg.
-55
-60
-65
-70
-75
-80
-85
-90
-95
-100
-105
Power dBm
0
20
40
60
80
100
120
140
feet

Figure 19.g

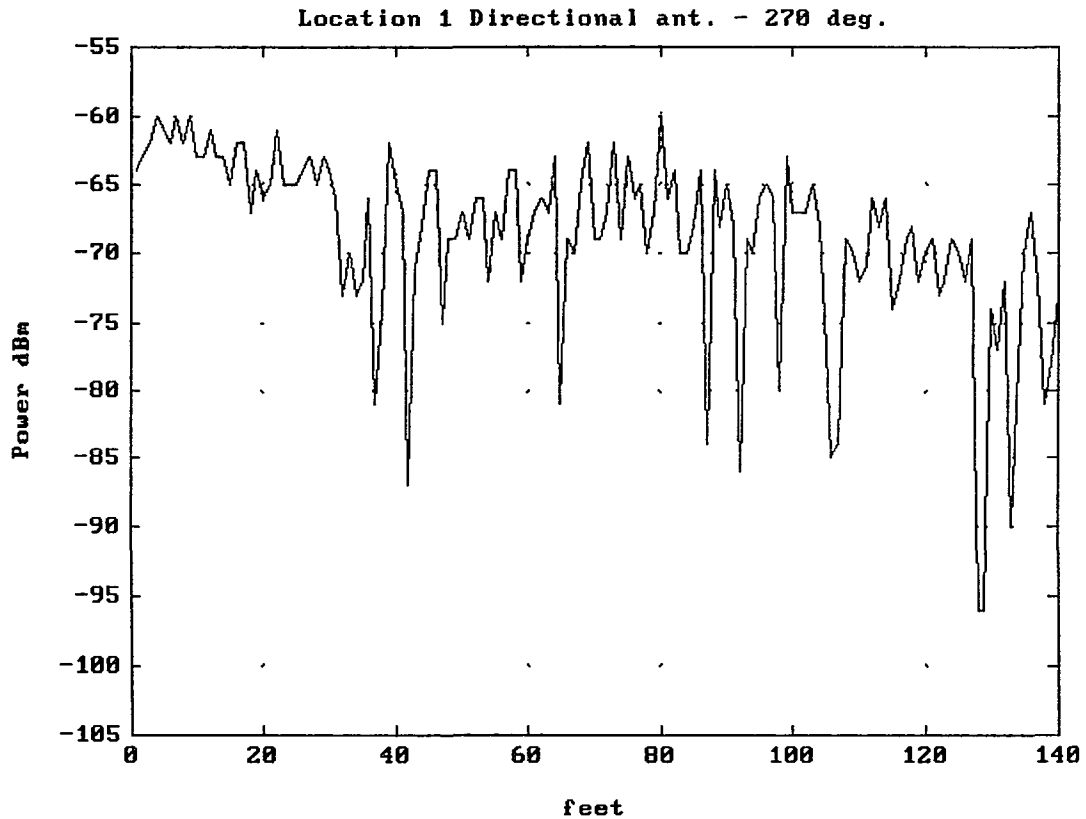
Location 1 Directional ant. - 270 deg.
Power dBm
-55
-60
-65
-70
-75
-80
-85
-90
-95
-100
-105
0
20
40
60
80
100
120
140
feet

Figure 19.h

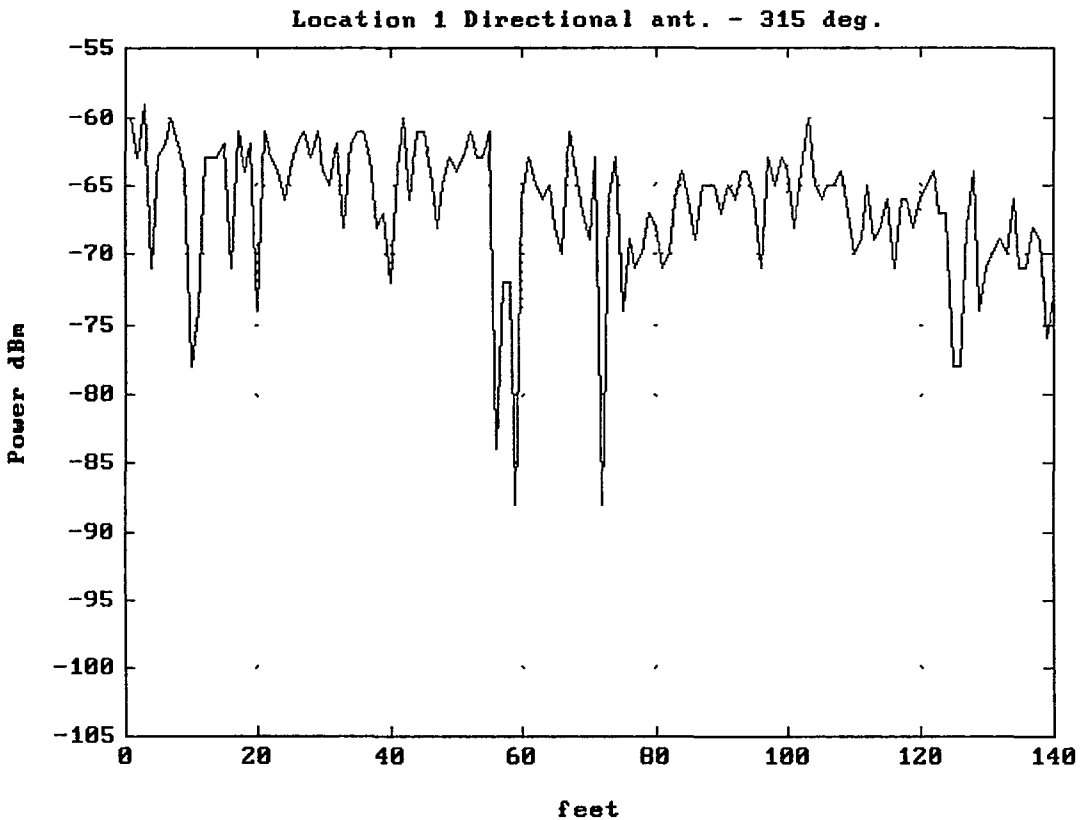
Location 1 Directional ant. - 315 deg.
Power dBm
-55
-60
-65
-70
-75
-80
-85
-90
-95
-100
-105
0
20
40
60
80
100
120
140
feet

Figure 19.i

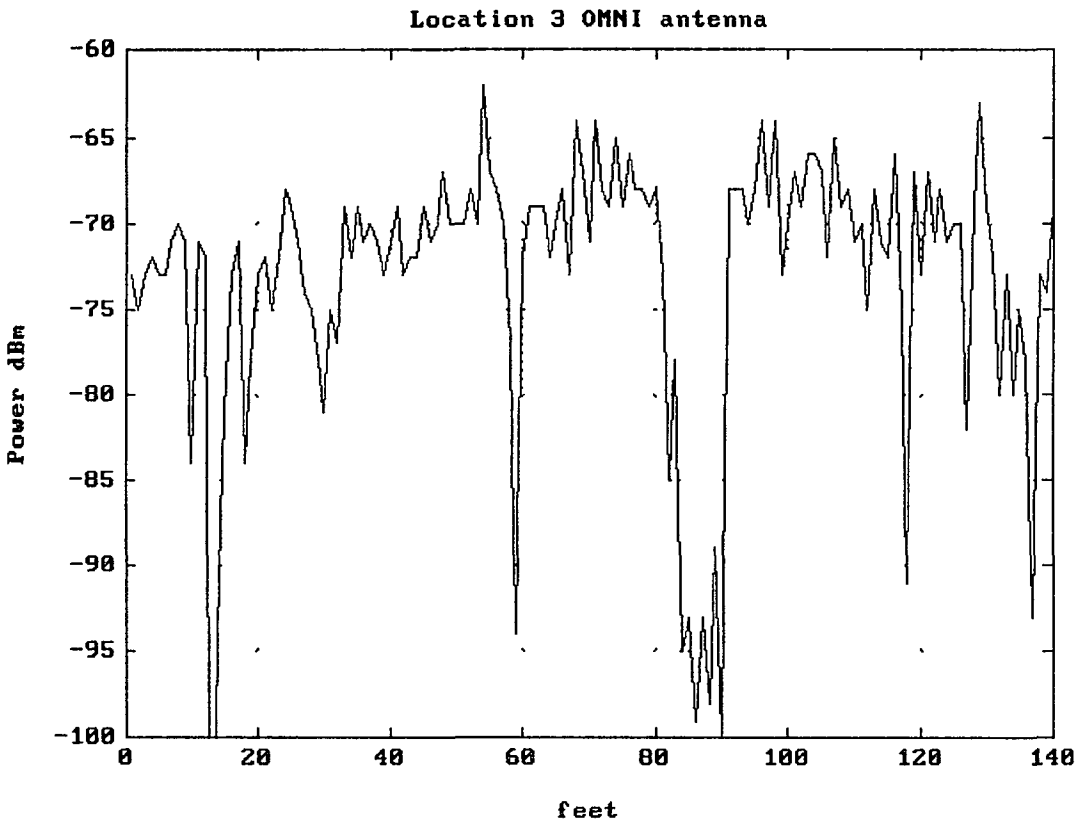
Location 3 OMNI antenna
Power dBm
-60
-65
-70
-75
-80
-85
-90
-95
-100
0
20
40
60
80
100
120
140
feet

Figure 20.a

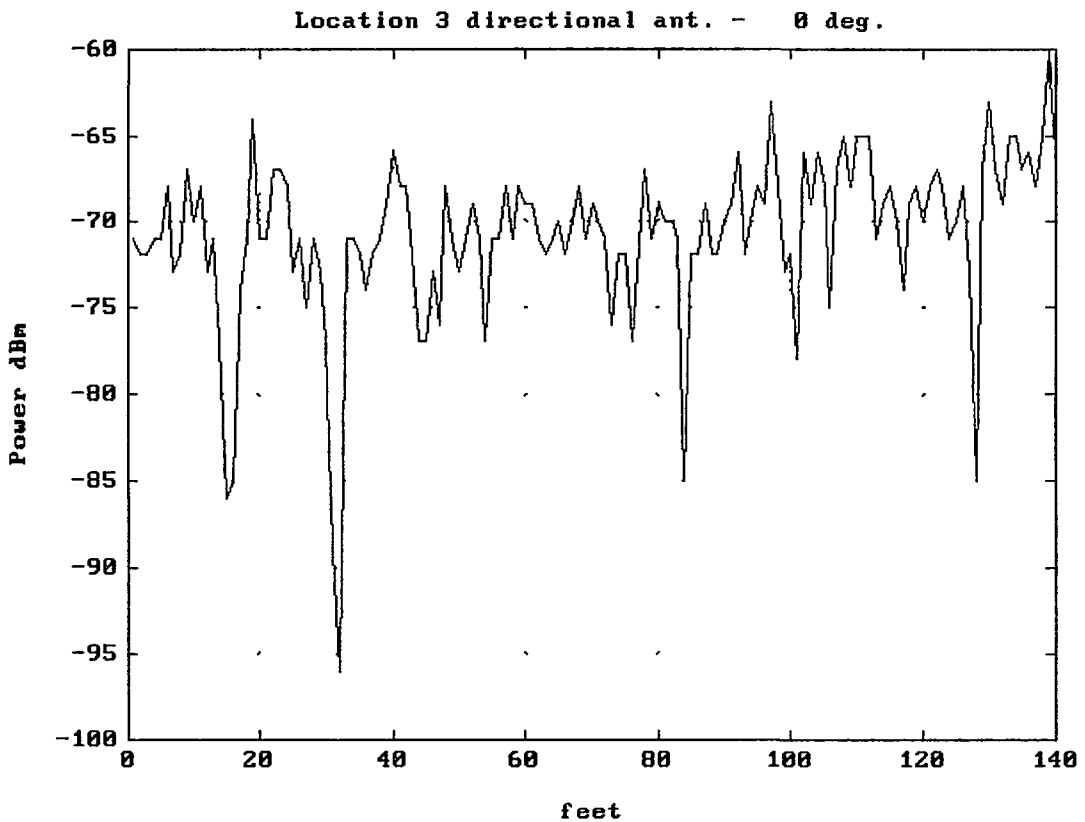
Location 3 directional ant. - 0 deg.
Power dBm
-60
-65
-70
-75
-80
-85
-90
-95
-100
0
20
40
60
80
100
120
140
feet

Figure 20.b

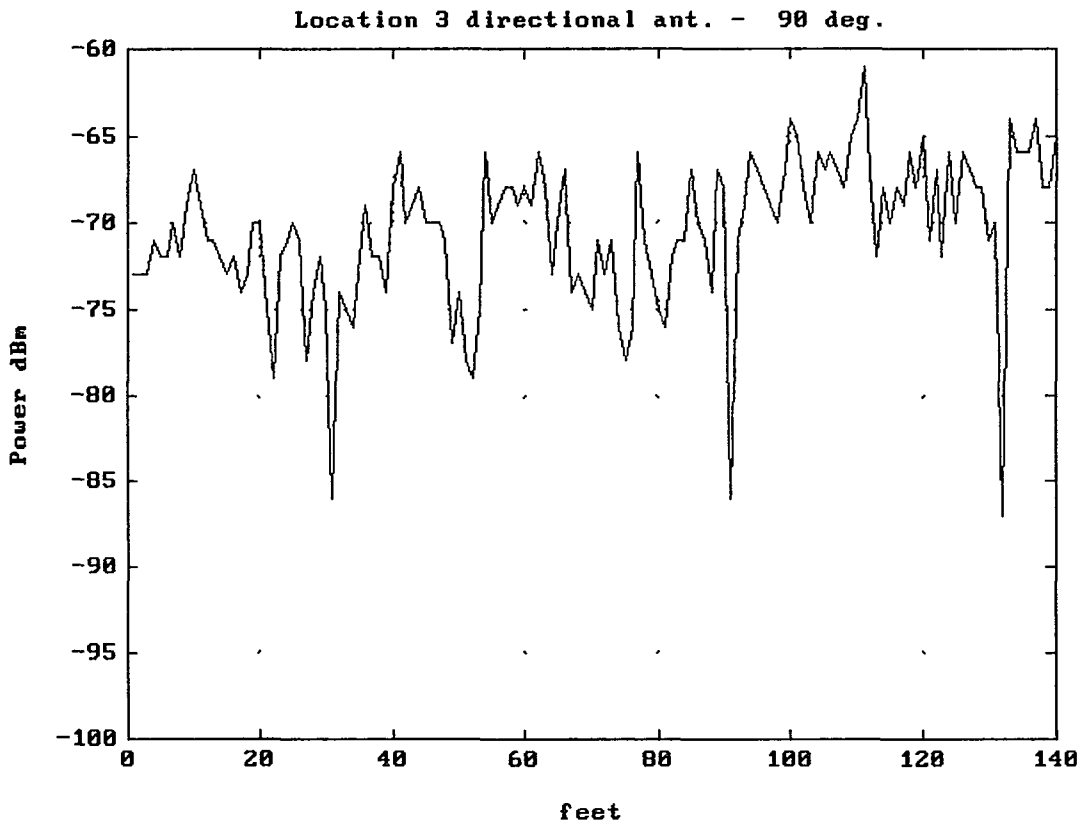
Location 3 directional ant. - 90 deg.
Power dBm
-60
-65
-70
-75
-80
-85
-90
-95
-100
0
20
40
60
80
100
120
140
feet

Figure 20.c

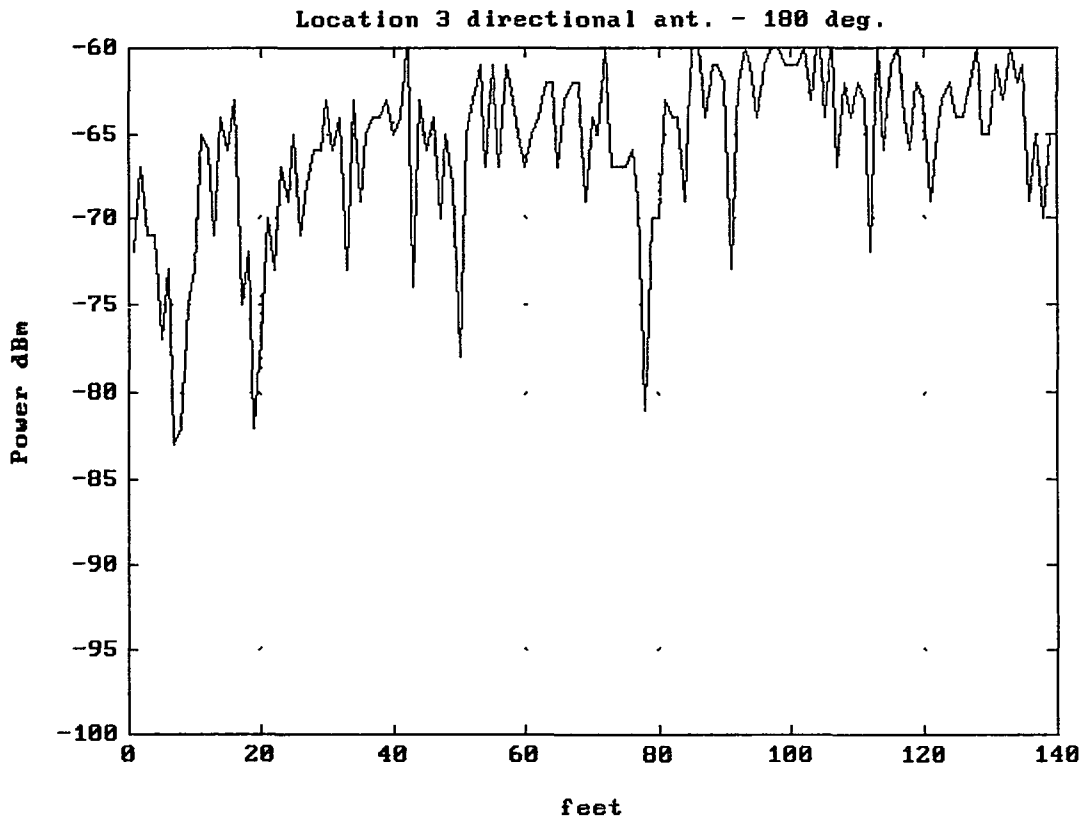
Location 3 directional ant. - 180 deg.
Power dBm
-60
-65
-70
-75
-80
-85
-90
-95
-100
0
20
40
60
80
100
120
140
feet

Figure 20.d

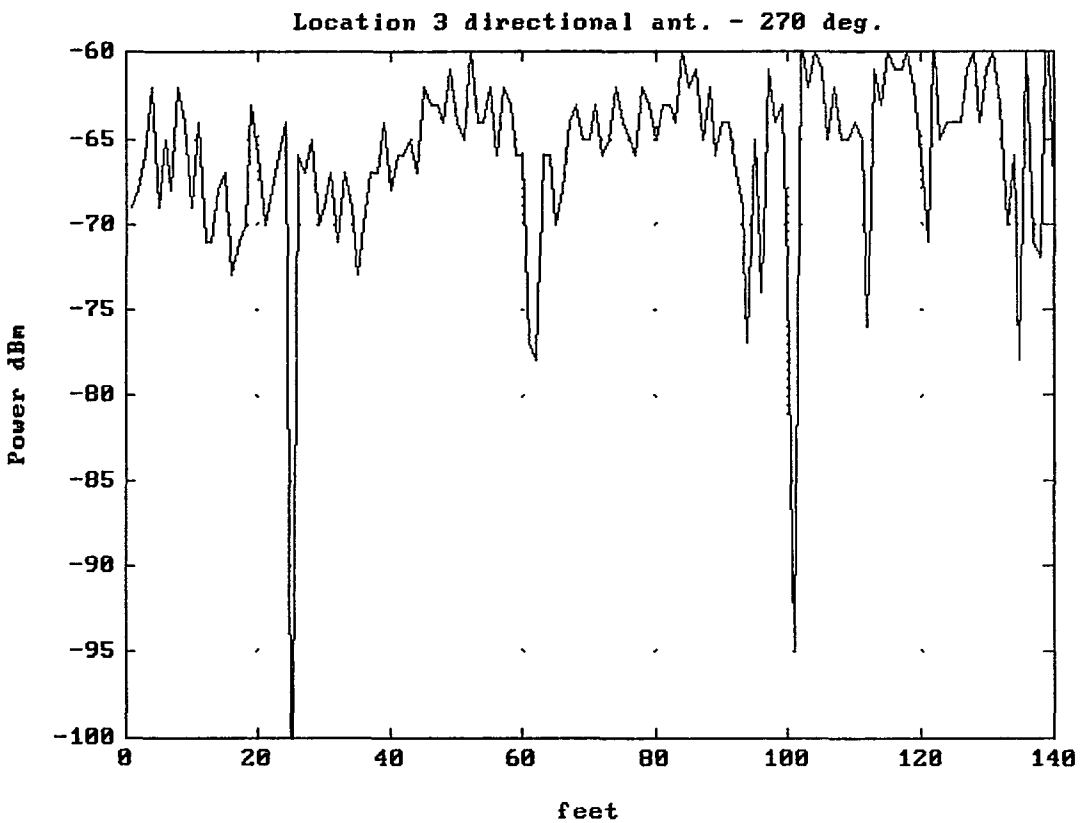
Location 3 directional ant. - 270 deg.
Power dBm
-60
-65
-70
-75
-80
-85
-90
-95
-100
0
20
40
60
80
100
120
140
feet

Figure 20.e

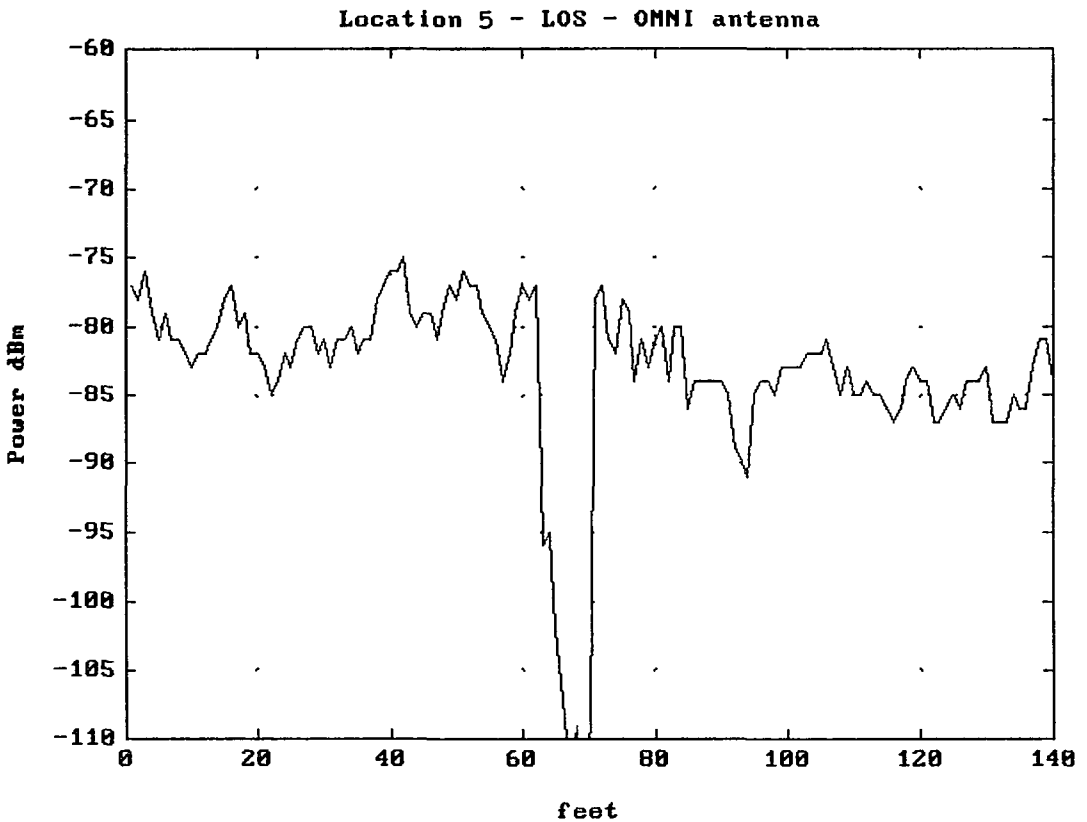
Location 5 - LOS - OMNI antenna
Power dBm
-60
-65
-70
-75
-80
-85
-90
-95
-100
-105
-110
0
20
40
60
80
100
120
140
feet

Figure 21.a

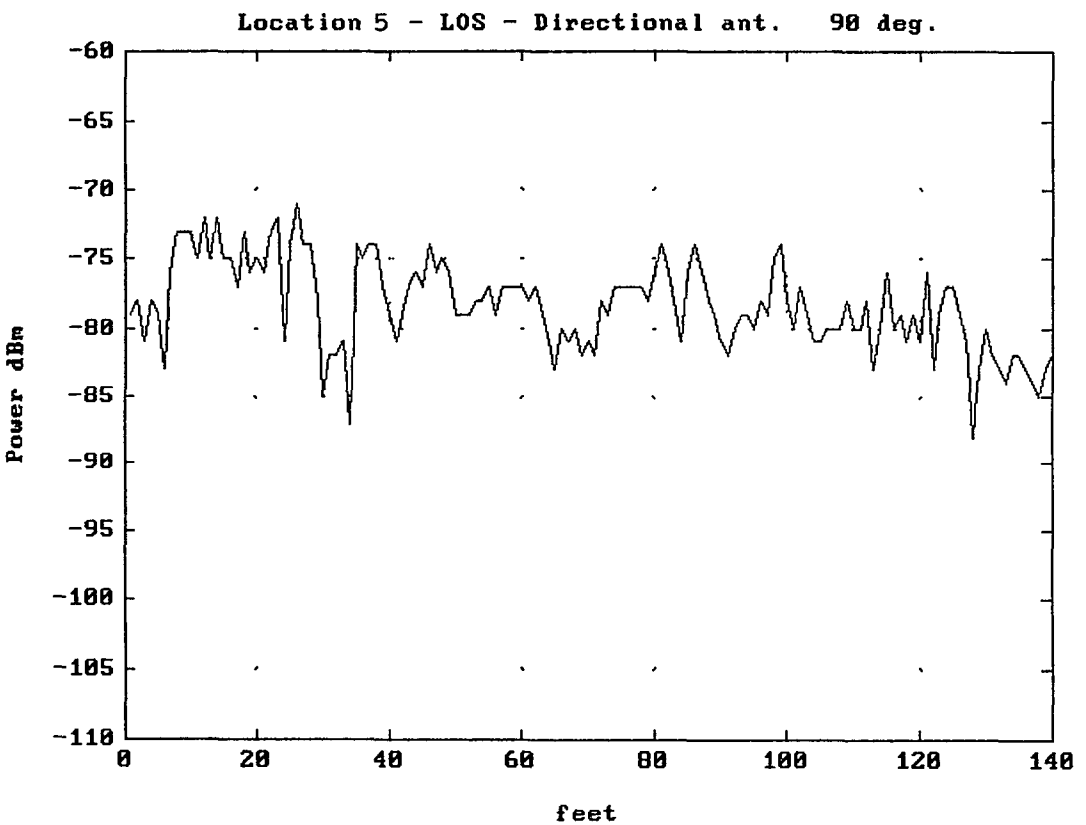
Location 5 - LOS - Directional ant. 90 deg.
Power dBm
-60
-65
-70
-75
-80
-85
-90
-95
-100
-105
-110
0
20
40
60
80
100
120
140
feet

Figure 21.b

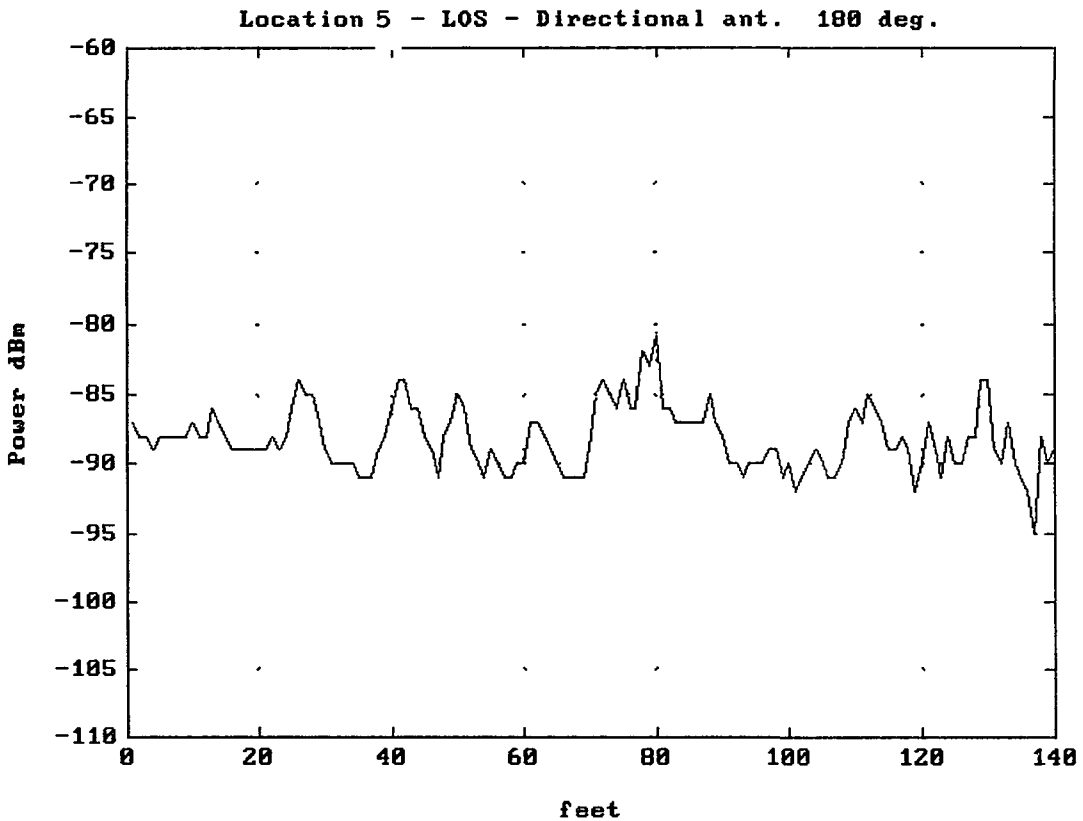
Location 5 - LOS - Directional ant. 180 deg.
Power dBm
-60
-65
-70
-75
-80
-85
-90
-95
-100
-105
-110
0
20
40
60
80
100
120
140
feet

Figure 21.c

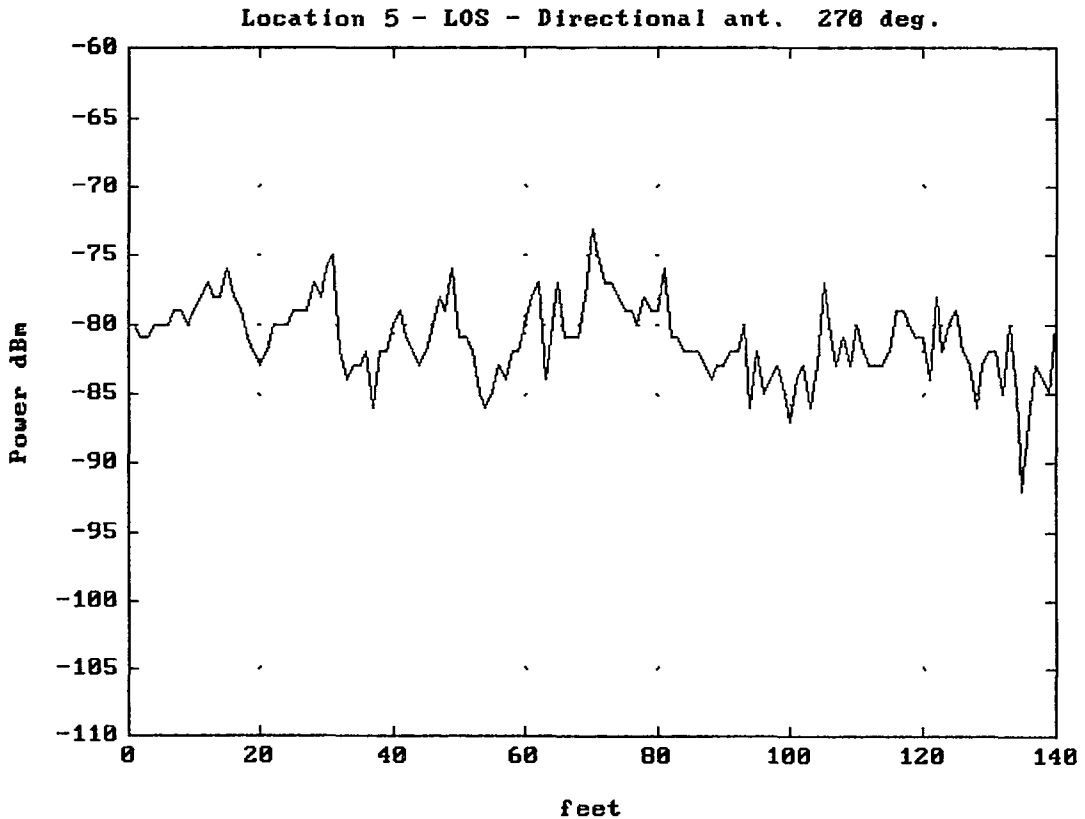
Location 5 - LOS - Directional ant. 270 deg.
Power dBm
-60
-65
-70
-75
-80
-85
-90
-95
-100
-105
-110
0
20
40
60
80
100
120
140
feet

Figure 21.d

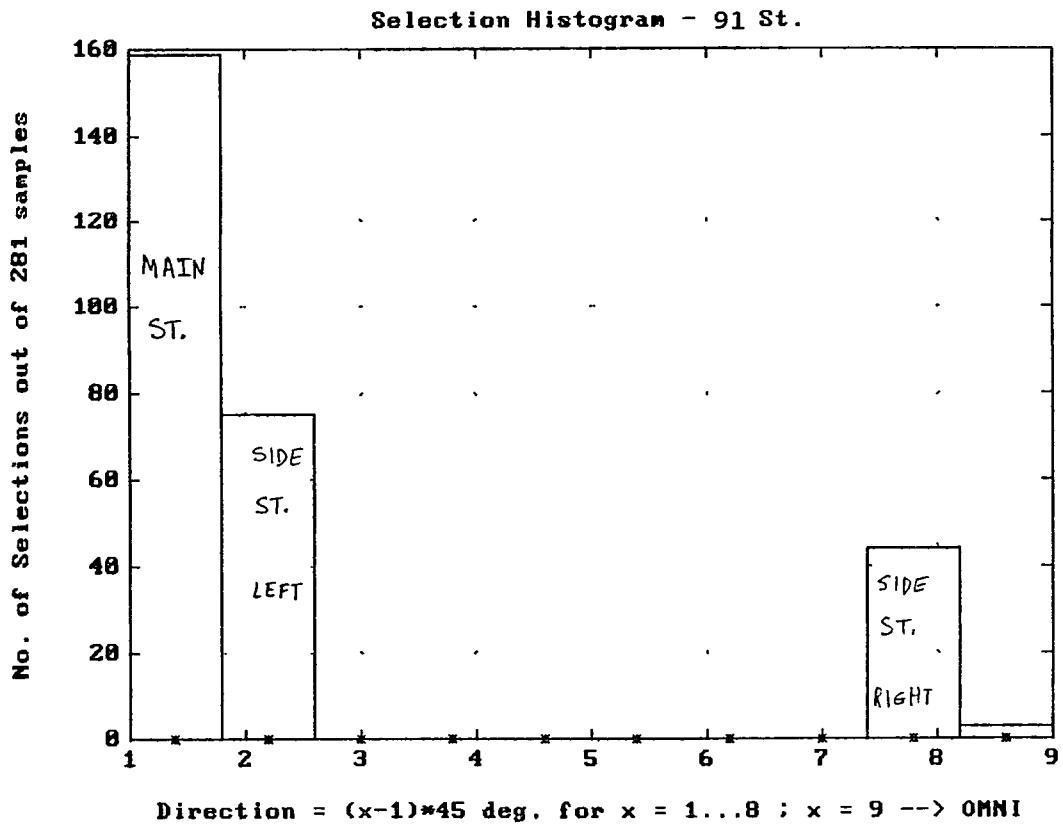
Selection Histogram - 91 St.
No. of Selections out of 281 samples
160
140
120
100
80
60
40
20
0
MAIN ST.
SIDE ST. LEFT
SIDE ST. RIGHT
1
2
3
4
5
6
7
8
9
Direction = (x-1)*45 deg. for x = 1...8 ; x = 9 --> OMNI

Figure 22.a

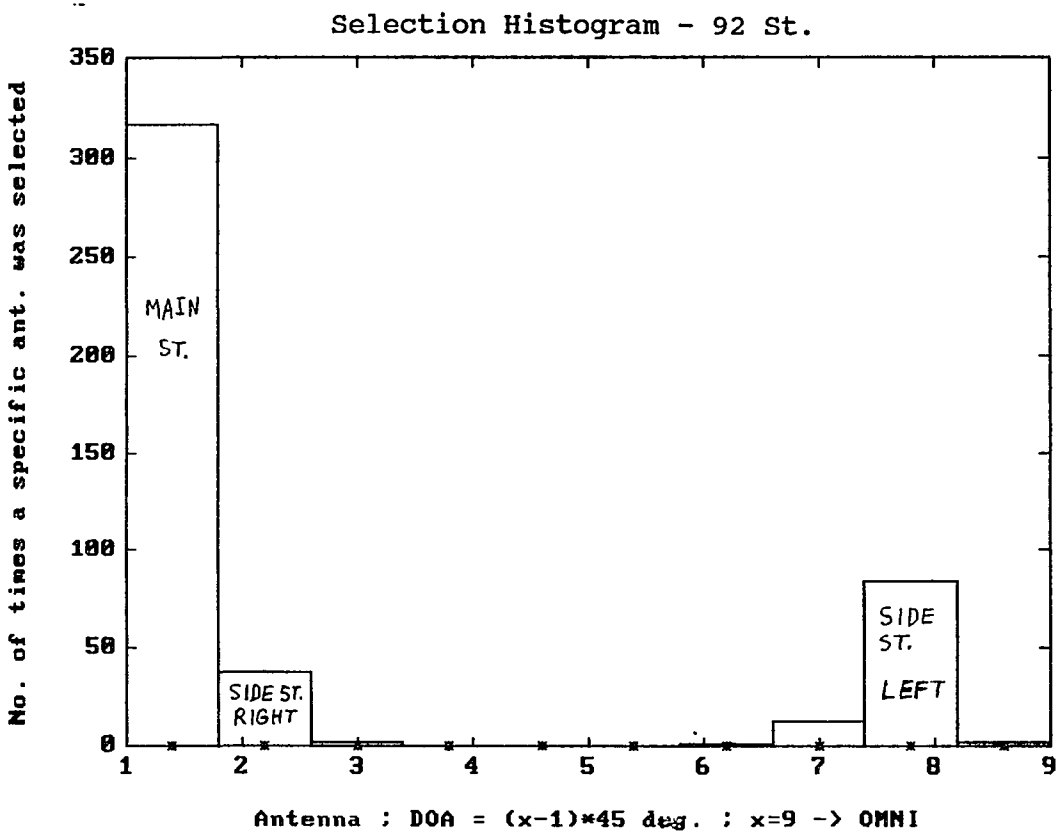
Selection Histogram - 92 St.
No. of times a specific ant. was selected
350
300
250
200
150
100
50
0
MAIN ST.
SIDE ST. RIGHT
SIDE ST. LEFT
1
2
3
4
5
6
7
8
9
Antenna ; DOA = (x-1)*45 deg. ; x=9 -> OMNI

Figure 22.b

References

[1] W.C.Y. Lee, "Preliminary Investigation of Mobile radio Signal Fading Using Directional Antenna on the Mobile Unit", IEEE Trans. on Vehicular Communications, Vol. VC-15, No. 2, Oct. 1966 : 8-15

[2] J.R. Stidham, "Experimental Study of UHF Mobile Radio Transmission Using a Directive Antenna", IEEE Trans. on Vehicular Communications, Vol. VC-15, No. 2, Oct. 1966 : 16-24

[3] W.C. Jakes, Jr. "Microwave Mobile Communications", J. Wiley & Sons, New York, 1974

[4] W.C.Y. Lee, "Mobile Cellular Communications Systems", McGraw Hill, New York, 1989

[5] A.L. Davidson, W.J. Turney, "Mobile Antenna Gain in the Multipath Environment at 900 MHz", IEEE Trans. on Vehicular Technology, Vol. VT-26, No. 4, Nov. 1977 : 345-348

[6] J.D. Kraus, "Antennas", McGraw Hill, New York, 1988

[7] H. Taub and D.L. Schilling, "Principles of Communications Systems", McGraw Hill, New York, 1986

[8] W.C.Y. Lee, "Overview of Cellular CDMA", IEEE Trans. on Vehicular Technology, Vol. 40, No. 2, May 1991 : 291-302

[9] W.C.Y. Lee, "Mobile Communications Engineering", McGraw Hill, New York, 1982

[10] B.K. Levitt, The Effect of Activity Factor on Performance of CDMA Voice Communication Links, JPL, MSAT X Magazin, 1992 : 13-17

[11] K.A. Norton, "The Calculation of Ground Wave Field Intensity Over a Finite Conducting Spherical Earth", Proc. IRE 29, December 1941 : 623-639

[12] K. Bullington, "Radio Propagation fundamentals", Bell System Tech. Journal 36, May 1957 : 593-626

[13] Y. Okumura et al., "Field Strength and its Variability in UHF and VHF Land Mobile Radio Services", Rev. Elec. Commm. Lab.,16, Sep.-Oct. 1968

[14] M. Hata, "Empirical Formula for Propagation Loss in Land Mobile Radio Services", IEEE Trans. on Vehicular Technology, Vol. VT-29, No. 3, August 1980 : 317-325

[15] W.C.Y. Lee, R. H. Brandt, "the Elevation Angle of Mobile Radio Signal Arrival", IEEE Trans. on Communications, Vol. COM-21, No. 11, Nov. 1973 : 1194-1197

[16] A.J. Rustako, N. Amitay, G.J. Owens, S.R.Roman, "Radio Propagation at Microwave Frequencies for Line of Sight Microcellular Mobile and personal Communications", IEEE Trans. on Vehicular Technology, Vol. 40, No. 1, Feb. 1991 : 203-210

[17] V. Erceg, D.L. Schilling, S. Gassemzadeh, D.Li, M. Taylor, "Out of Sight Propagation Modeling and Measurements in an Urban and Sub Urban Environment Using Broad Band Sequence Spread Spectrum", Communications Magazine, June 1993

[18] D.L. Schilling et al., "Broadband CDMA for Personal Communications Systems", IEEE Communications Magazine, Nov. 1991 : 86-93

[19] Helstrom, "Statistical Theory of Signal Detection", Pergamon Press, London, 1960

[20] A.D. Whalen, "Detection of Signals in Noise", Academic Press, New York, 1971

[21] Bennet, "Methods of Solving Noise Problems", Proc. IRE, May 1956 : 609-638

[22] Rice," Mathematical Analysis of Random Noise", Bell System Tech. Journal, Vol. 23, 1944 : 282-236

[23] H.H. Jenkins, "Small aperture Radio Direction Finding", Artech House, Boston, 1991

[24] R.L. Pickholtz, L.B. Milstein, D.L. Schilling, M. Kullback, D. Fishman, W.H. Biederman, "Field Tests Designed to Demonstrate Increased Spectral Efficiency

for Personal Communications", IEEE, 26.1.1 - 26.1.5, Globcom 1991 : 878-882

[25] AT&T, "Application for New or Modified Radio Station Authorization Under Part 5 of FCC Rules - Experimental Radio Service", submitted to the FCC, Washington DC, Feb. 1990

[26] R.L. Pickholtz, L.B. Milstein, D.L. Schilling, "Spread Spectrum for Mobile Communications", IEEE Trans. on Vehicular Technology, May 1991 :313 322

[27] D. Parsons, "The Mobile Radio Propagation Channel", Halsted Press; J. Wiley & Sons, New York, 1992